Electronic Supporting Information

Nitrogen activation and cleavage by a multimetallic uranium complex

Megan Keener,[a] Farzaneh Fadaei-Tirani,[a] Rosario Scopelliti,[a] Ivica Zivcovic,[b] and Marinella Mazzanti*[a]

[a]Institut des Sciences et Ingénierie Chimiques, École Polytechnique Fédérale de Lausanne (EPFL), CH-1015 Lausanne, Switzerland.
[b]Laboratory for Quantum Magnetism, Institute of Physics, Ecole Polytechnique Fédérale de Lausanne (EPFL), CH-1015 Lausanne, Switzerland
*Email to whom correspondence should be addressed: mmazzanti@epfl.ch

Table of Contents

S1. Materials and Physical Measurements 2
S2. Synthesis 4
S3. Reactivity studies 8
S3.1. Protonolysis of complex I. 8
S3.2. Reactivity of heteroleptic-nitride complexes, 1 and 4. 8
S3.3. Reactivity of complex $[U^{III}(OSi(O^tBu)_3)_2I(THF)_3]$: generating complexes "$[U^{III}(OSi(O^tBu)_3)_2(N(SiMe_3)_2)]$", "$[U^{III}(OSi(O^tBu)_3)_2(N(SiMe_3)_2)(toluene)_x]$", and 2. 8
S3.4. Reactivity of heteroleptic-nitride complex, 3-Cs. 9
S3.5. Reactivity of heteroleptic-nitride complexes, 6-K, 6-Cs, X, and 7. 10
S4. General procedure for the formation of NH_3 and $N(SiMe_3)_2$-containing species from HCl. 12
S5. NMR Spectroscopy Data 13
S5.1. NMR spectra for protonolysis studies with complex I. 13
S5.2. NMR spectra for the synthesis of complex 3-Cs 14
S5.3. NMR spectra for isolated heteroleptic complexes. 20
S5.3.1. U(IV)/U(IV) heteroleptic complexes, 1, 3-Cs, and 3b-Cs. 20
S5.3.2. U(III)/U(IV) heteroleptic complexes, 4, 5, 6-K, 6-Cs. 29
S5.3.3. U(V)/U(V) heteroleptic complex, 7. 39
S5.4. NMR spectra for the reactivity of heteroleptic-nitride complexes. 42
S5.4.1. Reactivity of complexes, 1 and 4. 42
S5.4.2. Reactivity of complex 3-Cs. 47
S5.4.3. Reactivity of complexes 6-K, 6-Cs, X, and 7. 55
S5.5. NMR spectra for the formation of NH_3 and $N(SiMe_3)_2$-containing species from addition of HCl. 67
S6. X-Ray Crystallography Data 72
S7. EPR and Magnetism Data 74
S8. Supplementary Schemes 76
S9. References 77

S1. Materials and Physical Measurements

General Considerations

Unless otherwise noted, all manipulations were performed under an atmosphere of dry, oxygen-free Ar or N_2 by means of standard Schlenk or glovebox techniques (MBraun (equipped with a -40 °C freezer) glovebox). Anhydrous solvents were dried over potassium/benzophenone (THF, toluene, and diethyl ether (Et_2O)), sodium sand/benzophenone (*n*-hexanes) and distilled. Deuterated solvents for NMR spectroscopy were purchased from Cortecnet: d_8-THF was distilled over potassium/benzophenone and freeze-degassed, d_6-DMSO was freeze-degassed and dried over 3 Å molecular sieves for several days prior to use. $^{15}N_2$ (98% ^{15}N) were purchased from Cortecnet and stored over activated 3 Å molecular sieves. Depleted uranium turnings were purchased from IBILABS, Florida, USA. Unless otherwise noted, reagents were purchased from commercial suppliers and used as received. $[\{U^{IV}((N(SiMe_3)_2)_3\}[\{U^{IV}((N(SiMe_3)_2)_2(OSi(O^tBu)_3)\}(\mu\text{-}N)][Na(DME)_3]$ (**I**),[1] $[(U^{IV}((N(SiMe_3)_2)_2(THF))_2(\mu\text{-}N)][BPh_4]$ (**E**),[2] were prepared as previously described.

Caution: *Depleted uranium (primary isotope ^{238}U) is a weak α-emitter (4.197 MeV) with a half-life of 4.47 x 10^9 years. Manipulations and reactions should be carried out in monitored fume hoods or in an inert glovebox in a radiation laboratory equipped with α- and β-counting equipment.*

Physical Measurements

NMR spectra were obtained on a AVANCENEO 400 MHz spectrometer, and referenced to residual solvent resonances of THF (d_8-THF), toluene (d_8-toluene), or dimethylsulfoxide (d_6-DMSO) in Pyrex NMR tubes adapted with J. Young valves.

Elemental analyses were performed under an inert atmosphere of nitrogen with a ThermoScientific Flash 2000 Organic Elemental Analyzer.

EPR analysis were performed on a Bruker Elexsys E500 spectrometer working at 9.4 GHz frequency with an Oxford ESR900 cryostat for 4-300 K operation. Simulations were performed with the Easyspin 5.1.3 program.[3]

Magnetic measurements were performed using a Quantum Design MPMS-5T superconducting quantum interference device (SQUID) magnetometer in a temperature range 2-250 K. The powder sample was enclosed in an evacuated quartz capsule and placed inside a plastic straw. The measurements were performed with applied magnetic field of 1 T in the zero-field cooled (ZFC) regime. Diamagnetic corrections were applied using Pascal's constants.[4] The magnetic moment was calculated per uranium using the formula:

$$\mu_{eff} = \sqrt{\frac{8\chi T}{2}}$$

X-ray crystallography data for the analyzed crystal structures were collected using Cu K_α radiation on a Rigaku SuperNova dual system in combination with Atlas type CCD detector or a XtaLAB Synergy R, DW system, HyPix-Arc 150 diffractometer, both operating at T = 140.01(10) K.

Single clear intense orange prism crystals of complex **1** (dimensions 0.43 × 0.15 × 0.08 mm^3), single clear dark brown plate-shaped crystals of complex **2** (dimensions 0.19 × 0.12 × 0.12 mm^3), single clear light brown prism-shaped crystals of complex **3-Cs** (dimensions 0.14 × 0.07 × 0.05 mm^3), single clear pale-yellow needle-shaped crystals of complex **3b-Cs** (dimensions 0.14 × 0.04 × 0.02 mm^3), single clear light brown crystals of complex **3-K** (0.28 × 0.12 × 0.09 mm^3), single lustrous dark black prism-shaped crystals of complex **4** (dimensions 0.24 × 0.11 × 0.08 mm^3), single metallic dark black irregular crystals of complex **5 (**dimensions 0.45 × 0.37 × 0.22 mm^3**)**, single clear intense red plate-shaped crystals of complex **6-K** (0.28 × 0.15 × 0.03 mm^3), single clear light orange plate-shaped crystals of complex **6-Cs** (0.24 × 0.11 × 0.02 mm^3), single clear dark brown plate-shaped crystals of complex **7 (**dimensions 0.20 × 0.10 × 0.08 mm^3), single clear light yellow plate-shaped crystals of complex **8** (0.17 × 0.07 × 0.03 mm^3), and single clear pale green prism-shaped crystals of complex **9** were (0.25 × 0.08 × 0.07 mm^3) were used as supplied. The following data reduction and correction were carried out by *CrysAlis^{Pro}*.[5] The solutions and refinements were performed by *SHELXT* and *SHELXL*,[6, 7] respectively. The crystal structures were refined using full-matrix least-squares based on $\boldsymbol{F^2}$ with all non-H atoms defined in anisotropic manner.

Hydrogen atoms were placed in calculated positions by means of the "riding" model. The refinement of the crystal structures needed some restraints dealing with atomic distances (SADI. DFIX, DANG cards) or anisotropic refinement (RIGU, SIMU instructions). This was due to the disorder displayed, mostly, by some ligands or solvent molecules.
CCDC numbers are 2174705 (complex **1**); 2174938 (complex **2**); 2101093 (complex **3-Cs**); 2141646 (complex **3b-Cs**); 2174960 (complex **3-K**); 2174751 (complex **4**); 2174754 (complex **5**); 2141660 (complex **6-K**); 2141333 (complex **6-Cs**); 2174752 (complex **7**); 2142105 (complex **8**); and 2174753 (complex **9**).

S2. Synthesis

Synthesis of [K{U^{IV}(OSi(O^{t}Bu)$_3$)(N(SiMe$_3$)$_2$)$_2$}$_2$(μ-N)] (1): A 20 mL reaction tube equipped with a glass-coated magnetic stirbar was charged with **E** (159.5 mg, 0.1 mmol) and 3 mL of THF. In a separate vial, KOSi(O^{t}Bu)$_3$ (60.5 mg, 0.2 mmol, 2.0 equiv.) was dissolved in 1 mL of THF. The solution of KOSi(O^{t}Bu)$_3$ was then added dropwise to the stirring solution of **E**, where the solution went from dark brown to pale-red with immediate precipitation of a white solid ($KBPh_4$) from the reaction mixture. This was stirred at room temperature for 1 hour. Stirring was discontinued and the mixture was filtered over a porosity 4 filter frit to yield a pale-red solution. All volatiles were removed under vacuum at room temperature yielding a microcrystalline pink solid. The solid was extracted into minimal *n*-hexanes and filtered over a 0.22 μm porosity filter frit to remove the remaining $KBPh_4$. The volatiles were removed under vacuum, yielding a pink microcrystalline solid (139.2 mg, 82 % yield). Orange single crystals suitable for XRD analysis formed over 24 hours from a concentrated Et_2O or hexane solution of **1** kept at -40ºC. Complex **1** is soluble in all common solvents (THF, *n*-hexanes, toluene, and Et_2O).
^{1}H NMR (400 MHz, d_8-THF, 298K): δ 1.06 (singlet, OSi(O^{t}Bu)$_3$); δ -2.13 ppm (broad singlet, N(SiMe$_3$)$_2$) (**Figure S10**). **^{1}H NMR** (400 MHz, d_8-toleuene, 298K): δ -3.81 (singlet, OSi(O^{t}Bu)$_3$); δ -0.10 (singlet, N(SiMe$_3$)$_2$) (**Figure S8**). **Variable temperature ^{1}H NMR** (400 MHz, d_8-THF, (233K): δ 35.68; δ 0.25; δ -15.02; δ -39.59; δ -54.15 ppm; (213K): δ 42.66; δ 1.55; δ -15.50; δ -34.01; δ -43.27; δ -57.95 ppm; (193K): δ -7.28; δ -20.58; -27.48; -35.03; -43.70; -52.92 ppm (**Figure S11**). **Variable temperature ^{1}H NMR** (400 MHz, d_8-toluene, (233K): δ 0.42; δ 23.57 ppm; (213K): δ 2.30 (broad); δ -23.25; δ -30.95 ppm; (193K): δ 10.50; δ 3.44; δ -10.63; δ -25.47; δ -35.14 ppm (**Figure S9**). *Anal*. *Calcd*. for $C_{48}H_{126}N_5KO_8Si_{10}U_2$: C, 33.96; H, 7.48: N, 4.13. *Found*: C, 33.85; H, 7.52: N, 4.23.

Modified synthesis of [U^{III}(OSi(O^{t}Bu)$_3$)$_2$I(THF)$_3$][8]: A 20 mL reaction tube equipped with a magnetic stirbar was charged with $UI_3(THF)_{3.5}$ (749.2 mg, 0.86 mmol, 1 equiv.) in 1 mL of THF. A solution of KOSi(O^{t}Bu)$_3$ (520.4 mg, 1.72mmol, 2 equiv.) in 2 mL of THF was added to the stirring suspension of $UI_3(THF)_{3.5}$, where the solution went immediately from blue to dark brown. The reaction mixture was stirred at room temperature for 6 hours, in which the color became dark red with a colorless precipitate. The reaction mixture was filtered on a porosity 4 frit and the filter cake was washed with minimal, prechilled THF (-40ºC). The volatiles were removed under vacuum and the resultant solid was dissolved in 2 mL of THF. The solution was kept at -40°C overnight, affording complex [U^{III}(OSi(O^{t}Bu)$_3$)$_2$I(THF)$_3$] as a dark brown-purple crystalline solid (669.9 mg, 70 % yield).
^{1}H NMR (400 MHz, d_8-THF, 298K): δ 6.1 ppm (singlet, OSi(O^{t}Bu)$_3$). *Anal*. *Calcd*. for $C_{36}H_{75}O_{11}Si_2U$: C, 39.02; H, 7.10. *Found*: C, 38.94; H, 7.19 (**Figure S2**).

Synthesis of [Cs{U^{IV}(OSi(O^{t}Bu)$_3$)$_2$(N(SiMe$_3$)$_2$)}$_2$(μ-N)] (3-Cs):
Step 1. A 20 mL reaction tube equipped with a glass-coated magnetic stirbar was charged with [U^{III}(OSi(O^{t}Bu)$_3$)$_2$I(THF)$_3$] (741.5 mg, 0.67 mmol) and 2 mL of THF. In a separate vial, KN(SiMe$_3$)$_2$ (133,7 mg, 0.67 mmol, 1.0 equiv.) was dissolved in 2 mL of THF. Both solutions were cooled to -40°C. The solution of KN(SiMe$_3$)$_2$ was then added dropwise to the stirring solution of [U^{III}(OSi(O^{t}Bu)$_3$)$_2$I(THF)$_3$], where the solution went from dark purple to brown-red with immediate precipitation of a white solid (KI) from the reaction mixture. This was stirred at -40°C for 2 hours. Stirring was discontinued and the mixture was filtered over a prechilled 0.22 μm porosity filter frit to yield a brown-red solution. All volatiles were removed under vacuum at room temperature yielding a red-brown residue (*in-situ* "[U^{III}(OSi(O^{t}Bu)$_3$)$_2$(N(SiMe$_3$)$_2$)]").
Step 2. The residue of "[U^{III}(OSi(O^{t}Bu)$_3$)$_2$(N(SiMe$_3$)$_2$)]" was equipped with a glass-coated magnetic stirbar and cooled to -40°C. Prechilled Et_2O and neat CsN_3 (57.7 mg, 0.33 mmol, 0.5 equiv.) were added and the reaction mixture was stirred at -40°C for four days yielding a pink-brown solution. The mixture was filtered over a 0.22 μm porosity filter frit to yield a brown-pink solution. All the volatiles were removed under vacuum at room temperature yielding a pink-brown microcrystalline solid. The solid was recrystallized by extracting into minimal *n*-hexanes and placing the reaction mixture at -40°C, yielding a pink microcrystalline solid over three crops (368.8 mg, 56% yield). Light brown

single crystals suitable for XRD analysis formed over 24 hours from a concentrated Et_2O or *n*-hexane solution of **3-Cs** kept at -40ºC.

Complex **3-Cs** is soluble in all common solvents (THF, *n*-hexanes, toluene, and Et_2O), but care needs to be taken dependent on solvent utilized. Complex **3-Cs** is stable in toluene at -40°C for one month, whereas in THF, begins to decompose after 1 hour and full decomposition after 24 hours to **3b-Cs**. Both toluene and THF solutions of **3-Cs** at room temperature shows decomposition within 30 minutes. Alternately, **3-Cs** is stable in THF at -80°C for up to 8 hours.

^{1}H NMR (400 MHz, d_8-THF, 298K): δ 1.64 (singlet, $OSi(O^tBu)_3$); δ -13.91 ppm (broad singlet, $N(SiMe_3)_2$) (**Figure S14**). **^{1}H NMR** (400 MHz, d_8-toluene, 298K): δ 1.76 (singlet, $OSi(O^tBu)_3$); δ -16.31 ppm (broad singlet, $N(SiMe_3)_2$) (**Figure S12**). **Variable temperature ^{1}H NMR** (400 MHz, d_8-THF, (233K): δ 3.47; δ -31.34 ppm; (213K): δ 4.18; δ -41.49 ppm; (193K): δ 21.57; δ -2.76 ppm (**Figure S15**). **Variable temperature ^{1}H NMR** (400 MHz, d_8-toluene, (233K); δ 1.13; δ -19.58 ppm; (213K): δ 12.64; δ 1.14; δ -5.64; δ -21.43 ppm; (193K): δ 13.41; δ -6.30 ppm (**Figure S13**). *Anal*. *Calcd*. for $C_{60}H_{144}N_3CsO_{16}Si_8U_2$: C, 36.08; H, 7.27: N, 2.10. *Found*: C, 36.39; H, 7.31: N, 2.07.

Synthesis of [Cs{$(OSi(O^tBu)_3)_3U^{IV}$}(μ-NH)(μ-κ^2:*C,N*−$CH_2SiMe_2NSiMe_3$)-{$U^{IV}(N(SiMe_3)_2)(OSi(O^tBu)_3)$}] (3b-Cs): A 4 mL vial equipped a glass-coated magnetic stirbar was charged with **3-Cs** (19.9 mg, 0.01 mmol) and 0.5 mL THF. The solution was stirred at room temperature for 24 hours, where the solution went from pink to golden yellow in color. Stirring was discontinued and all volatiles were removed under vacuum at room temperature yielding a yellow residue. The residue was dissolved in minimal *n*-hexanes and placed at -40ºC, yielding crystals suitable for XRD analysis (17.7 mg, 89% yield). **^{1}H NMR** (400 MHz, d_8-THF, 298K): δ 51.66; δ 35.40; δ 2.10; δ 1.63; δ -8.23; δ -13.84; δ -31.59; - δ -38.39; -324.81 ppm (**Figure S16**). *Anal*. *Calcd*. for $C_{60}H_{144}N_3CsO_{16}Si_8U_2$: C, 36.08; H, 7.27: N, 2.10. *Found*: C, 36.21; H, 7.22: N, 2.03.

Synthesis of [K{$U^{IV}(OSi(O^tBu)_3)(N(SiMe_3)_2)_2$}$_2$(μ-N)][$K(THF)_6$] (4): A 4 mL vial was charged with **1** (29.0 mg, 0.017 mmol). In a separate vial, KC_8 (22.9 mg, 0.17 mmol, 10.0 equiv.) was suspended in 1.0 mL of THF. Both vials were cooled to -80°C. The mixture of KC_8 was then added in one single portion to the vial containing **1**, where the solution went to a dark brown color with immediate precipitation of graphite. After 1 hour stirring at -80°C, the resulting dark brown suspension was evaporated while maintaining the reaction flask at a cold temperature, and the resulting residue was extracted with 0.5 mL of cold *n*-hexanes. The suspension was filtered over a prechilled por 4 porosity filter frit to removed excess KC_8 and graphite, which were then washed with cold *n*-hexanes (0.5 mL). The filtrate was concentrated to 0.2 mL, 10 drops of cold THF were added, and the resulting mixture was placed at -40°C. After 10 minutes, dark black crystals suitable for XRD analysis were formed and collected on a cold filter (28.6 mg, 78% yield). Complex **4** is soluble in all common solvents (THF, *n*-hexanes, toluene, and Et_2O) at -40°C. However, the complex begins to decompose in THF over 24 hours at -40°C (**Figure S18**), and is completely transformed to the U(IV)/U(IV) starting material, **1**, in toluene over 24 hours at -40°C (**Figure S20**).

Variable temperature ^{1}H NMR (400 MHz, d_8-THF, (233K): δ 0.40; δ -12.39 ppm; (213K): δ 0.25; δ -14.30; δ -27.59 ppm; (193K): δ -0.14; δ -30.97 ppm (**Figure S17**). **Variable temperature ^{1}H NMR** (400 MHz, d_8-toluene, (233K): δ 3.42; δ 1.24; δ 0.07 ppm; (213K): δ 3.19; δ 0.98; δ -23.70; δ -32.17 ppm; (193K): δ 37.88; δ 19.80; δ 11.02; δ 3.76; δ 1.01; δ -10.76; δ -19.76; δ -33.22; δ -37.12; δ -65.67 ppm (**Figure S19**). *Anal*. *Calcd*. for $C_{72}H_{169}N_5K_2O_{14}Si_{10}U_2$: C, 39.96; H, 7.87: N, 3.24. *Found*: C, 39.71; H, 7.65: N, 3.12.

Synthesis of [$((Me_3Si)_2N)_2U^{IV}(OSi(O^tBu)_3)$(μ-NH)($\mu$-$\kappa^2$:*C,N*−$CH_2SiMe_2NSiMe_3$)-$U^{III}(N(SiMe_3)_2)(OSi(O^tBu)_3)$][$(K(2.2.2\text{-cryptand}))_2$] (5): A 4 mL vial equipped with a magnetic stirbar was charged with **4** (21.6 mg, 0.01 mmol) and dissolved in 0.25 mL of THF. In a separate vial, 2.2.2-cryptand (7.5 mg, 0.02 mmol, 2.0 equiv.) was dissolved in 0.5 mL of THF. Both solutions were cooled to -40°C. The solution of 2.2.2-cryptand was then added dropwise to the vial containing **4**. After 1 hour stirring at -40°C, the resulting dark brown solution was concentrated to 0.2 mL, 1 drop of cold *n*-hexanes were added, and the resulting mixture were placed at -40°C. After

12 hours, dark black crystals suitable for XRD analysis were formed and collected on a cold filter (18.4 mg, 74% yield). Complex **4** is soluble in most common solvents (THF, *n*-hexanes, and Et_2O).
Variable temperature ^{1}H NMR (400 MHz, d_8-THF, (233K): δ 84.93; δ 26.97; δ -13.33; δ -15.47; δ -42.73 ppm; (213K): δ 36.21; δ -14.99; δ -34.31; δ -49.37 ppm; (193K): δ 39.73; δ 33.76; δ -17.86; δ -54.30; δ -77.37 ppm (**Figure S21**). *Anal. Calcd.* for $C_{84}H_{198}N_9K_2O_{20}Si_{10}U_2$: C, 40.52; H, 8.02: N, 5.06. *Found*: C, 40.44; H, 7.85: N, 4.98.

Synthesis of $[K_2\{U^{IV/III}(OSi(O^tBu)_3)_2(N(SiMe_3)_2)\}_2(\mu\text{-}N)]$ (6-K): A reaction tube was charged with **3-Cs** (49.9 mg, 0.025 mmol). In a separate 4 mL vial, KC_8 (33.8 mg, 0.25 mmol, 10.0 equiv.) was suspended in 1.5 mL of Et_2O. Both vessels were cooled to -40°C. The mixture of KC_8 was then added in one single portion to the reaction tube containing **3-Cs**, where the solution went to a dark red-brown color with immediate precipitation of graphite. After 30 minutes stirring at -40°C, the resulting dark red-brown suspension was evaporated while maintaining the reaction flask at a cold temperature, and the resulting residue was extracted with 1.0 mL of cold *n*-hexanes. The suspension was filtered over a prechilled por 4 porosity filter frit to remove excess KC_8 and graphite, which were then washed with cold *n*-hexanes (1.0 mL). The filtrate was concentrated to 0.3 mL and the resulting reaction mixture was placed at -40°C. After 24 hours, dark brown crystals were formed and collected on a cold filter (34.9 mg, 72% yield). Intense red crystals suitable for XRD analysis could be formed from a concentrated *n*-hexanes or toluene solution at -40°C. Complex **6-K** is soluble in all common solvents (THF, *n*-hexanes, toluene, and Et_2O) at -40°C, and is stable in toluene at -40°C, however, the complex decomposes in THF over 24 hours at -40°C.
Variable temperature ^{1}H NMR (400 MHz, d_8-toluene, (233K): δ 4.26; δ 2.65; δ -23.13; δ -24.79; δ -26.28 ppm; (213K): δ 4.66; δ -30.40 ppm; (193K): δ 2.73 (broad); δ -34.93 ppm (**Figure S22**). **Variable temperature ^{1}H NMR** (400 MHz, d_8-THF, (233K): δ 1.48; δ 0.19; δ -17.29 ppm; (213K): δ -1.42; δ -23.53 ppm; (193K): δ -1.94; δ -10.15; δ -26.75 ppm (**Figure S23**). *Anal. Calcd.* for $C_{60}H_{144}N_3K_2O_{16}Si_8U_2$: C, 37.09; H, 7.47: N, 2.16. *Found*: C, 37.12; H, 7.41: N, 2.10.

Synthesis of $[Cs_2\{U^{III/IV}(OSi(O^tBu)_3)_2(N(SiMe_3)_2)\}_2(\mu\text{-}N)]$ (6-Cs): A reaction tube was charged with **3-Cs** (49.9 mg, 0.025 mmol). In a separate 4 mL vial, CsC_8 (57.2 mg, 0.25 mmol, 10.0 equiv.) was suspended in 1.5 mL of THF. Both vessels were cooled to -40°C. The mixture of CsC_8 was then added in one single portion to the reaction tube containing **3-Cs**, where the solution went to a dark red-brown color with immediate precipitation of graphite. After 30 minutes stirring at -40°C, the resulting dark red-brown suspension was evaporated while maintaining the reaction flask at a cold temperature, and the resulting residue was extracted with 1.0 mL of cold *n*-hexanes. The suspension was filtered over a prechilled por 4 porosity filter frit to remove excess KC_8 and graphite, which were then washed with cold *n*-hexanes (1.0 mL). The filtrate was concentrated to 0.3 mL and the resulting reaction mixture was placed at -40°C. After 24 hours, dark brown crystals were formed and collected on a cold filter (41.5 mg, 78% yield). Light orange crystals suitable for XRD analysis were formed from a concentrated *n*-hexanes or toluene solution at -40°C. Complex **6-Cs** is soluble in all common solvents (THF, *n*-hexanes, toluene, and Et_2O) at -40°C, and is stable in toluene at -40°C, however, slight decomposition is observed in THF over 24 hours at -40°C (**Figure S26**).
Variable temperature ^{1}H NMR (400 MHz, d_8-toluene, (233K): δ 2.65; δ -26.69 ppm; (213K): δ 2.57; δ -30.76 ppm; (193K): δ -2.56; δ -36.23 ppm (**Figure S24**). **Variable temperature ^{1}H NMR** (400 MHz, d_8-THF, (233K): δ 65.96; δ 22.82; δ 1.31; δ 6.58; δ -11.20; δ -17.96 ppm; (213K): δ 74.22; δ 1.30; δ -8.57; δ -23.09; δ -74.00 ppm; (193K): δ 86.27; δ -3.92; δ -9.85; δ -26.53; δ -68.16; δ -88.86 ppm (**Figure S25**). *Anal. Calcd.* for $C_{60}H_{144}N_3Cs_2O_{16}Si_8U_2$: C, 33.83; H, 6.81: N, 1.97. *Found*: C, 33.63; H, 6.62: N, 1.74.

Synthesis of *in-situ* generated "$[K_3\{U^{III}(OSi(O^tBu)_3)_2(N(SiMe_3)_2)\}_2(\mu\text{-}N)]$" (X): A reaction tube was charged with **3-Cs** (49.9 mg, 0.025 mmol). In a separate 4 mL vial, KC_8 (33.8 mg, 0.25 mmol, 10.0 equiv.) was suspended in 1.5 mL of THF. Both vessels were cooled to -40°C. The mixture of KC_8 was then added in one single portion to the reaction tube containing **3-Cs**, where the solution went to a dark purple color with immediate precipitation of graphite. After 30 minutes stirring at -40°C, the resulting dark purple suspension was evaporated while maintaining the reaction flask at a cold temperature, and the resulting residue was extracted with 1.0 mL of cold *n*-hexanes. The suspension

was filtered over a prechilled por 4 porosity filter frit to remove excess KC_8 and graphite, which were then washed with cold *n*-hexanes (1.0 mL). The volatiles were removed under vacuum while maintaining the reaction flask at a cold temperature, yielding a microcrystalline purple solid. Complex **X** was utilized immediately after synthesis to reduce decomposition. Attempts to isolate single crystals of **X** proved unsuccessful due to decomposition at -40°C over 24 hours in the solution-state.

***In-situ* variable temperature ^{1}H NMR** (400 MHz, d_8-THF, (233K): δ 21.99; δ 2.68; δ -14.99 ppm; (213K): 3.17 (broad); -1.41 ppm; (193K): δ 8.56; δ 1.04; -3.40; -8.69; -33.58 ppm (**Figure S38**-**Figure S39**).

***In-situ* variable temperature ^{1}H NMR** (400 MHz, d_8-toluene, (233K): δ 2.96; δ -15.25; δ -23.19 ppm; (213K): δ 3.03; δ 17.32 ppm; (193K): δ 2.67; δ -15.95; δ -24.57 ppm (**Figure S40**).

Synthesis of $[K_3\{U^V(OSi(O^tBu)_3)_2(N(SiMe_3)_2)\}_2(\mu\text{-}N)(\mu\text{-}\eta^2\text{:}\eta^2\text{-}N_2)]$ (7):

Step 1. A reaction tube was charged with **3-Cs** (119.8 mg, 0.06 mmol). In a separate 4 mL vial, KC_8 (33.8 mg, 0.25 mmol, 10.0 equiv.) was suspended in 3 mL of THF. Both vials were cooled to -40°C. The mixture of KC_8 was then added in one single portion to the vial containing **3-Cs**, where the solution went to a dark purple color with immediate precipitation of graphite. After 30 minutes stirring at -40°C, the resulting dark purple suspension was evaporated while maintaining the reaction flask at a cold temperature, and the resulting residue was extracted with 3 mL of cold *n*-hexanes. The suspension was filtered over a prechilled por 4 porosity filter frit to remove excess KC_8 and graphite, which were then washed with cold *n*-hexanes (1.0 mL). The volatiles were removed under vacuum while maintaining the reaction flask at a cold temperature, generating complex **X**.

Step 2. *In-situ* generated complex **X** was cooled to -80°C and dissolved in 7 mL of cold toluene, yielding a dark purple solution. This was then transferred to a Schlenk tube equipped with a J-Young valve under argon in the glovebox. The flask was then connected to a Schlenk line and evacuated while keeping the flask at -100°C. The solution was exposed to N_2 (1 atm) for 5 minutes at -100°C and vigorously stirred, resulting in a color change from purple to light brown. The solution was then brought to -80°C and reacted for 1 hour. The light brown solution was transferred into a nitrogen glovebox and placed at -40°C. After 24 hours, complex **7** precipitated from the solution as a brown microcrystalline solid, in which the supernatant was removed and the crystals were washed (3x) with cold (-40°C) toluene. The crystals were collected and dried under vacuum at -80°C (67.5 mg, 56% yield). Crystals suitable for XRD analysis were formed from a small-scale reaction of **3-Cs** (14.0 mg, 0.007 mmol) in toluene solution at -40°C. Complex **7** is insoluble in most common solvents (*n*-hexanes and toluene) at -40°C. Complex **7** is soluble in THF, however, the composition of the complex changes (**Figure S29**), and begins to decomposes at -80°C, forming an unknown species at -0.2 ppm.

Variable temperature ^{1}H NMR (400 MHz, d_8-toluene, (233K): δ 19.38; δ 4.55; δ 5.17; δ -12.44; δ -15.49; δ -27.53 ppm; (213K): δ 32.30; δ 22.25; δ 12.38; δ -0.98; δ -4.96; δ -6.22; δ -14.73; δ -17.63 ppm; (193K): δ 37.24; δ 26.15; δ 15.51; δ -1.83; δ -5.94; δ -7.70; δ -17.70; δ -20.49 ppm (**Figure S27**). **Variable temperature ^{1}H NMR** (400 MHz, d_8-THF, (233K): δ 3.32; δ -11.33 ppm; (213K): 2.33 (broad); .5.68; -11.60 ppm; (193K): δ 18.11; δ 11.44; -5.33; -8.20; -15.76 ppm (**Figure S28**). *Anal*. *Calcd*. for $C_{60}H_{144}N_5K_3O_{16}Si_8U_2$: C, 35.86; H, 7.22: N, 3.48. *Found*: C, 35.91; H, 7.36: N, 3.25.

Note: After complex **7** crystallizes from the reaction mixture at -40°C after 24 hours, the supernatant (5 mL) was separated and the solution was concentrated to roughly 0.5 mL of toluene and placed at -40°C. Over four independent trials, complex **8** was identified once, while complex **9** was identified on three occasions. Each crystallization of the supernatant always led to a mixture of crystals, in which the only other product that could be crystallographically identified was **3-K**. The other species that coprecipitated were not suitable for XRD analysis and could therefore not be identified.

S3. Reactivity studies

S3.1. Protonolysis of complex I.

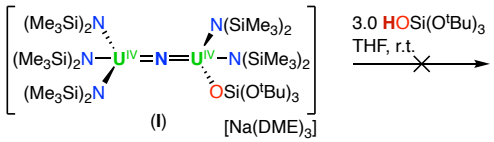

Reaction of I with HOSi(O^{t}Bu)$_3$. A 4 mL vial was charged with **I** (6.0 mg, 0.0035 mmol) and dissolved in 0.25 mL d_8-THF. In a separate 1 mL vial, HOSi(O^{t}Bu)$_3$ (1.0 mg, 0.0035 mmol, 1.0 equiv.) was added and dissolved in 0.25 mL d_8-THF. The solution of HOSi(O^{t}Bu)$_3$ was added in a single portion to the solution of **I**, where upon addition the solution remained pink-brown in color. The mixture was transferred to a NMR tube equipped with a J-Young valve and monitored over 5 days by ^{1}H NMR spectroscopy (**Figure S1**), resulting in unreacted complex **I** and HOSi(O^{t}Bu)$_3$.

S3.2. Reactivity of heteroleptic-nitride complexes, 1 and 4.

Reduction of 1 with 10.0 equiv. KC$_8$. In an argon filled glovebox, a NMR tube equipped with a J-Young valve was charged with complex **1** (5.9 mg, 0.0035 mmol). In a 1 mL vial, KC$_8$ (4.7 mg, 0.035 mmol, 10.0 equiv.) was suspended in 0.5 mL of d_8-THF. Both vials were chilled to -80°C. The chilled suspension of KC$_8$ was added in a single portion to the NMR tube containing **1**, where upon addition, the solution turned dark red-brown in color with contaminant formation of graphite. The mixture was analyzed by variable temperature ^{1}H NMR spectroscopy (**Figure S31**), resulting in consumption of complex **1**, formation of **4**, as well as multiple unidentifiable species. The following reduction can also be performed at -40°C, but results in higher quantities of the unknown species (**Figure S30**).

Reaction of 4 with 2.2.2-cryptand. In an argon filled glovebox, a NMR tube equipped with a J-Young valve was charged with complex **4** (5.0 mg, 0.0023 mmol). In a 1 mL vial, 2.2.2-cryptand (1.7 mg, 0.046 mmol, 2.0 equiv.) was dissolved in 0.5 mL of d_8-THF. Both were chilled to -40°C. The chilled suspension of 2.2.2-cryptand was added in a single portion to the NMR tube containing **4**, where upon addition, the solution turned dark brown in color. The mixture was analyzed by variable temperature ^{1}H NMR spectroscopy (**Figure S32**), resulting in consumption of complex **4**, formation of **5**, as well as minor unidentifiable species.

Reaction of 4 with 1 atm N$_2$. In a nitrogen filled glovebox, a NMR tube equipped with a J-Young valve was charged with complex **4** (5.0 mg, 0.0023 mmol) a nd chilled to -80°C. Prechilled solvent (d_8-THF or d_8-toluene) was added to the tube containing **4** and mixed while maintaining the NMR tube at a cold temperature. The mixture was analyzed by variable temperature ^{1}H NMR spectroscopy after 6 hours, resulting in unreacted **4** (**Figure S33** and **Figure S34**). The mixture was then brought to -40°C and monitored by ^{1}H NMR spectroscopy, resulting in unreacted **4** and decomposition products found in both THF and toluene solutions.

S3.3. Reactivity of complex [U^{III}(OSi(O^{t}Bu)$_3$)$_2$I(THF)$_3$]: generating complexes "[U^{III}(OSi(O^{t}Bu)$_3$)$_2$(N(SiMe$_3$)$_2$)]", "[U^{III}(OSi(O^{t}Bu)$_3$)$_2$(N(SiMe$_3$)$_2$)(toluene)$_x$]", and 2.

Synthesis of *in-situ* generated "[U^{III}(OSi(O^{t}Bu)$_3$)$_2$(N(SiMe$_3$)$_2$)]": A 1 mL vial equipped with a glass-coated stirred was charged with [U^{III}(OSi(O^{t}Bu)$_3$)$_2$I(THF)$_3$] (15.5 mg, 0.014 mmol) and 0.25 mL of d_8-THF. In a separate 1 mL vial, KN(SiMe$_3$)$_2$ (2.8 mg, 0.014 mmol, 1.0 equiv.) was dissolved in 0.25 mL of d_8-THF. Both solutions were cooled to -40°C. The solution of KN(SiMe$_3$)$_2$ was then added dropwise to the stirring solution of [U^{III}(OSi(O^{t}Bu)$_3$)$_2$I(THF)$_3$], where the solution went from dark purple to brown-red with immediate precipitation of a white solid (KI) from the reaction mixture. After stirring at -40°C for 1 hour, the mixture was transferred to a prechilled NMR tube equipped with a J-Young valve and the solution was analyzed by ^{1}H NMR spectroscopy (**Figure S3**), resulting in a mixture of the major species, "[U^{III}(OSi(O^{t}Bu)$_3$)$_2$(N(SiMe$_3$)$_2$)]", with minor species, "[U^{III}(OSi(O^{t}Bu)$_3$)$_2$(N(SiMe$_3$)$_2$)(toluene)$_x$]", [{U^{III}(OSi(O^{t}Bu)$_3$}$_2$],[9] [U^{III}(OSi(O^{t}Bu)$_3$)$_2$I(THF)$_3$], and **2**. The nature of byproducts, "[U^{III}(OSi(O^{t}Bu)$_3$)$_2$(N(SiMe$_3$)$_2$)(toluene)$_x$]", and **2**, were determined via alternative synthetic routes (see below), in

which **2** was unambiguously determined by X-Ray diffraction studies (**Figure S60**). Attempts to isolate X-Ray quality crystals of the proposed major species, "[{U^{IV}($OSi(O^tBu)_3$)$_2$($N(SiMe_3)_2$)]", proved unsuccessful, leading to the isolation of ligand scrambling products, such as the previously reported complex, [U^{III}($OSi(O^tBu)_3$)$_3$]$_2$,[10] or transformation to the byproducts "[U^{III}($OSi(O^tBu)_3$)$_2$($N(SiMe_3)_2$)(toluene)$_x$]" and **2** in the presence of non-polar solvents. **^{1}H NMR** (400 MHz, d_8-THF, 298K): δ 3.93 (singlet, $OSi(O^tBu)_3$); δ -7.56 ppm (broad singlet, $N(SiMe_3)_2$) (**Figure S3**).

Synthesis of *in-situ* generated "[U^{III}($OSi(O^tBu)_3$)$_2$($N(SiMe_3)_2$)(toluene)$_x$]": A 1 mL vial equipped with a glass-coated stirbar was charged with [U^{III}($OSi(O^tBu)_3$)$_2$I(THF)$_3$] (15.5 mg, 0.014 mmol) and 0.25 mL of d_8-toluene. In a separate 1 mL vial, $KN(SiMe_3)_2$ (2.8 mg, 0.014 mmol, 1.0 equiv.) was dissolved in 0.25 mL of d_8-toluene. The solution of $KN(SiMe_3)_2$ was then added dropwise to the stirring solution of [U^{III}($OSi(O^tBu)_3$)$_2$I(THF)$_3$], where the solution went from dark purple to brown-red with immediate precipitation of a white solid (KI) from the reaction mixture. The mixture was transferred to a NMR tube equipped with a J-Young valve and the solution was analyzed by ^{1}H NMR spectroscopy (a, **Figure S4**), resulting in a mixture of the major species, "[U^{III}($OSi(O^tBu)_3$)$_2$($N(SiMe_3)_2$)(toluene)$_x$]", and minor unidentifiable species. The volatiles were then removed under vacuum, yielding a brown residue. This was further dissolved in d_8-THF and analyzed by ^{1}H NMR spectroscopy (b, **Figure S4**), resulting in a mixture of the major species, "[U^{III}($OSi(O^tBu)_3$)$_2$($N(SiMe_3)_2$)(toluene)$_x$]", and minor unidentifiable species. **^{1}H NMR** (400 MHz, d_8-THF, 298K): δ 1.65 (singlet, $OSi(O^tBu)_3$); δ -8.83 ppm (broad singlet, $N(SiMe_3)_2$).

Synthesis of [U^{III}($OSi(O^tBu)_3$)$_2$($N(SiMe_3)_2$)$_2$K] (2): A 1 mL vial equipped with a glass-coated stirred was charged with [U^{III}($OSi(O^tBu)_3$)$_2$I(THF)$_3$] (15.5 mg, 0.014 mmol) and 0.25 mL of d_8-THF. In a separate 1 mL vial, $KN(SiMe_3)_2$ (5.6 mg, 0.028 mmol, 2.0 equiv.) was dissolved in 0.25 mL of d_8-THF. Both solutions were cooled to -40°C. The solution of $KN(SiMe_3)_2$ was then added dropwise to the stirring solution of [U^{III}($OSi(O^tBu)_3$)$_2$I(THF)$_3$], where the solution went from dark purple to brown-red with immediate precipitation of a white solid (KI) from the reaction mixture. After stirring at -40°C for 1 hour, the mixture was transferred to a prechilled NMR tube equipped with a J-Young valve and the solution was analyzed by ^{1}H NMR spectroscopy (**Figure S5**), resulting in **2** as the major species. The mixture was filtered over a 0.22 um por filter frit, and the volatiles were removed under vacuum. The brown residue was dissolved in minimal toluene and placed at -40°C. After 24 hours, brown crystals suitable for XRD analysis (**Figure S60**) were obtained (14.1 mg, 92% yield). **^{1}H NMR** (400 MHz, d_8-THF, 298K): δ 2.75 (singlet, $OSi(O^tBu)_3$); δ -12.27 ppm (broad singlet, $N(SiMe_3)_2$) (**Figure S5**). **^{1}H NMR** (400 MHz, d_8-toluene, 298K): δ 0.10 (singlet, $OSi(O^tBu)_3$); δ -11.35 ppm (broad singlet, $N(SiMe_3)_2$) (**Figure S6**). *Anal*. *Calcd*. for $C_{36}H_{90}N_2KO_8S6U$: C, 38.44; H, 8.07: N, 2.49. *Found*: C, 38.39; H, 7.88: N, 2.45.

S3.4. Reactivity of heteroleptic-nitride complex, 3-Cs.

Reduction of 3-Cs with 1.0 equiv. KC_8 in THF. In an argon filled glovebox, a NMR tube equipped with a J-Young valve was charged with complex **3-Cs** (15.9 mg, 0.008 mmol). In a 1 mL vial, KC_8 (1.0 mg, 0.008 mmol, 10.0 equiv.) was suspended in 0.5 mL of d_8-THF. Both vessels were chilled to -40°C. The chilled suspension of KC_8 was added in a single portion to the NMR tube containing **3-Cs**, where upon addition, the solution turned dark red-brown in color with contaminant formation of graphite. The mixture was analyzed by variable temperature ^{1}H NMR spectroscopy (**Figure S35**), resulting in a mixture of complex **3-Cs** and **6-K**.

Reduction of 3-Cs with 10.0 equiv. KC_8 in Et_2O. In an argon filled glovebox, a 4 mL vial was charged with complex **3-Cs** (7.0 mg, 0.0035 mmol). In a 1 mL vial, KC_8 (4.7 mg, 0.035 mmol, 10.0 equiv.) was suspended in 0.5 mL of Et_2O. Both vials were chilled to -40°C. The chilled suspension of KC_8 was added in a single portion to the vial containing **3-Cs**, where upon addition, the solution turned dark red-brown in color with contaminant formation of graphite. All the volatiles were removed under vacuum while maintaining the vial at a cold temperature. The mixture was extracted into d_8-toluene and analyzed by variable temperature ^{1}H NMR spectroscopy (**Figure S36**), resulting in the formation of **6-K**.

Reduction of 3-Cs with 10.0 equiv. CsC_8 in THF. In an argon filled glovebox, a NMR tube equipped with a J-Young valve was charged with complex **3-Cs** (7.0 mg, 0.0035 mmol). In a 1 mL vial, CsC_8 (8.0 mg, 0.035 mmol, 10.0 equiv.) was suspended in 0.5 mL of d_8-THF. Both vessels were chilled to -40°C. The chilled suspension of CsC_8 was added in a single portion to the NMR tube containing **3-Cs**, where upon addition, the solution turned dark red-brown in color with contaminant formation of graphite. The mixture was analyzed by variable temperature ^{1}H NMR spectroscopy (**Figure S37**), resulting in the formation of **6-Cs**.

Reduction of 3-Cs with 10.0 equiv. KC_8 in THF. In an argon filled glovebox, a NMR tube equipped with a J-Young valve was charged with complex **3-Cs** (7.0 mg, 0.0035 mmol). In a 1 mL vial, KC_8 (4.7 mg, 0.035 mmol, 10.0 equiv.) was suspended in 0.5 mL of d_8-THF. Both vessels were chilled to (-40°C or -80°C). The chilled suspension of KC_8 was added in a single portion to the NMR tube containing **3-Cs**, where upon addition, the solution turned dark purple in color with contaminant formation of graphite. The mixtures were analyzed by variable temperature ^{1}H NMR spectroscopy (-40°C; **Figure S39**) and (-80°C; **Figure S38**), resulting in complex **X** as the major species.

S3.5. Reactivity of heteroleptic-nitride complexes, 6-K, 6-Cs, X, and 7.

Reduction of 6-K with 10.0 equiv. KC_8 in THF. In an argon filled glovebox, a NMR tube equipped with a J-Young valve was charged with complex **6-K** (6.8 mg, 0.0035 mmol). In a 1 mL vial, KC_8 (4.7 mg, 0.035 mmol, 10.0 equiv.) was suspended in 0.5 mL of d_8-THF. Both vessels were chilled to -40°C. The chilled suspension of KC_8 was added in a single portion to the NMR tube containing **6-K**, where upon addition, the solution turned dark purple in color with contaminant formation of graphite. The mixture was analyzed by variable temperature ^{1}H NMR spectroscopy (**Figure S43**), resulting in complex **X** as the major species.

Reaction of 6-K with 1 atm N_2. In an argon filled glovebox, a NMR tube equipped with a J-Young valve was charged with complex **6-K** (6.8 mg, 0.0035 mmol). The tube was transferred into a nitrogen-filled glovebox, cooled to -80°C, and the argon headspace was removed under vacuum. Prechilled solvent (d_8-toluene or d_8-THF) was added in a single portion to the NMR tube containing **6-K**, where upon addition, the solution remained dark red-brown in color. The solution was analyzed by variable temperature ^{1}H NMR spectroscopy for both d_8-toluene (**Figure S45**) and d_8-THF (**Figure S44**) solutions, resulting in unreacted **6-K**, and an unknown species at -0.2 ppm in d_8-THF.

Reaction of 6-Cs with 1 atm N_2. In an argon filled glovebox, a NMR tube equipped with a J-Young valve was charged with complex **6-Cs** (7.4 mg, 0.0035 mmol). The tube was transferred into a nitrogen-filled glovebox, cooled to -80°C, and the argon headspace was removed under vacuum. Prechilled solvent (d_8-toluene or d_8-THF) was added in a single portion to the NMR tube containing **6-Cs**, where upon addition, the solution remained dark red-brown in color. The solution was analyzed by variable temperature ^{1}H NMR spectroscopy for both d_8-toluene (**Figure S47**) and d_8-THF (**Figure S46**) solutions, resulting in unreacted **6-Cs**, and an unknown species at -0.2 ppm in d_8-THF.

Reaction of *in-situ* generated X with 1 atm N_2.

Step 1. A 4 mL vial was charged with **3-Cs** (7.0 mg, 0.0035 mmol). In a separate 1 mL vial, KC_8 (4.7 mg, 0.035 mmol, 10.0 equiv.) was suspended in 0.5 mL of THF. Both vials were cooled to -40°C. The mixture of KC_8 was then added in one single portion to the vial containing **3-Cs**, where the solution went to a dark purple color with immediate precipitation of graphite. After 30 minutes stirring at -40°C, the resulting dark purple suspension was evaporated while maintaining the reaction flask at a cold temperature, and the resulting residue was extracted with 0.5 mL of cold *n*-hexanes. The suspension was filtered over a prechilled por 4 porosity filter frit to remove excess KC_8 and graphite, which were then washed with cold *n*-hexanes (0.5 mL). The solution was transferred to a prechilled NMR tube equipped with a J-Young valve and the volatiles were carefully removed under vacuum while maintaining the tube at a cold temperature, generating complex **X**.

Step 2. *In-situ* generated complex **X** was cooled to -80°C and dissolved in 0.5 mL of cold d_8-toluene, yielding a dark purple solution. The tube was then connected to a Schlenk line and evacuated while maintaining the tube at -100°C. The solution was exposed to N_2 (1 atm) at -100°C, resulting in an immediate color change from purple to light brown. The solution was brought to -80°C and mixed every 10 minutes for 1 hour. The solution was analyzed by variable temperature ^{1}H NMR spectroscopy (**Figure S48**), resulting in complex **7**.

Reaction of 7 with 1.0 equiv. of *in-situ* generated X.

Step 1. In an argon filled glovebox, a 4 mL vial was charged with **3-Cs** (14.0 mg, 0.007 mmol). In a separate 1 mL vial, KC_8 (9.4 mg, 0.07 mmol, 10.0 equiv.) was suspended in 1 mL of THF. Both vials were cooled to -40°C. The mixture of KC_8 was then added in one single portion to the vial containing **3-Cs**, where the solution went to a dark purple color with immediate precipitation of graphite. After 30 minutes stirring at -40°C, the resulting dark purple suspension was evaporated while maintaining the reaction flask at a cold temperature, and the resulting residue was extracted with 1 mL of cold *n*-hexanes. The suspension was filtered over a prechilled por 4 porosity filter frit to remove excess KC_8 and graphite, which were then washed with cold *n*-hexanes (0.5 mL). *In-situ* generated complex **X** was cooled to -80°C and dissolved in 0.5 mL of cold d_8-toluene, yielding a dark purple solution.

Step 2. A 4 mL vial equipped with a magnetic stirbar was charged with complex **7** (14.1 mg, 0.007 mmol) and cooled to -80°C. The prechilled solution of *in-situ* generated complex **X** (***step 1***) in d_8-toluene was added in a single portion to the vial containing **7**, where upon addition, the solution became dark red-brown in color with an orange-brown precipitate. The solution was reacted at -80°C for 1 hour, then brought to -40°C and stirred for an additional 24 hours. The reaction mixture was then transferred to a prechilled NMR tube equipped with a J-Young valve and analyzed by variable temperature ^{1}H NMR spectroscopy (**Figure S50**-**Figure S54**). 1,2 addition of a C–H bond of the $N(SiMe_3)_2$ ligand across the U–N–U bond, was confirmed by ^{1}H NMR spectroscopy, showing resonances of the imido (δ 627.91 ppm) and the methylene protons (δ -138.25 and -153.55 ppm).

The resulting mixture was filtered over a prechilled (-40°C) 0.22 μm porosity filter frit and the brown solution was concentrated and placed at -40°C for crystallization. Over 24 hours, a mixture of pale green and orange crystals suitable for XRD analysis were formed and identified as complexes, **9** and **3-K**, respectively.

S4. General procedure for the formation of NH_3 and $N(SiMe_3)_2$-containing species from HCl.

A NMR tube equipped with a J-Young valve was charged with $K(NSiMe_3)_2$, complexes **3-Cs**, **X**, **7**, or **7-$^{14/15}$N** (0.007 mmol), or the in-situ reaction mixture of complex **X** and **7**. An excess of a 1 M solution of HCl in Et_2O (0.5 mL) was added. The reaction mixture immediately turned colorless with precipitation of solids. After 1 hour, the solvent was removed under vacuum for 8 hours, d_6-DMSO and Me_2SO_2 as an analytical standard were added, and the signal of NH_4Cl and $N(SiMe_3)_2$-containing species was evaluated by quantitative ^{1}H NMR spectroscopy (120s relaxation delay) (**Figure S55**-**Figure S59**). Quantification of the NH_4Cl/$N(SiMe_3)_2$-containing resonances were performed for complexes **3-Cs** (283 %), **X** (275 %), **7** (287 %), **7-$^{14/15}$N** (293 %), and the *in-situ* reaction mixture of **X** and **7** (488 %: ~1.7 increase in the amount of NH_3 generated when compared to the nitride precursors).

S5. NMR Spectroscopy Data

S5.1. NMR spectra for protonolysis studies with complex I.

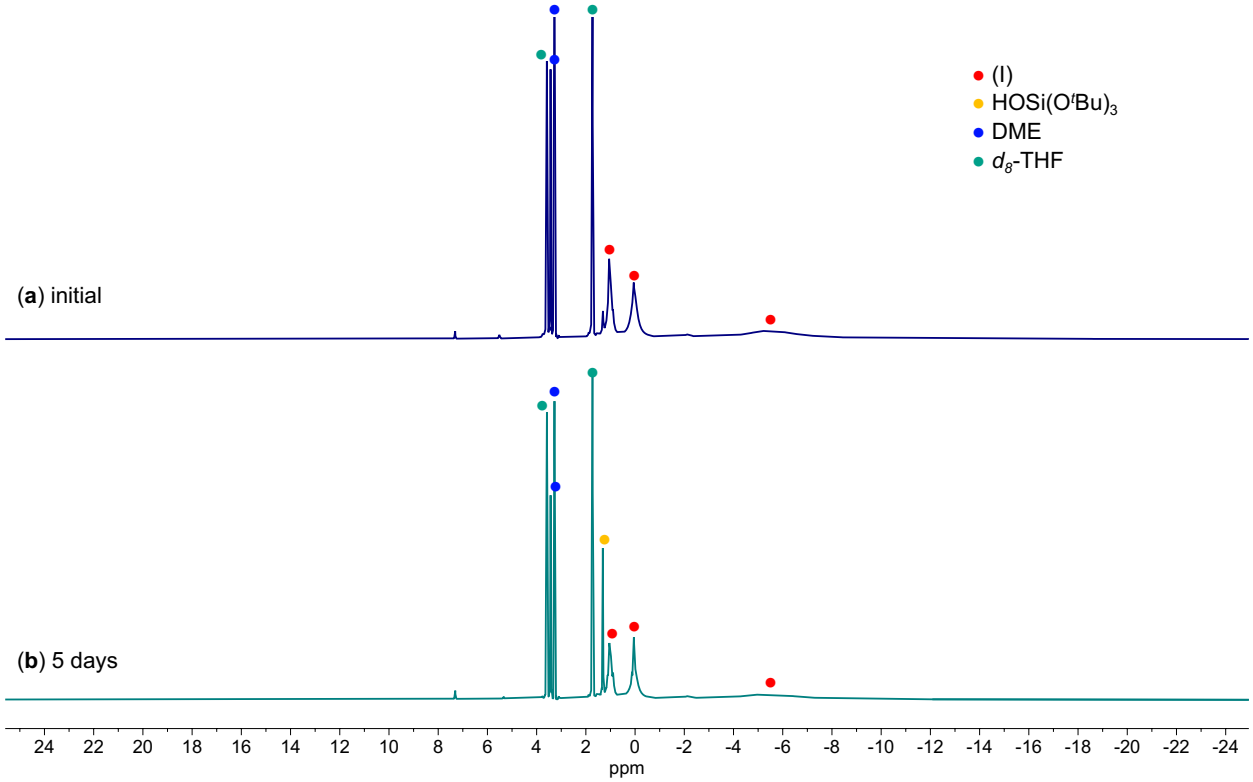

Figure S1. ^{1}H NMR (400 MHz, d_8-THF, 298K) spectra of complex **I** (a) initial, and in the presence of (**b**) 1.0 equiv. HOSi(O^{t}Bu)$_3$ over 5 days.

S5.2. NMR spectra for the synthesis of complex 3-Cs.

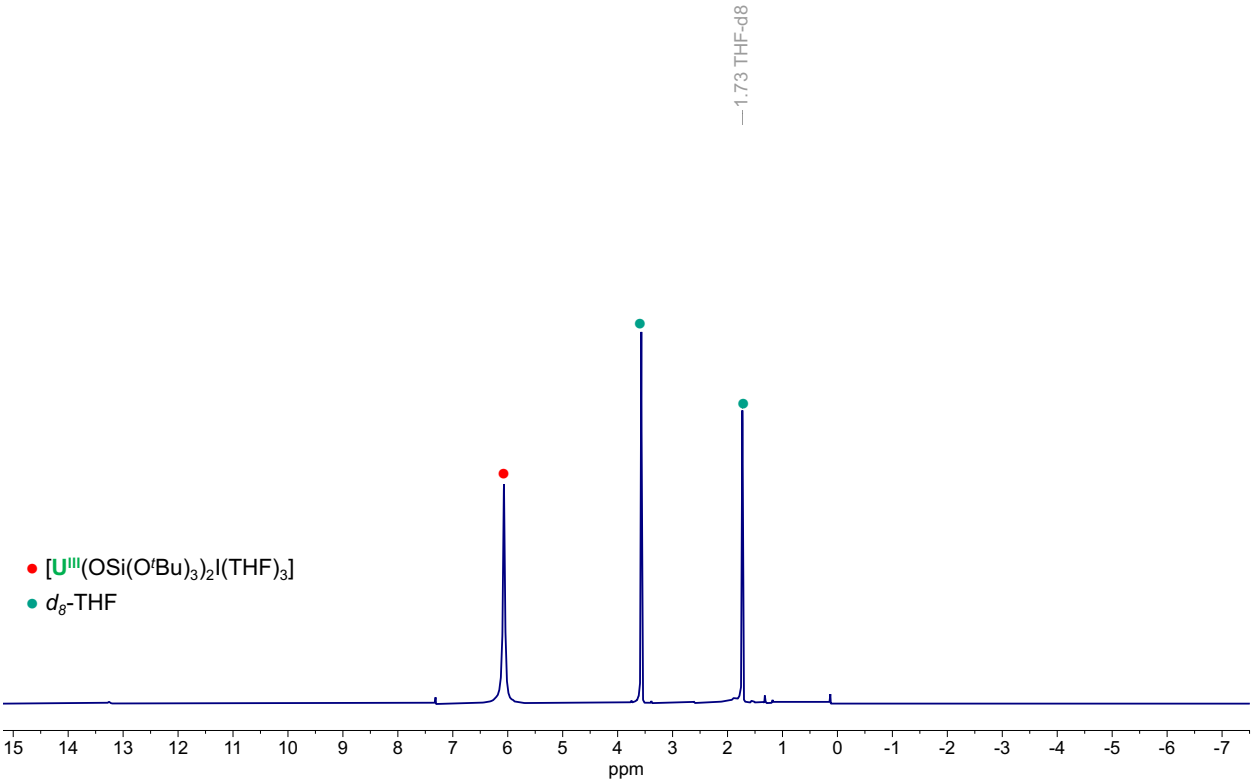

Figure S2. ^{1}H NMR (400 MHz, d_8-THF, 298K) spectra of isolated complex $[U^{III}(OSi(O^tBu)_3)_2I(THF)_3]$.

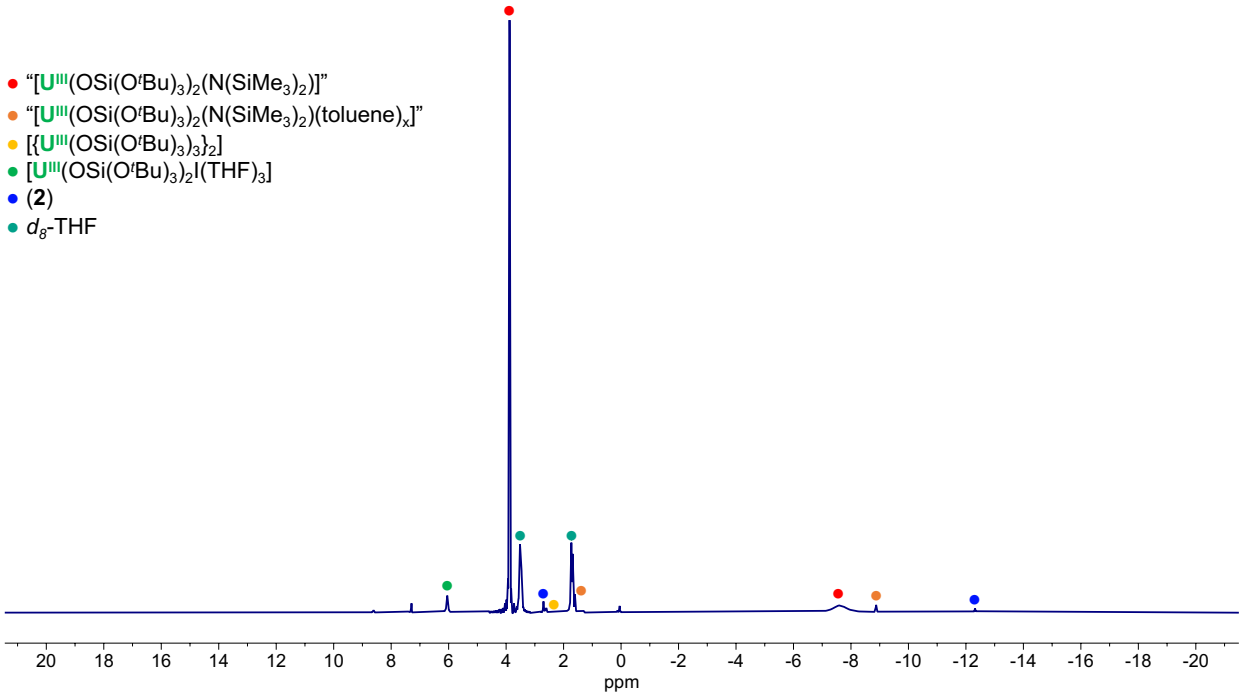

Figure S3. ^{1}H NMR (400 MHz, d_8-THF, 298K) spectra of complex [U^{III}(OSi(O^{t}Bu)$_3$)$_2$I(THF)$_3$] in the presence of 1.0 equiv. KN(SiMe$_3$)$_2$ at -40C, forming a mixture of the major species, "[U^{III}(OSi(O^{t}Bu)$_3$)$_2$(N(SiMe$_3$)$_2$)]", with minor species, "[U^{III}(OSi(O^{t}Bu)$_3$)$_2$(N(SiMe$_3$)$_2$)(toluene)$_x$]", [{U^{III}(OSi(O^{t}Bu)$_3$}$_2$],[9] [U^{III}(OSi(O^{t}Bu)$_3$)$_2$I(THF)$_3$], and **2**.

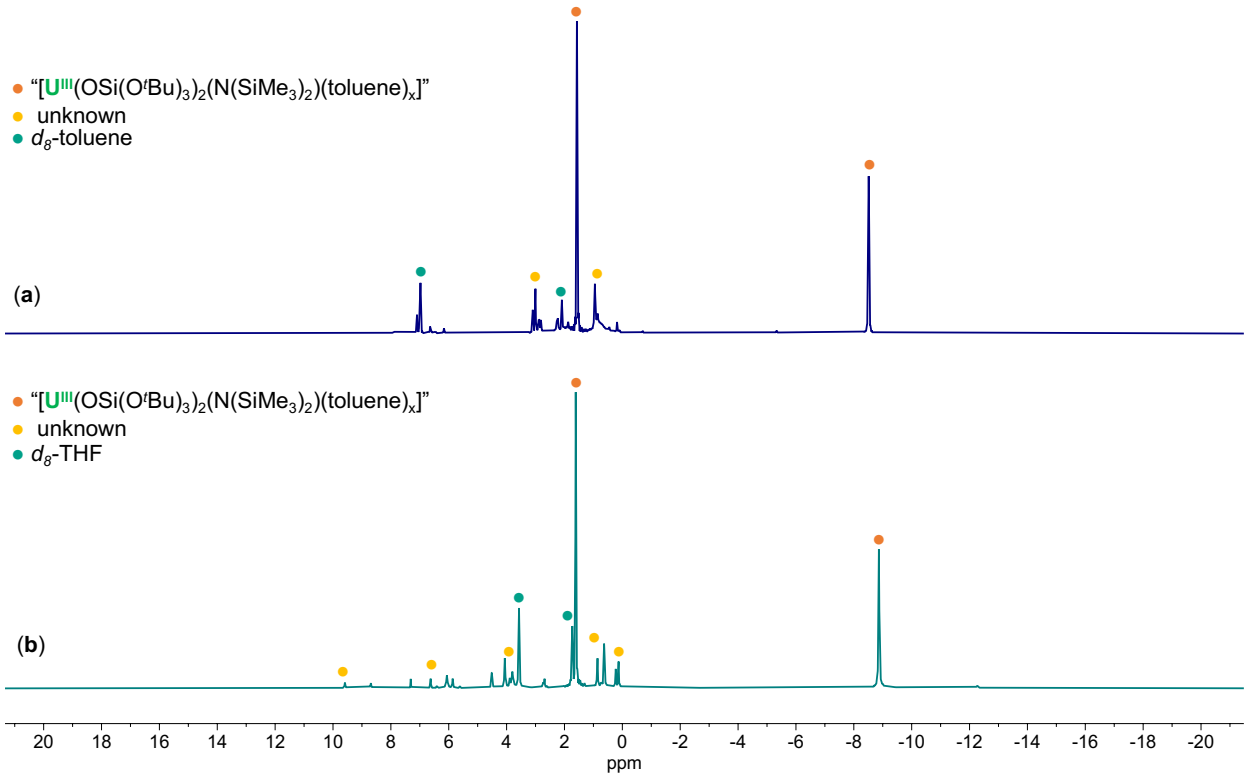

Figure S4. ^{1}H NMR (400 MHz, 298K) spectra of complex [U^{III}(OSi(O^{t}Bu)$_3$)$_2$I(THF)$_3$] in the presence of 1.0 equiv. KN(SiMe$_3$)$_2$ in (**a**) d_8-toluene. The reaction mixture from (**a**) was dried under vacuum and (**b**) dissolved in d_8-THF, forming a mixture of unknown resonances and "[U^{III}(OSi(O^{t}Bu)$_3$)$_2$(N(SiMe$_3$)$_2$)(toluene)$_x$]", as the major species.

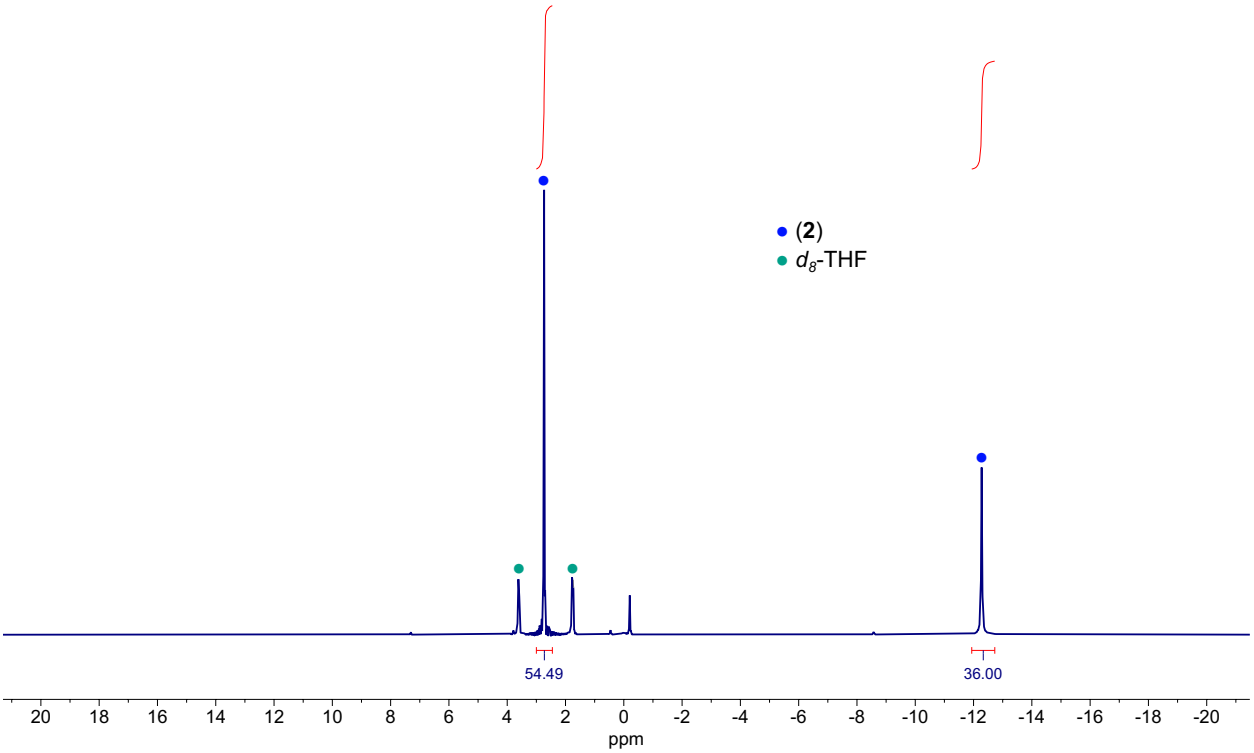

Figure S5. ^{1}H NMR (400 MHz, d_8-THF, 298K) spectrum of complex [U^{III}(OSi(O^{t}Bu)$_3$)$_2$I(THF)$_3$] in the presence of 2.0 equiv. KN(SiMe$_3$)$_2$, forming **2** as the major species.

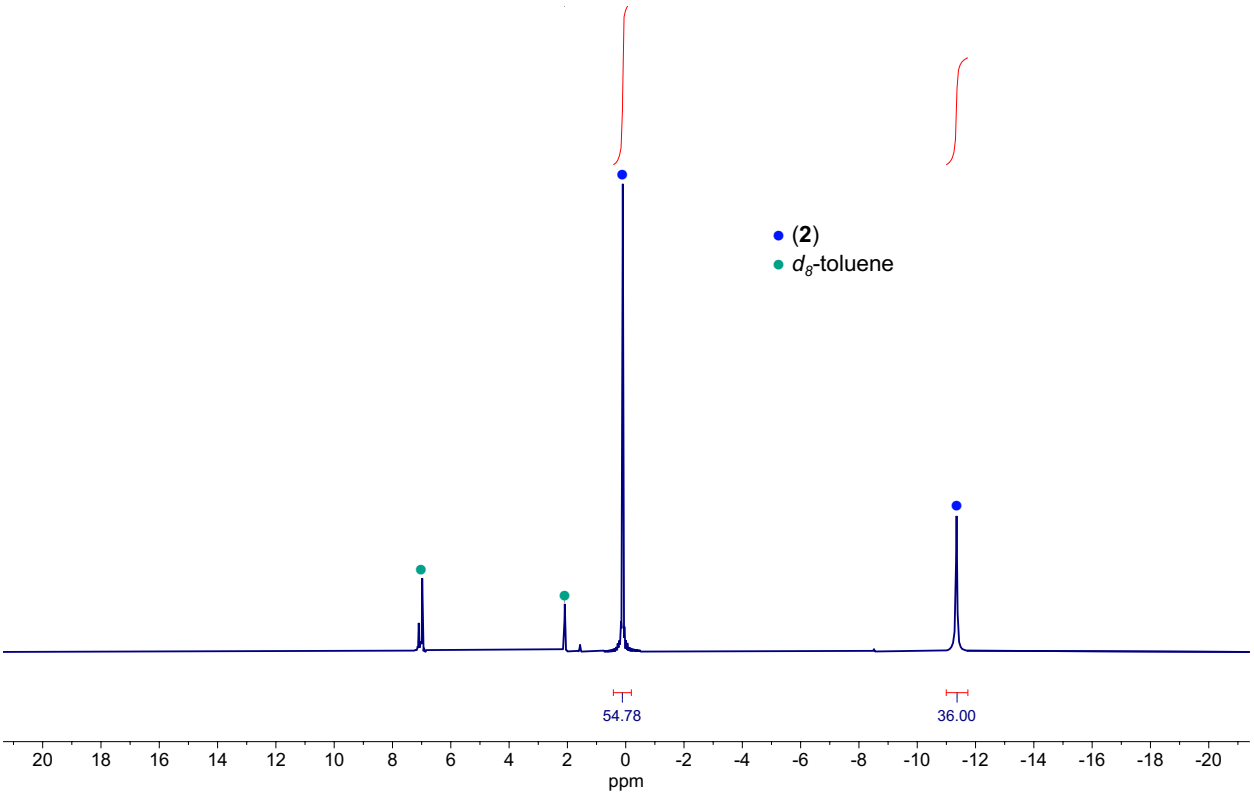

Figure S6. ^{1}H NMR (400 MHz, d_8-toluene, 298K) spectrum of isolated [{U^{III}(OSi(O^{t}Bu)$_3$)$_2$)(N(SiMe$_3$)$_2$)$_2$}K], **2**.

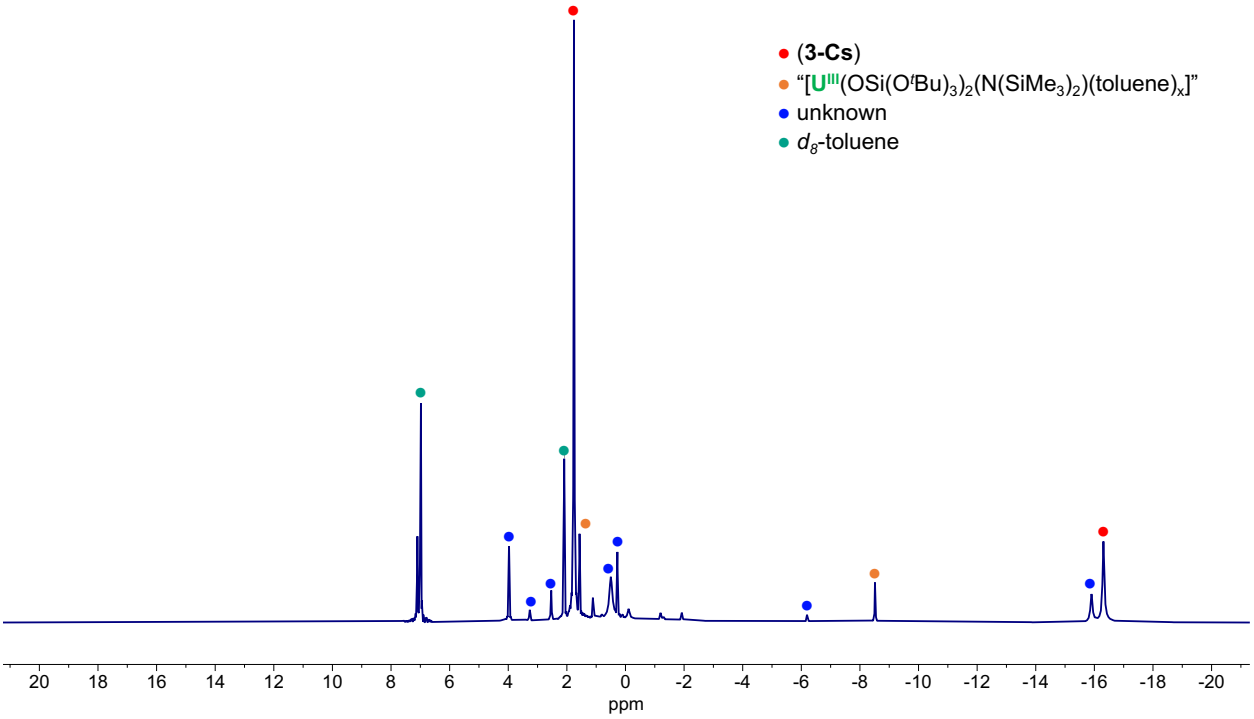

Figure S7. ^{1}H NMR (400 MHz, d_8-toluene, 298K) spectrum of the reaction mixture of *in situ* generated "[U^{III}(OSi(O^{t}Bu)$_3$)$_2$(N(SiMe$_3$)$_2$)]", in the presence of 0.5 equiv. CsN_3 in Et_2O after 4 days at -40°C, generating a mixture of species with **3-Cs** as the major product. Analytically pure **3-Cs** can be isolated from a concentrated hexanes or Et_2O solution at -40°C (*vide supra*, **Figure S12**).

S5.3. NMR spectra for isolated heteroleptic complexes.

S5.3.1. U(IV)/U(IV) heteroleptic complexes, 1, 3-Cs, and 3b-Cs.

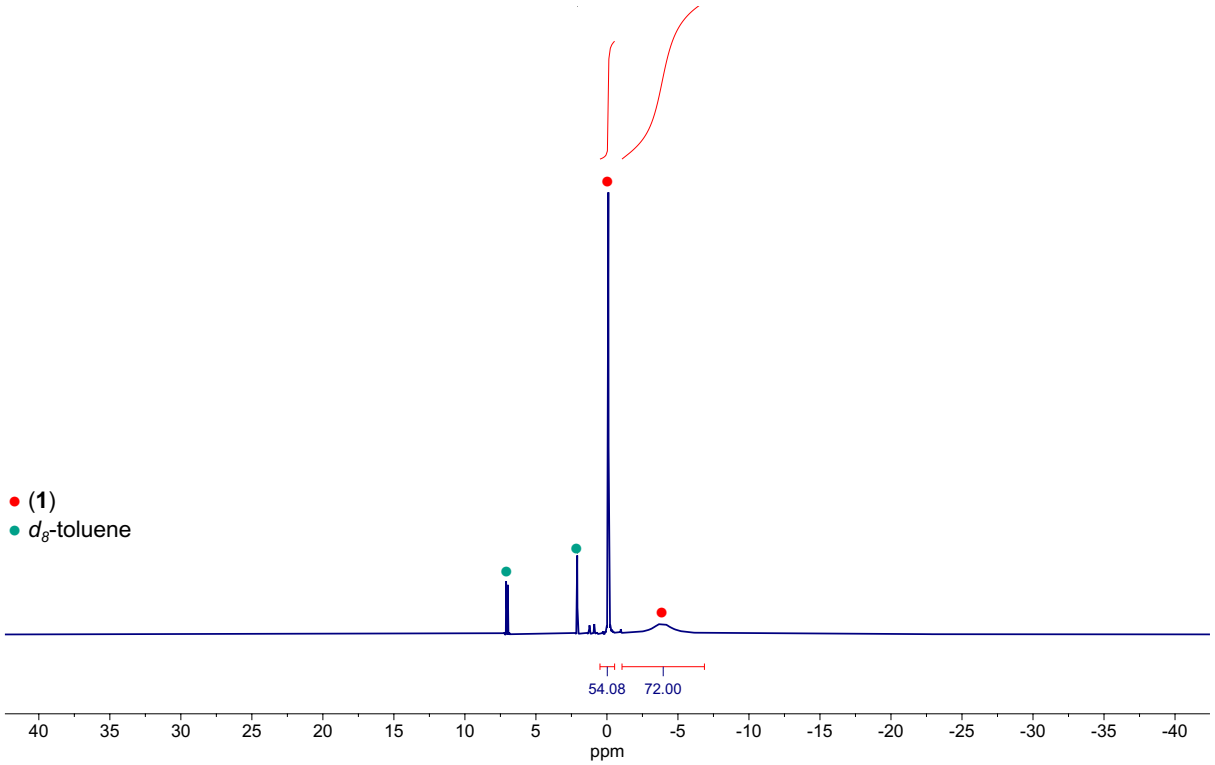

Figure S8. ^{1}H NMR (400 MHz, d_8-toluene, 298K) spectrum of [K{U^{IV}(OSi(O^{t}Bu)$_3$)(N(SiMe$_3$)$_2$)$_2$}$_2$(μ-N)], **1**.

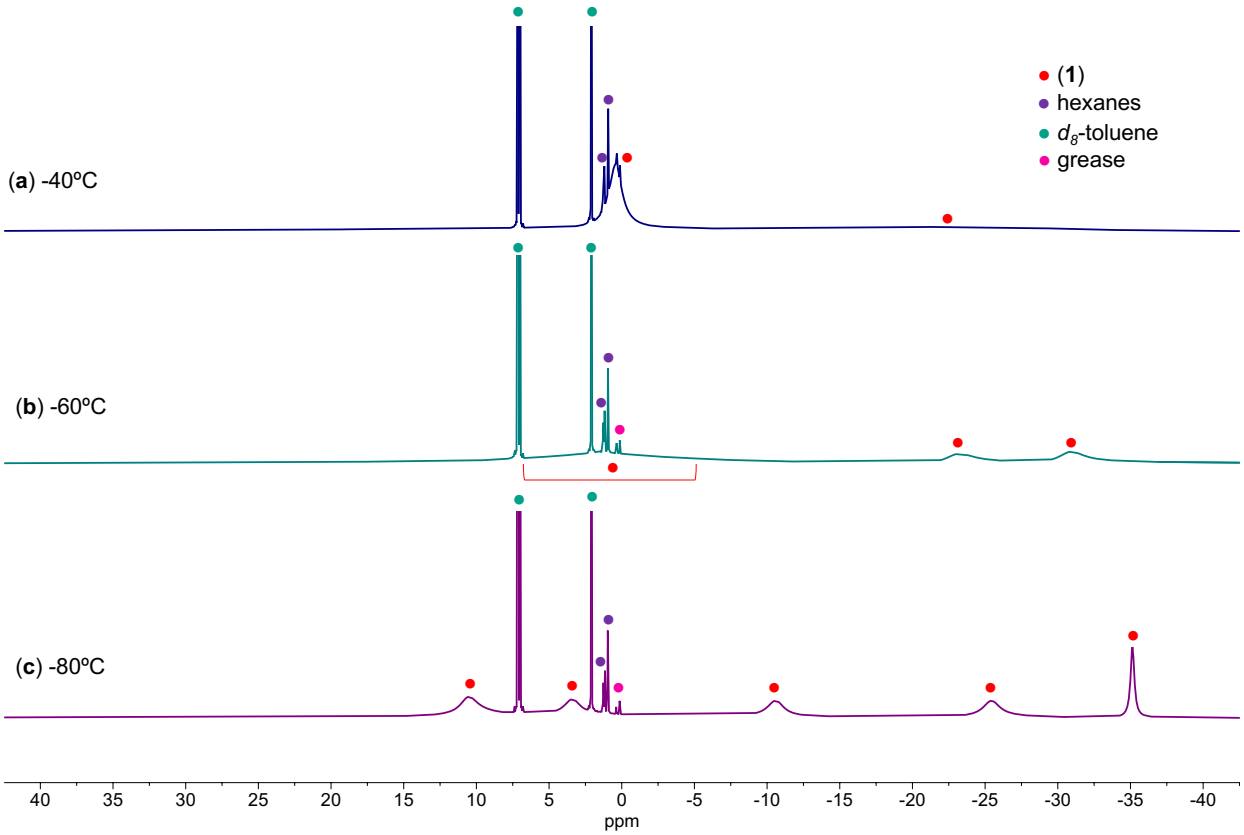

Figure S9. Variable temperature ^{1}H NMR (400 MHz, d_8-toluene, (**a**) 233K, (**b**) 213K, and (**c**) 193K) spectra of $[K\{U^{IV}(OSi(O^tBu)_3)(N(SiMe_3)_2)_2\}_2(\mu\text{-}N)]$, **1**.

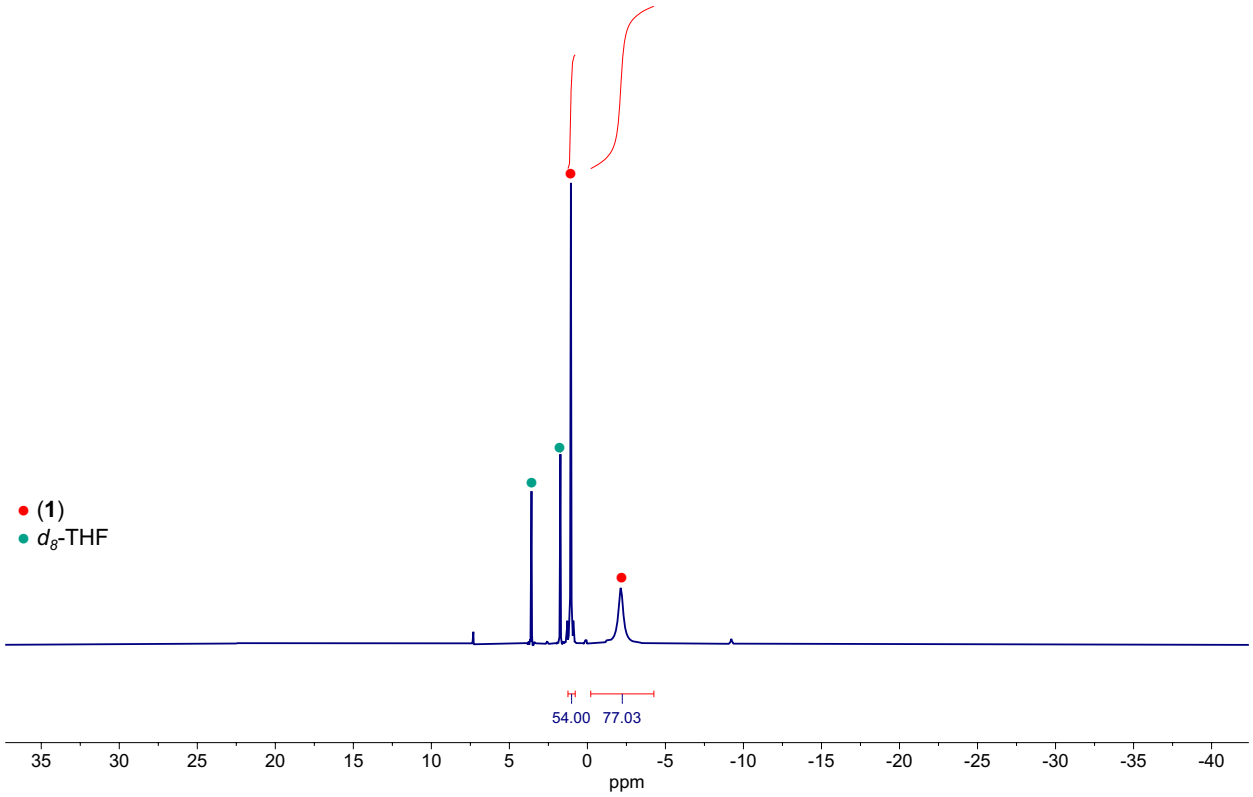

Figure S10. ^{1}H NMR (400 MHz, d_8-THF, 298K) spectra of [K{U^{IV}(OSi(O^{t}Bu)$_3$)(N(SiMe$_3$)$_2$)$_2$}$_2$(μ-N)], **1**.

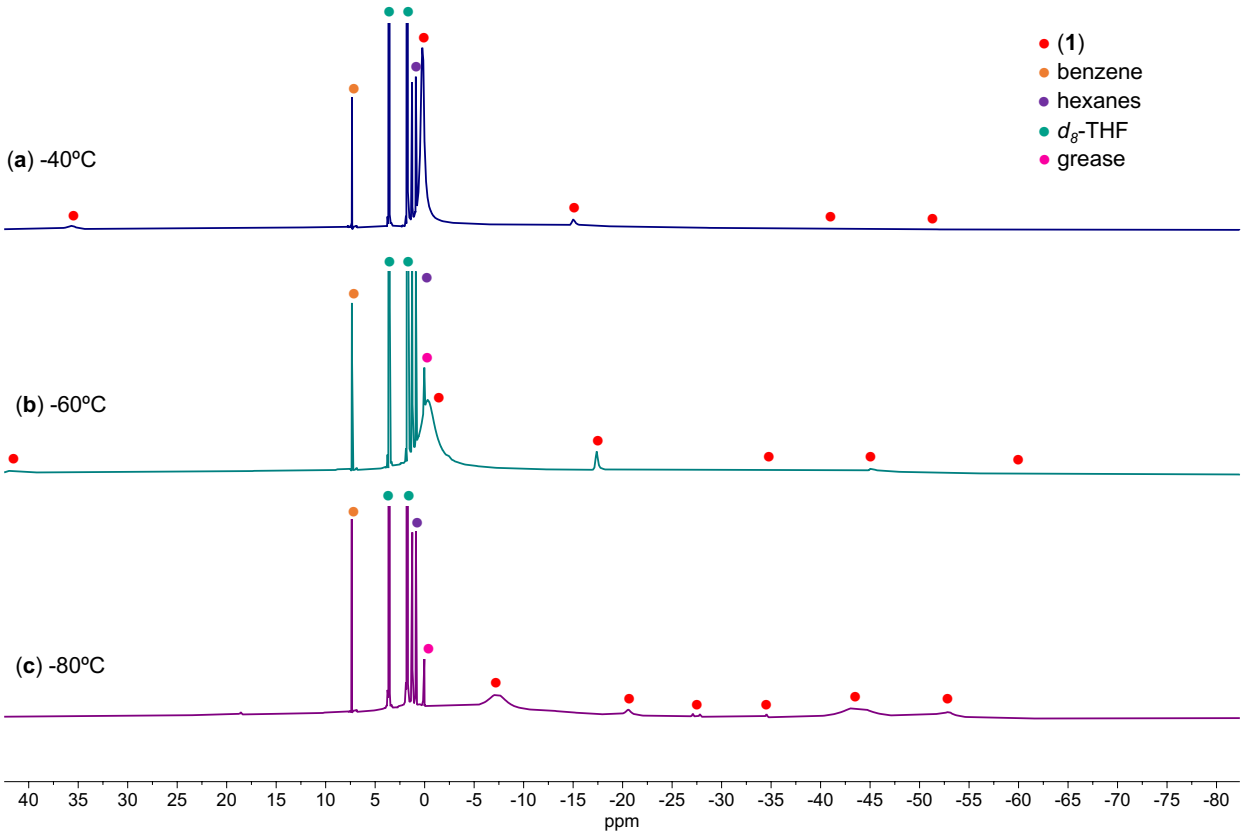

Figure S11. Variable temperature ^{1}H NMR (400 MHz, d_8-THF, (**a**) 233K, (**b**) 213K, and (**c**) 193K) spectra of $[K\{U^{IV}(OSi(O^tBu)_3)(N(SiMe_3)_2)_2\}_2(\mu\text{-}N)]$, **1**.

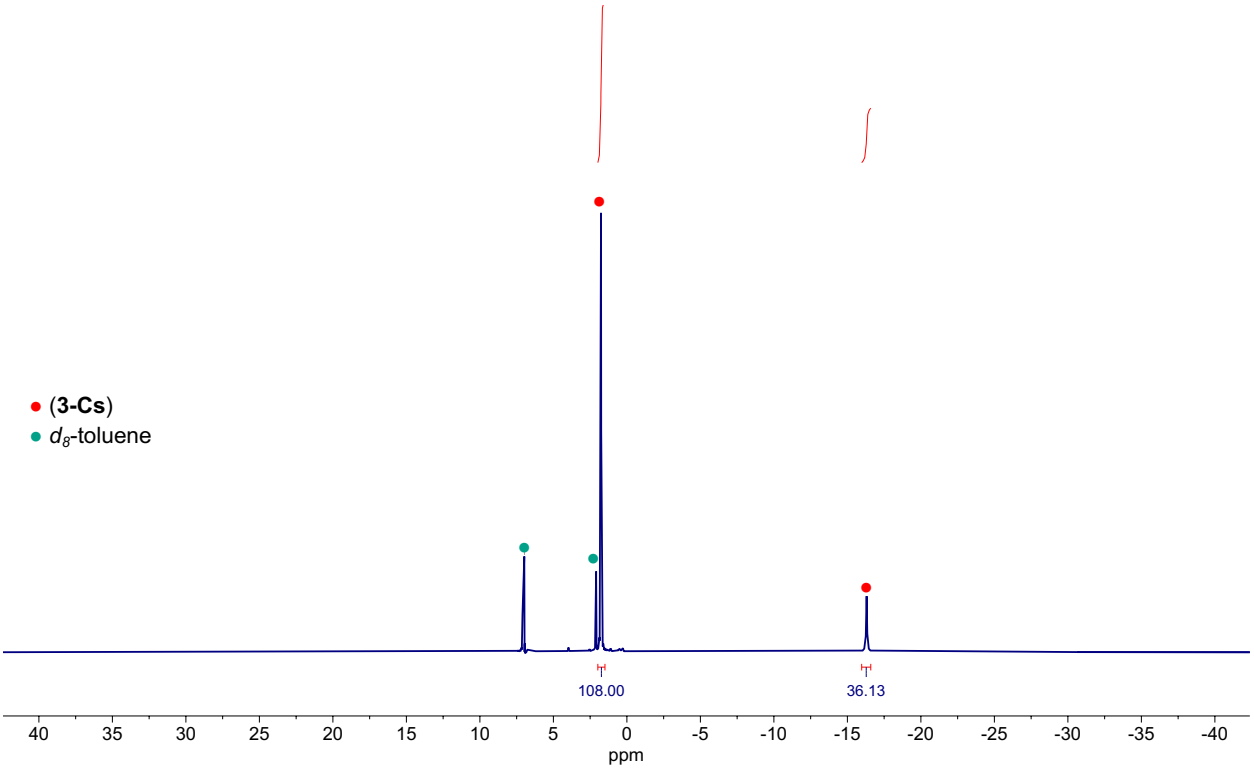

Figure S12. ^{1}H NMR (400 MHz, d_8-toluene, 298K) spectrum of [Cs{U^{IV}(OSi(O^{t}Bu)$_3$)$_2$(N(SiMe$_3$)$_2$)}$_2$(μ-N)], **3-Cs**.

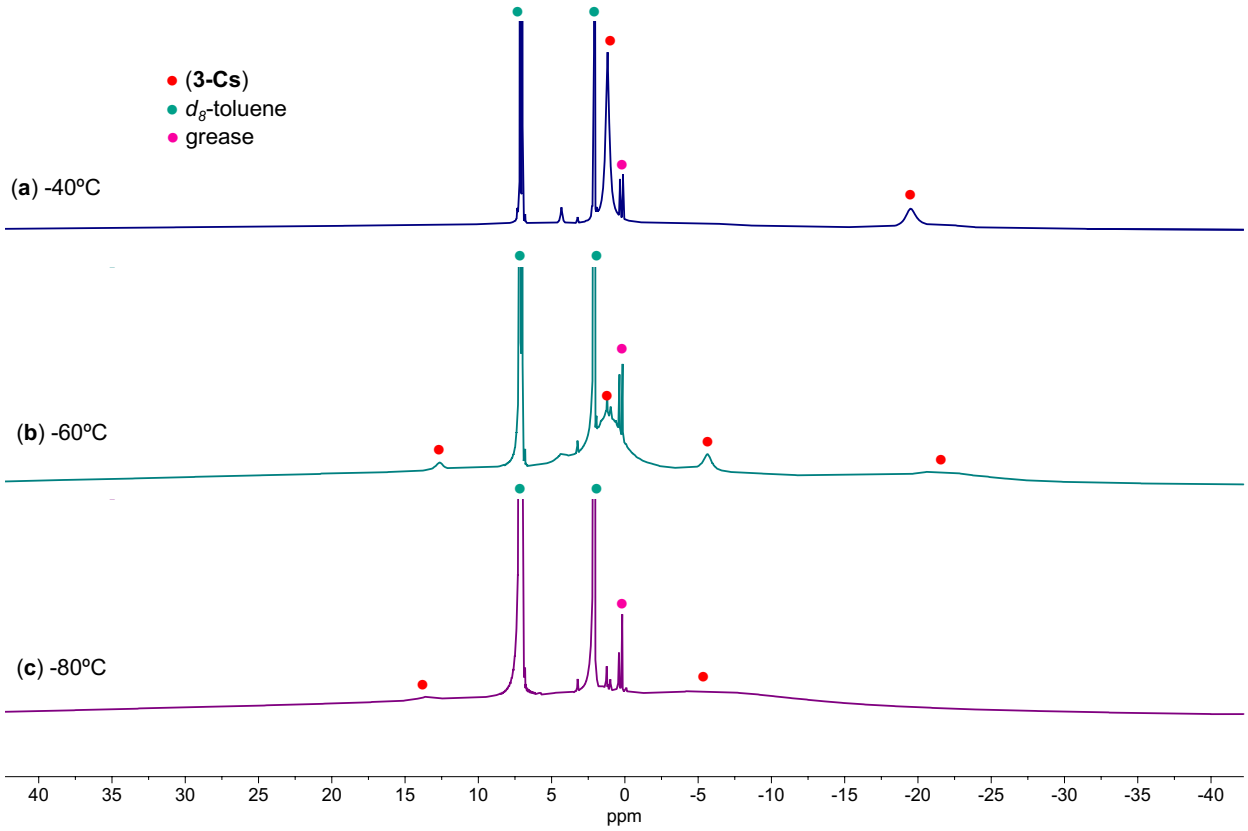

Figure S13. Variable temperature ^{1}H NMR (400 MHz, d_8-toluene, (**a**) 233K, (**b**) 213K, and (**c**) 193K) spectra of $[Cs\{U^{IV}(OSi(O^tBu)_3)_2(N(SiMe_3)_2)\}_2(\mu\text{-}N)]$, **3-Cs**. No decomposition is observed at -40°C.

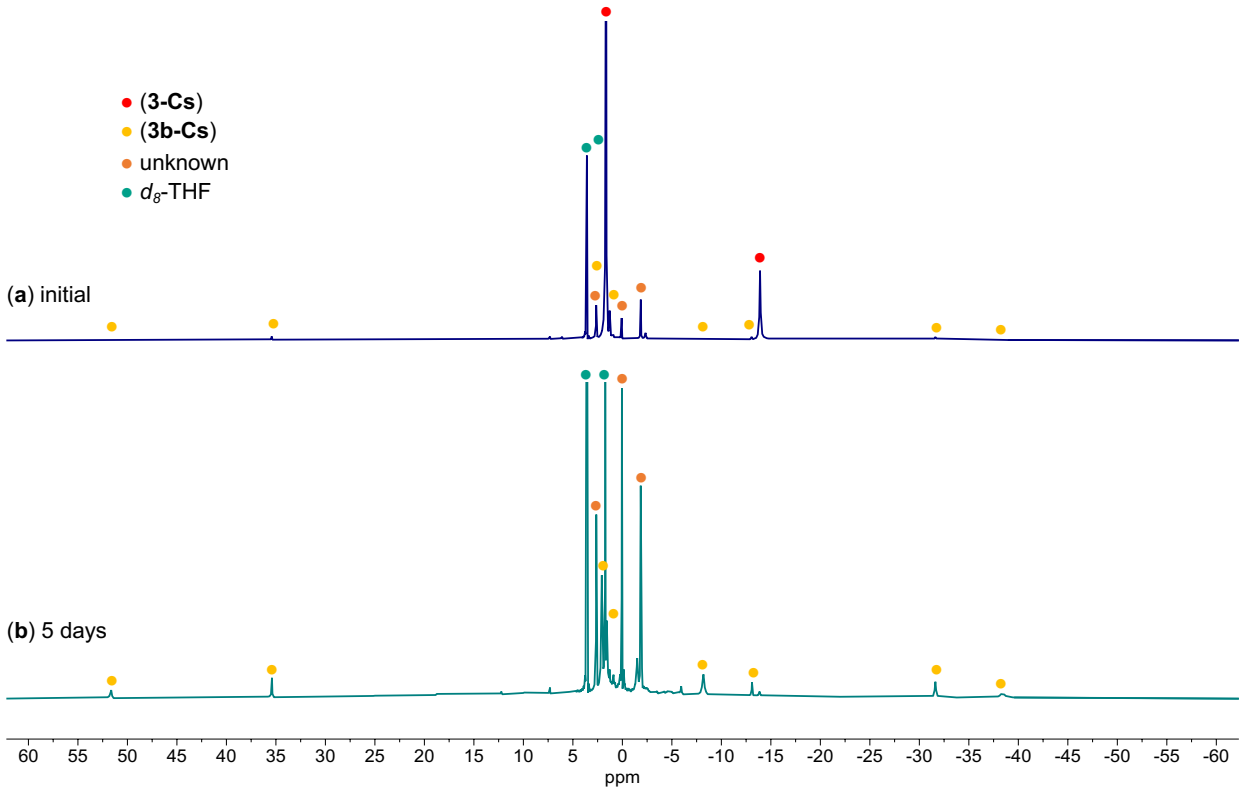

Figure S14. ^{1}H NMR (400 MHz, d_8-THF, 298K) spectra of [Cs{U^{IV}(OSi(O^{t}Bu)$_3$)$_2$(N(SiMe$_3$)$_2$)}$_2$(μ-N)], **3-Cs** after (**a**) 10 minutes and (**b**) 5 days at room temperature.

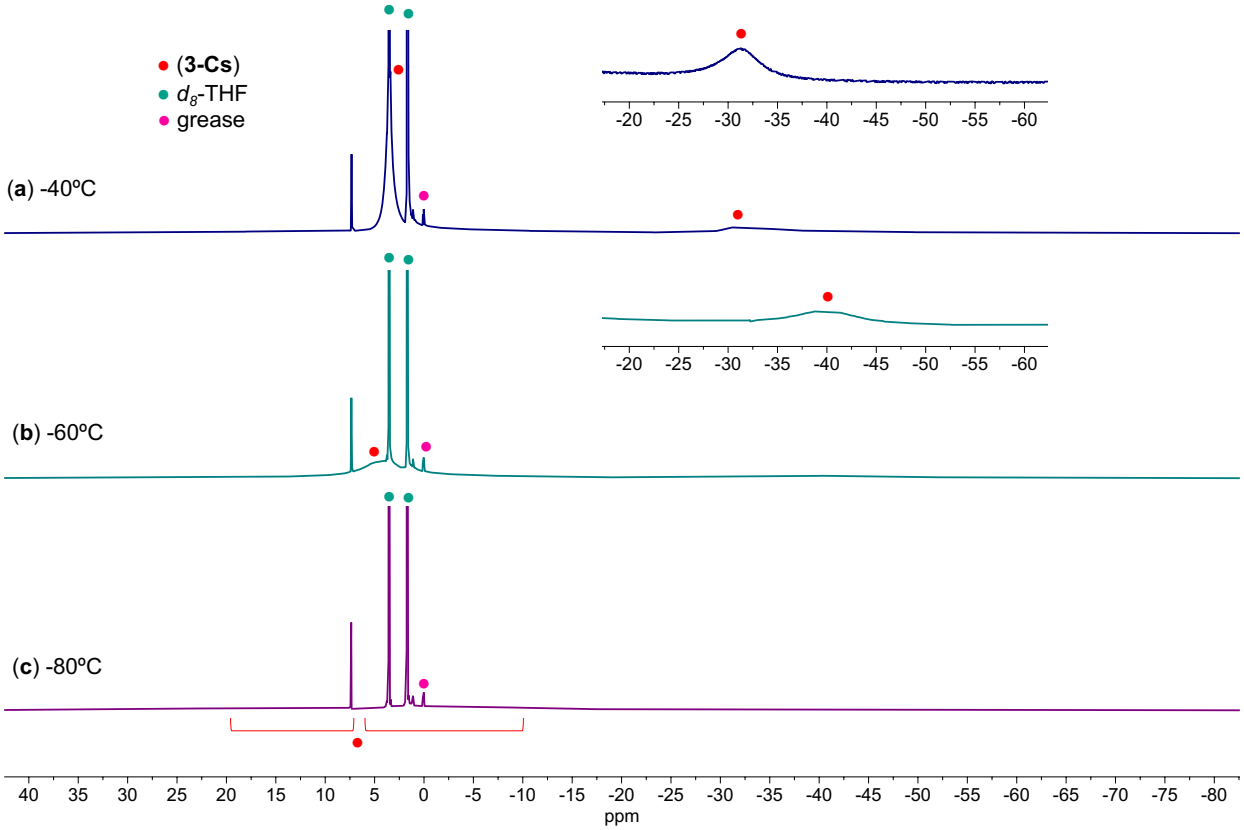

Figure S15. Variable temperature ^{1}H NMR (400 MHz, d_8-THF, (**a**) 233K, (**b**) 213K, and (**c**) 193K) spectra of [Cs{U^{IV}(OSi(O^{t}Bu)$_3$)$_2$(N(SiMe$_3$)$_2$)}$_2$(μ-N)], **3-Cs**, after 15 mins at -80°C. Decomposition is observed over 24 hours at -40°C.

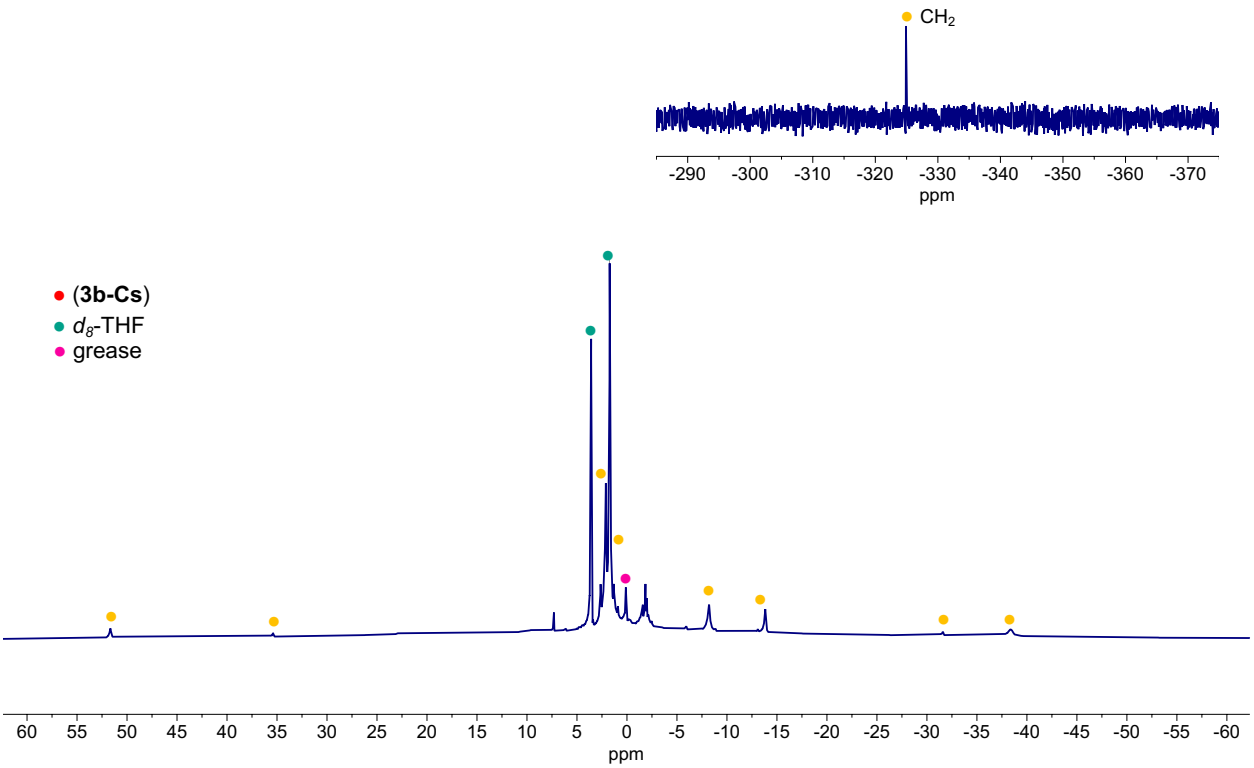

Figure S16. ^{1}H NMR (400 MHz, d_8-THF, 298K) spectrum of [Cs{(OSi(O^{t}Bu)$_3$)$_3$U^{IV}}(μ-NH)(*μ*-κ^2*:C,N*–CH$_2$SiMe$_2$NSiMe$_3$)-{U^{IV}(N(SiMe$_3$)$_2$)(OSi(O^{t}Bu)$_3$)}], **3b-Cs**.

S5.3.2. U(III)/U(IV) heteroleptic complexes, 4, 5, 6-K, 6-Cs.

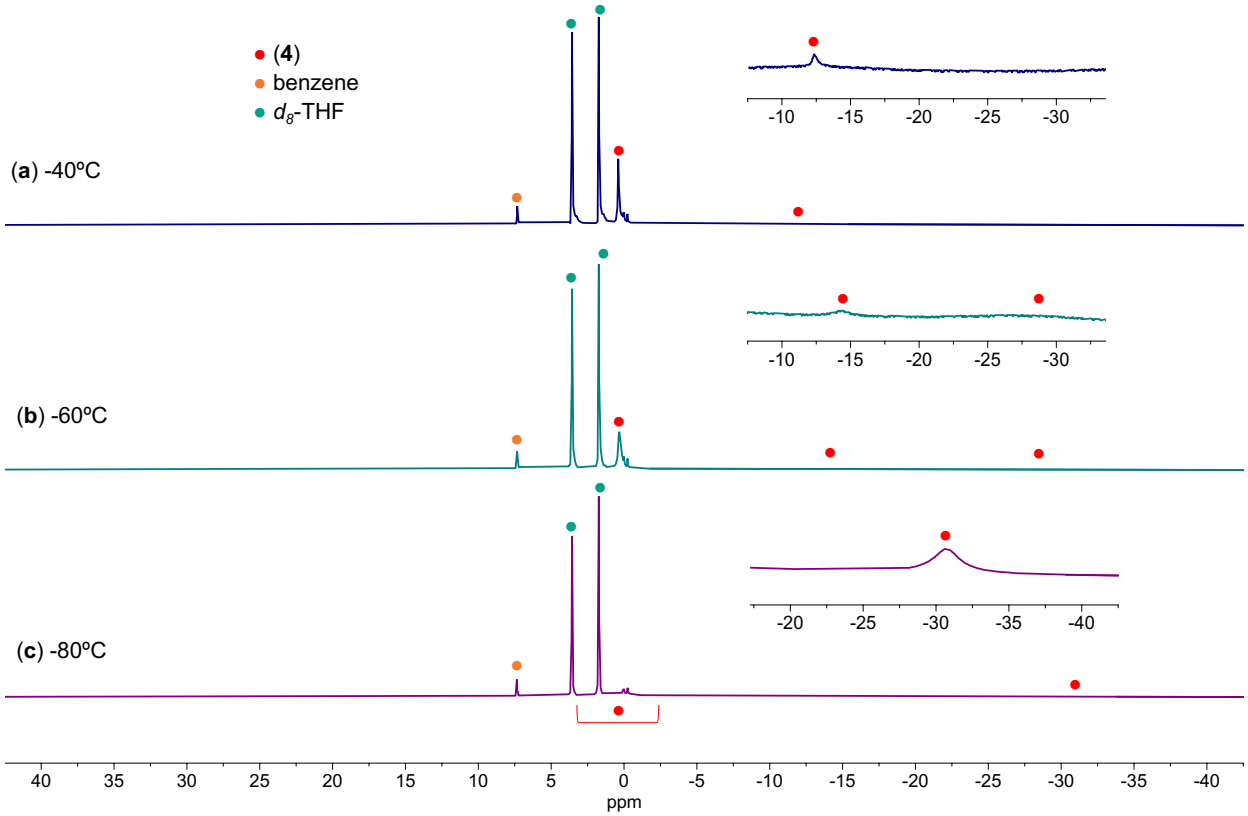

Figure S17. Variable temperature ^{1}H NMR (400 MHz, d_8-THF, (**a**) 233K, (**b**) 213K, and (**c**) 193K) spectra of $[K\{U^{III/IV}(OSi(O^tBu)_3)(N(SiMe_3)_2)_2\}_2(\mu\text{-}N)][K(THF)_6]$, **4**, after 15 minutes at -40°C. Slight decomposition is observed over 24 hours at -40°C (**Figure S18**).

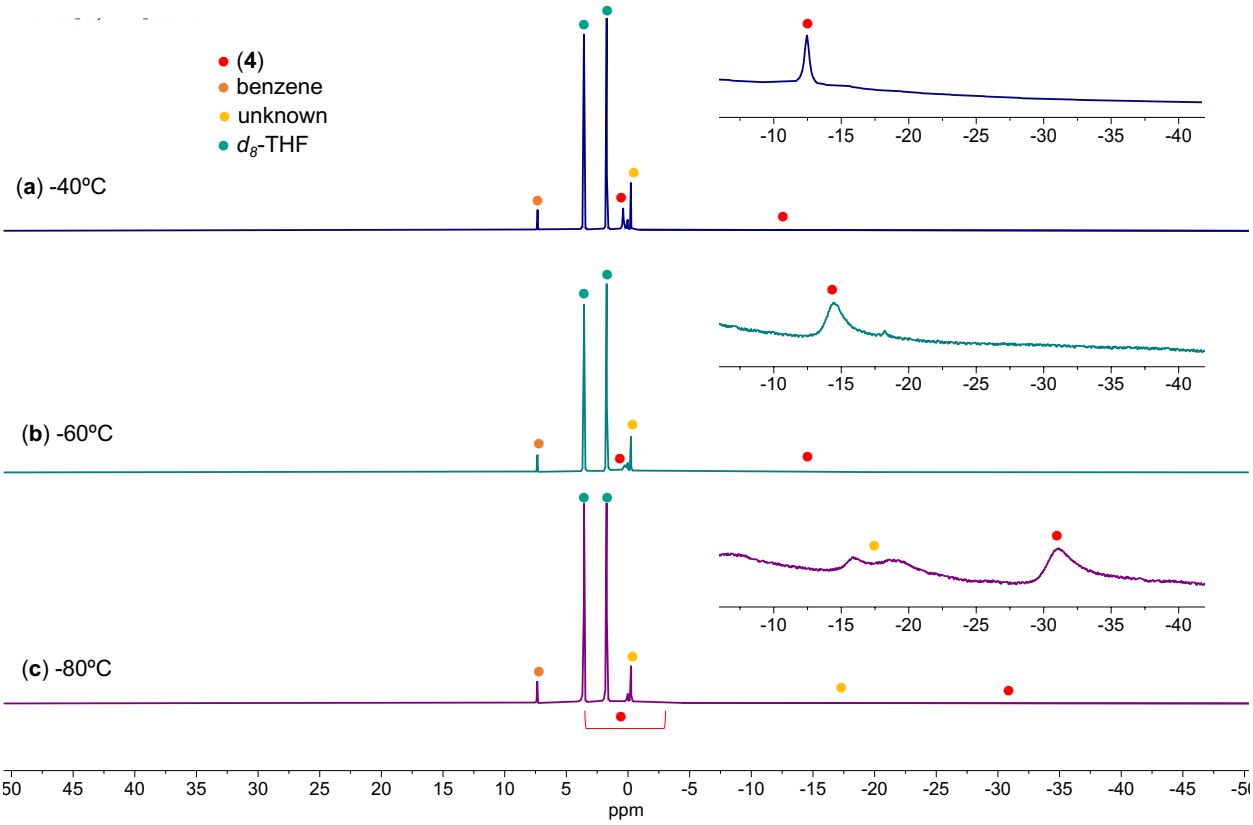

Figure S18. Variable temperature ^{1}H NMR (400 MHz, d_8-THF, (**a**) 233K, (**b**) 213K, and (**c**) 193K) spectra of $[K\{U^{III/IV}(OSi(O^tBu)_3)(N(SiMe_3)_2)_2\}_2(\mu\text{-}N)][K(THF)_6]$, **4**, after 24 hours at -40°C.

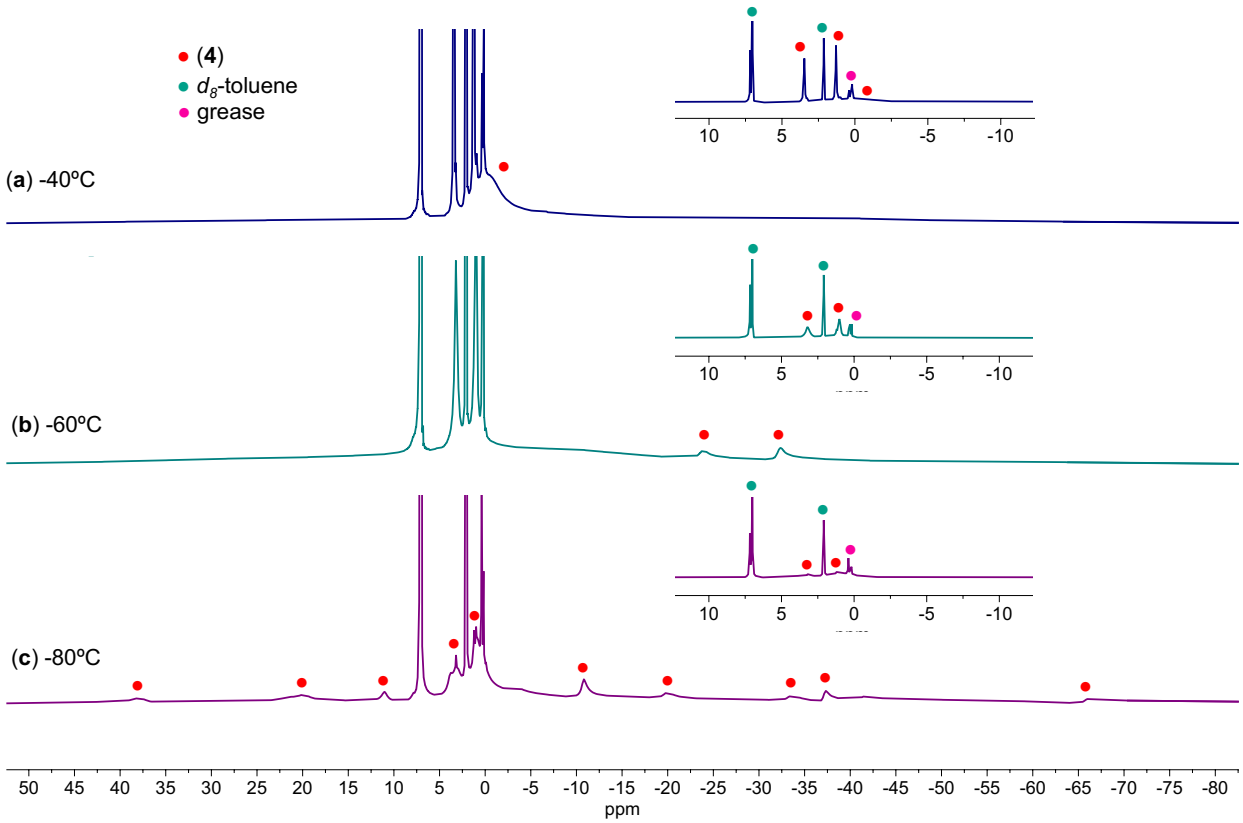

Figure S19. Variable temperature ^{1}H NMR (400 MHz, d_8-toluene, (**a**) 233K, (**b**) 213K, and (**c**) 193K) spectra of $[K\{U^{III/IV}(OSi(O^tBu)_3)(N(SiMe_3)_2)_2\}_2(\mu\text{-}N)][K(THF)_6]$, **4**, after 15 minutes at -40°C. Decomposition is observed over 24 hours at -40°C (**Figure S20**).

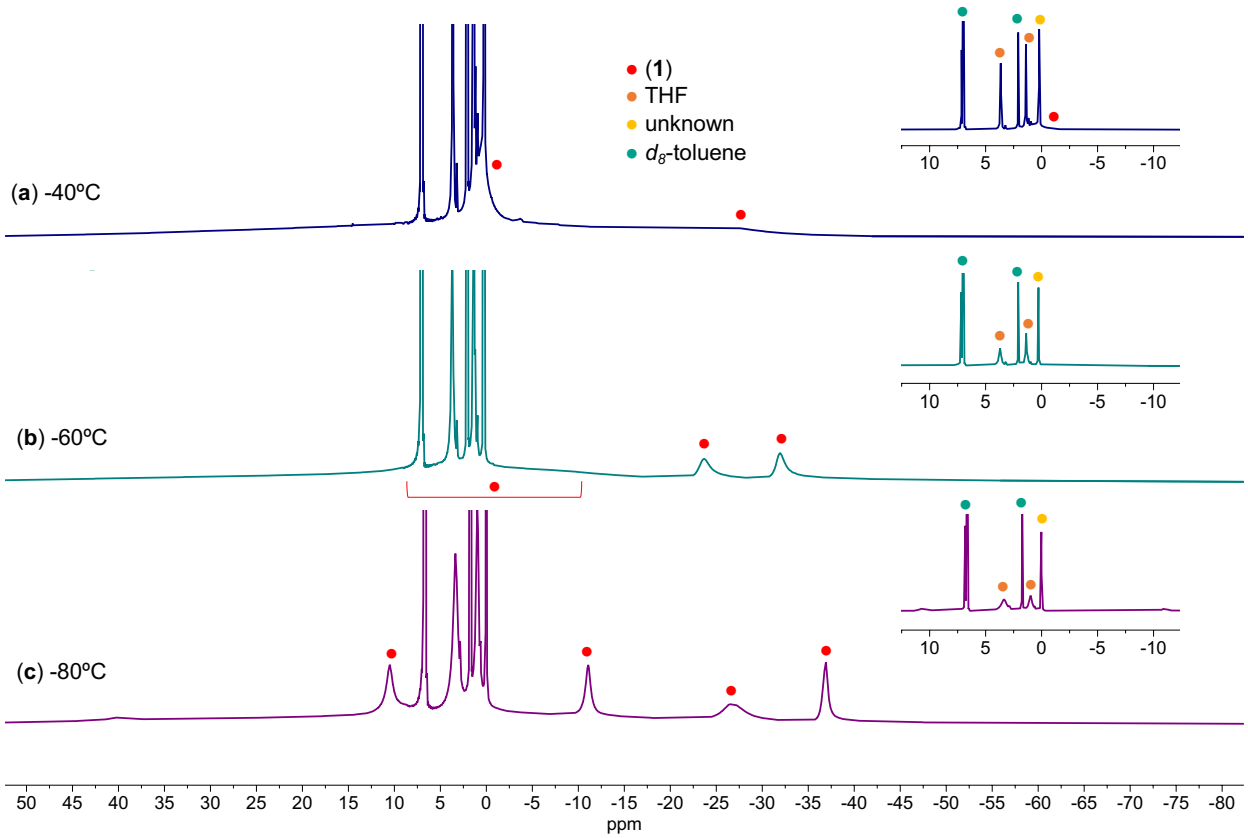

Figure S20. Variable temperature ^{1}H NMR (400 MHz, d_8-toluene, (**a**) 233K, (**b**) 213K, and (**c**) 193K) spectra of [K{$U^{III/IV}$(OSi(O^{t}Bu)$_3$)(N(SiMe$_3$)$_2$)$_2$}$_2$(μ-N)][K(THF)$_6$], **4**, after 24 hours at -40°C, resulting in full conversion to the U(IV)/U(IV) complex, **1**.

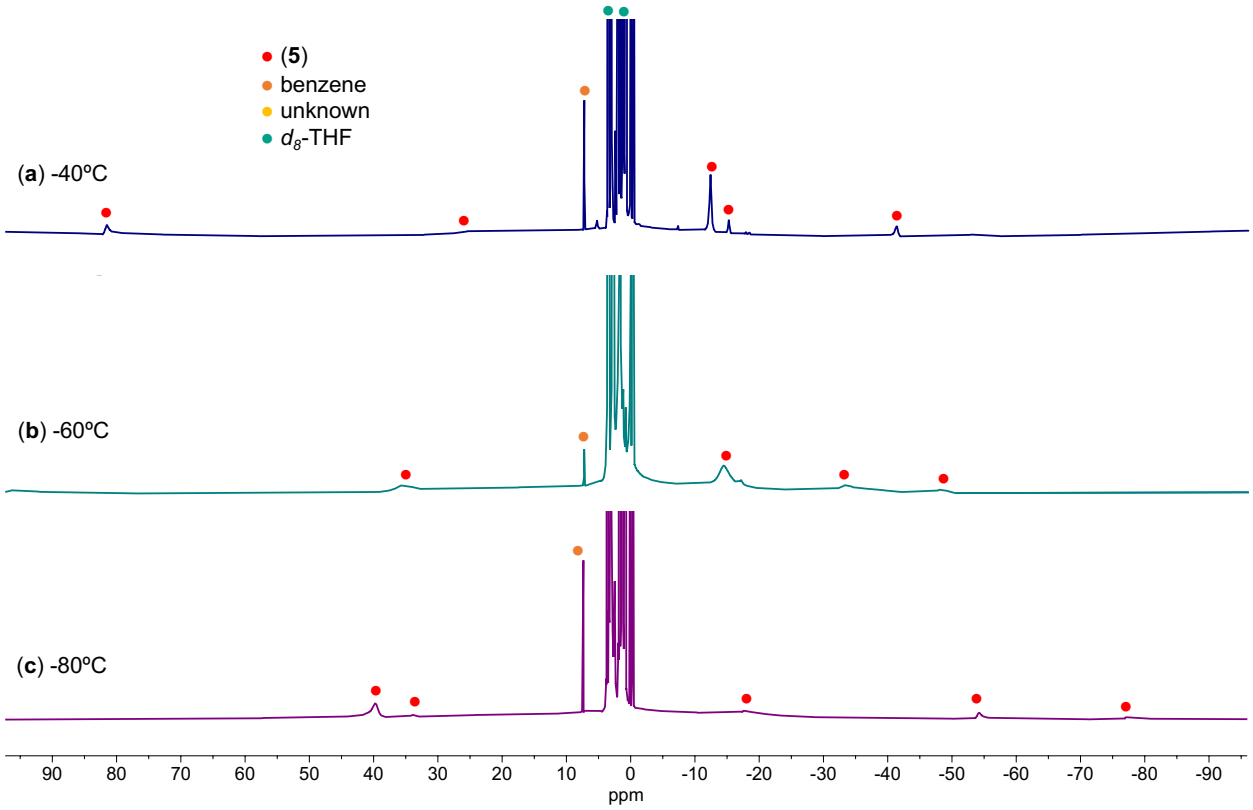

Figure S21. Variable temperature ^{1}H NMR (400 MHz, d_8-THF, (**a**) 233K, (**b**) 213K, and (**c**) 193K) spectra of $[((Me_3Si)_2N)_2U^{IV}(OSi(O^tBu)_3)(\mu\text{-NH})(\mu\text{-}\kappa^2\text{:}C,N\text{–}CH_2SiMe_2NSiMe_3)\text{-}U^{III}(N(SiMe_3)_2)(OSi(O^tBu)_3)][\{K(2.2.2\text{-cryptand})\}_2]$, **5**.

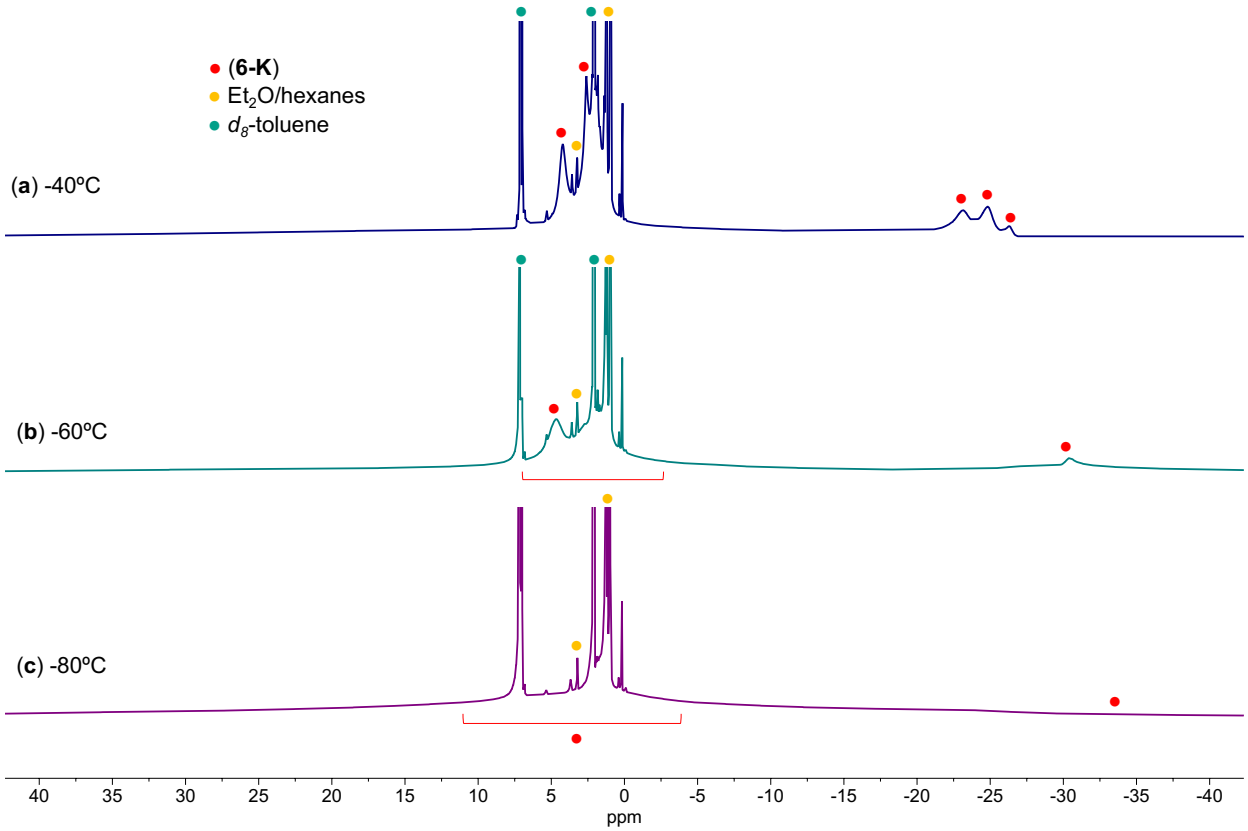

Figure S22. Variable temperature ^{1}H NMR (400 MHz, d_8-toluene, (**a**) 233K, (**b**) 213K, and (**c**) 193K) spectra of $[K_2\{U^{IV/III}(OSi(O^tBu)_3)_2(N(SiMe_3)_2)\}_2(\mu\text{-}N)]$, **6-K**, after 15 minutes at -80°C. No decomposition is observed at -40°C.

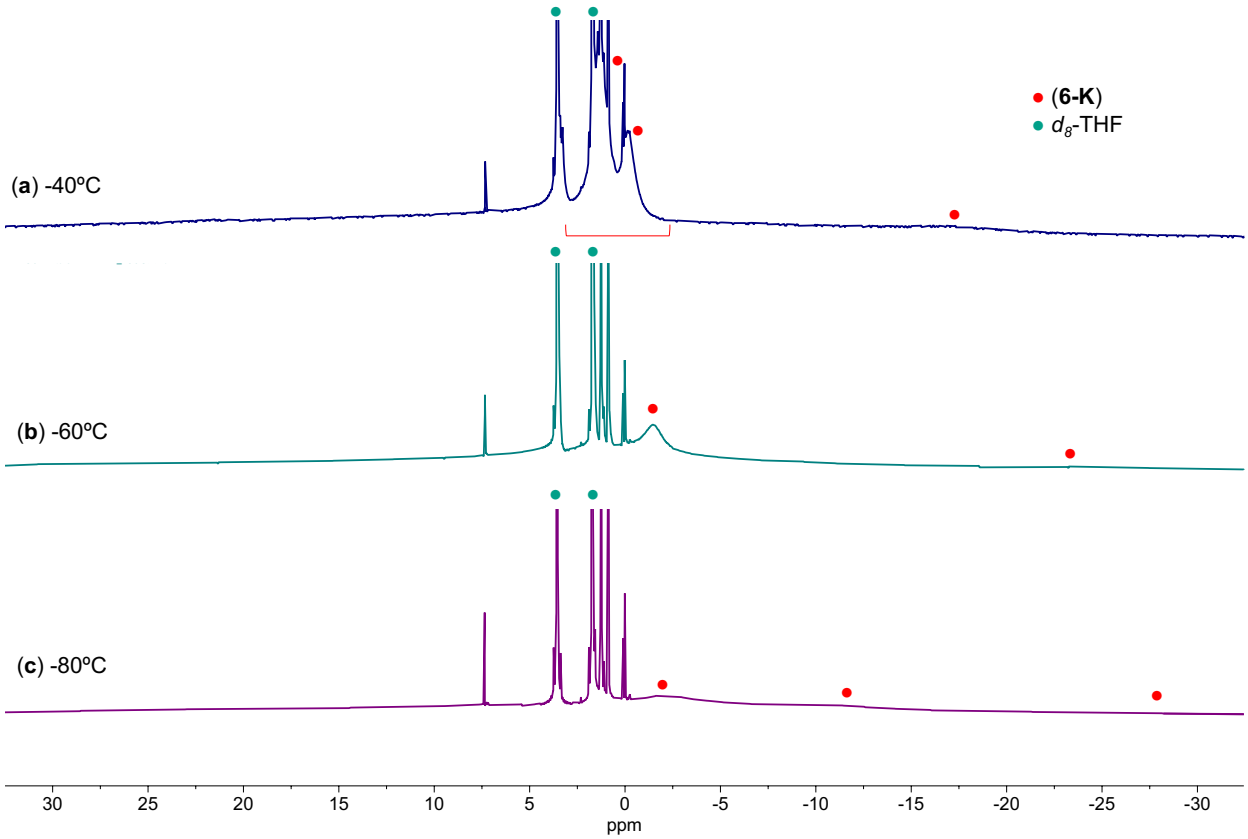

Figure S23. Variable temperature ^{1}H NMR (400 MHz, d_8-THF, (**a**) 233K, (**b**) 213K, and (**c**) 193K) spectra of $[K_2\{U^{IV/III}(OSi(O^tBu)_3)_2(N(SiMe_3)_2)\}_2(\mu\text{-}N)]$, **6-K**, after 15 minutes at -80°C. Decomposition and full consumption of **6-K** over 24 hours is observed at -40°C to unidentifiable species.

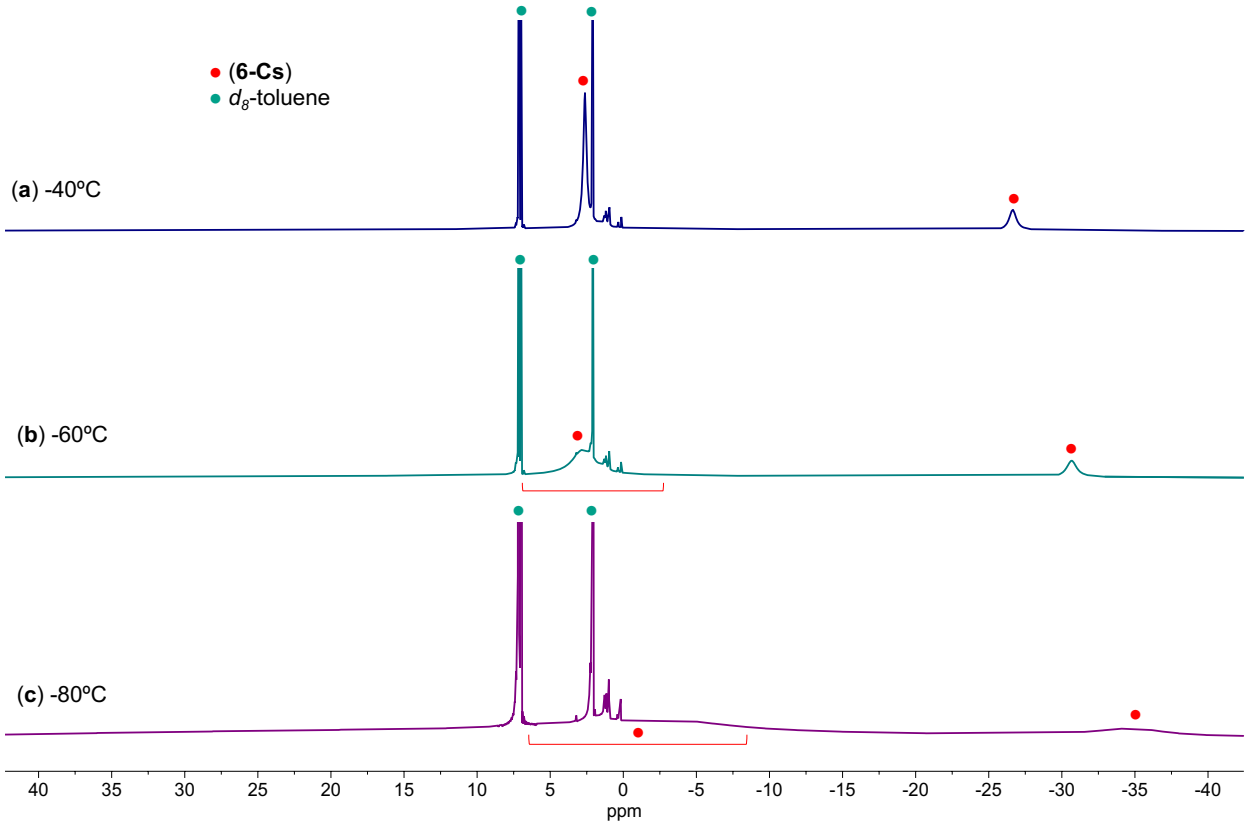

Figure S24. Variable temperature ^{1}H NMR (400 MHz, d_8-toluene, (**a**) 233K, (**b**) 213K, and (**c**) 193K) spectra of $[Cs_2\{U^{IV/III}(OSi(O^tBu)_3)_2(N(SiMe_3)_2)\}_2(\mu\text{-}N)]$, **6-Cs**, after 15 minutes at -80°C. No decomposition is observed at -40°C.

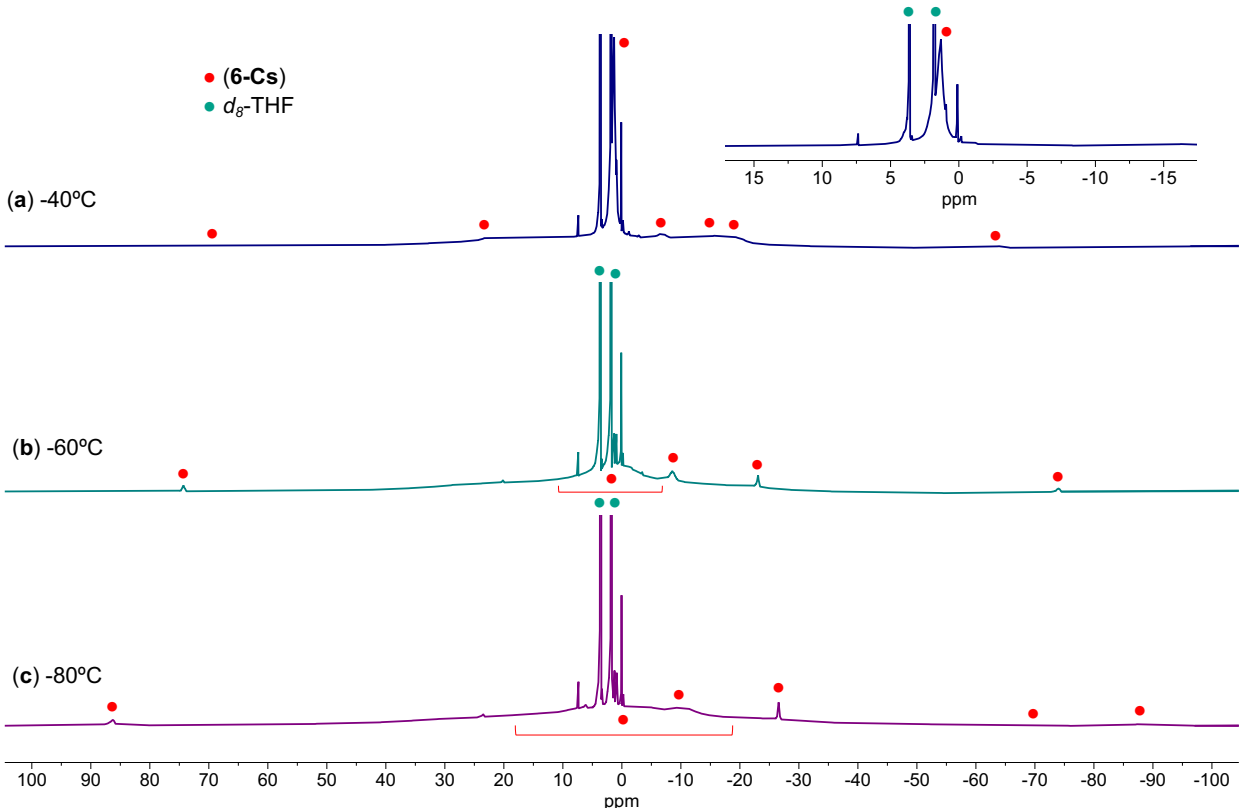

Figure S25. Variable temperature ^{1}H NMR (400 MHz, d_8-THF, (**a**) 233K, (**b**) 213K, and (**c**) 193K) spectra of $[Cs_2\{U^{IV/III}(OSi(O^tBu)_3)_2(N(SiMe_3)_2)\}_2(\mu\text{-}N)]$, **6-Cs**, after 15 minutes at -80°C. Slight decomposition is observed at -40°C after 24 hours (**Figure S26**).

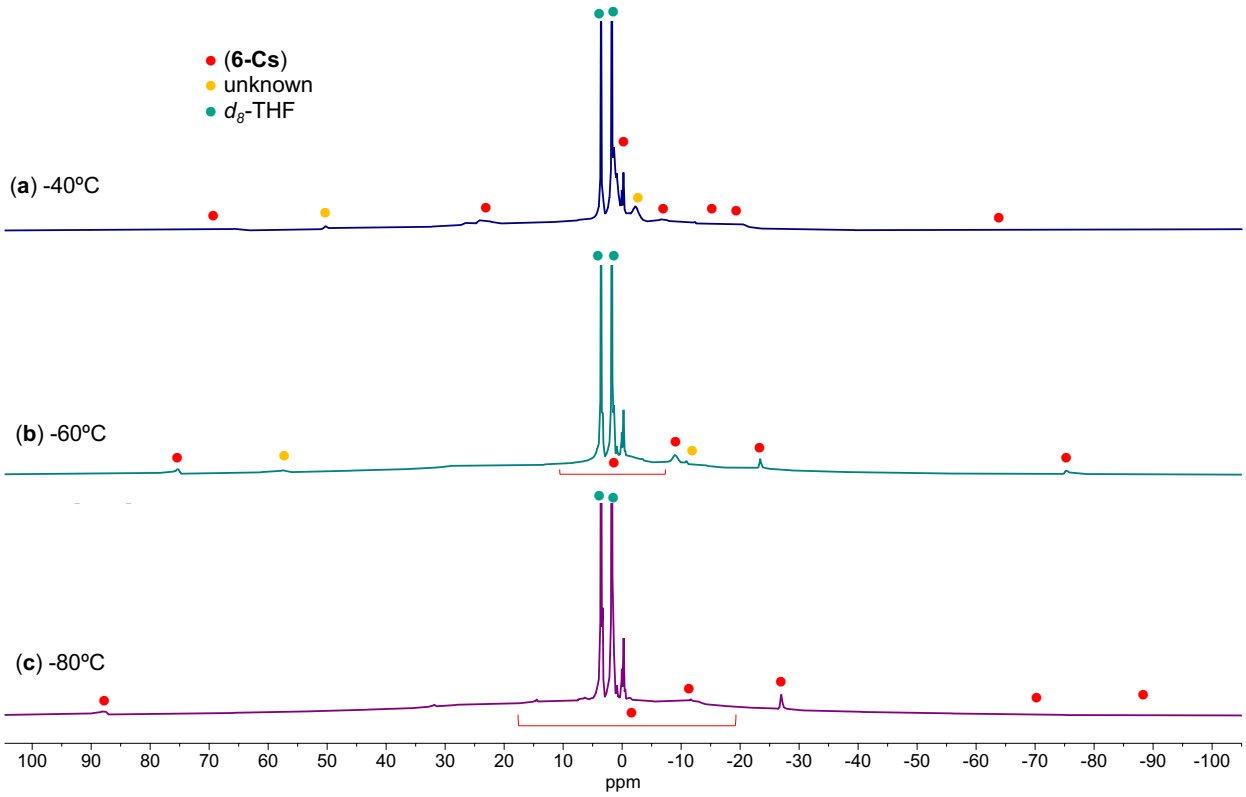

Figure S26. Variable temperature ^{1}H NMR (400 MHz, d_8-THF, (**a**) 233K, (**b**) 213K, and (**c**) 193K) spectra of $[Cs_2\{U^{IV/III}(OSi(O^tBu)_3)_2(N(SiMe_3)_2)\}_2(\mu\text{-}N)]$, **6-Cs**, after 24 hours at -40°C.

S5.3.3. U(V)/U(V) heteroleptic complex, 7.

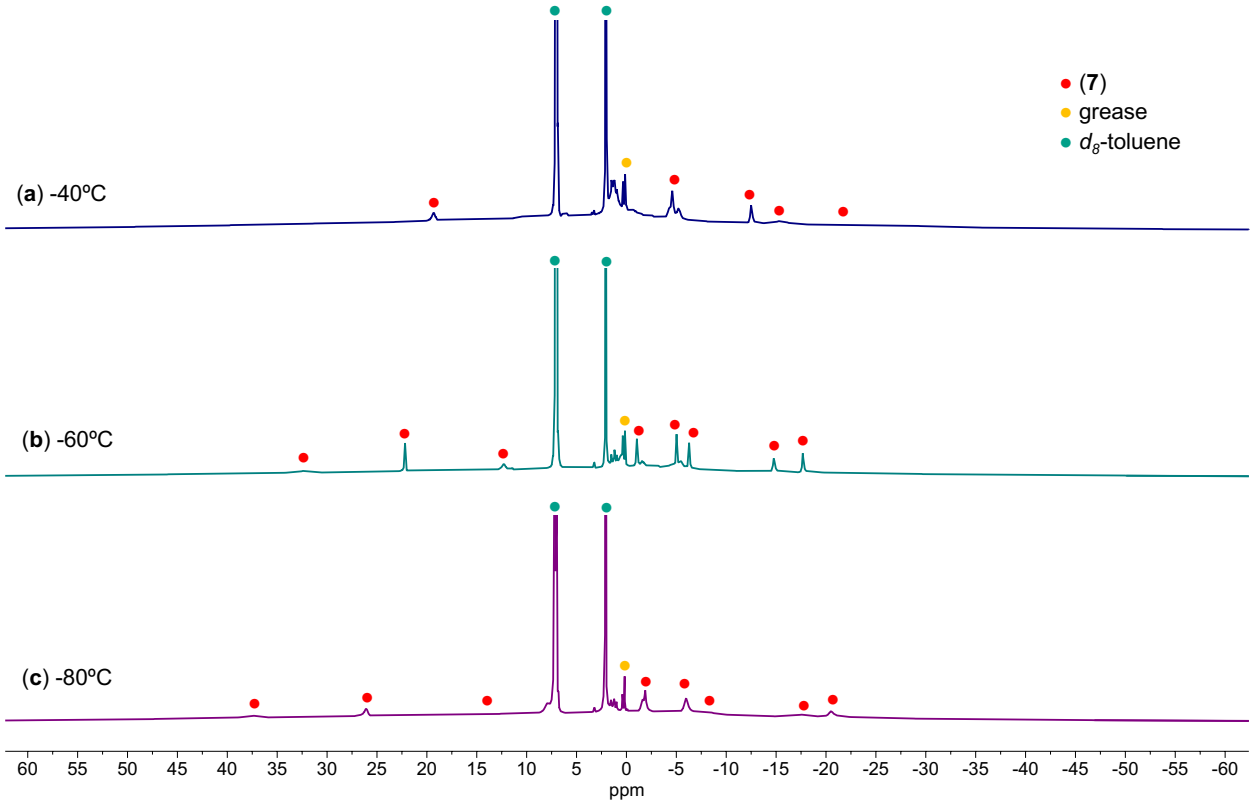

Figure S27. Variable temperature ^{1}H NMR (400 MHz, d_8-toluene, (**a**) 233K, (**b**) 213K, and (**c**) 193K) spectra of $[K_3\{U^V(OSi(O^tBu)_3)_2(N(SiMe_3)_2)\}_2(\mu\text{-}N)(\mu\text{-}\eta^2\text{:}\eta^2\text{-}N_2)]$, **7**. No decomposition is observed at -40°C.

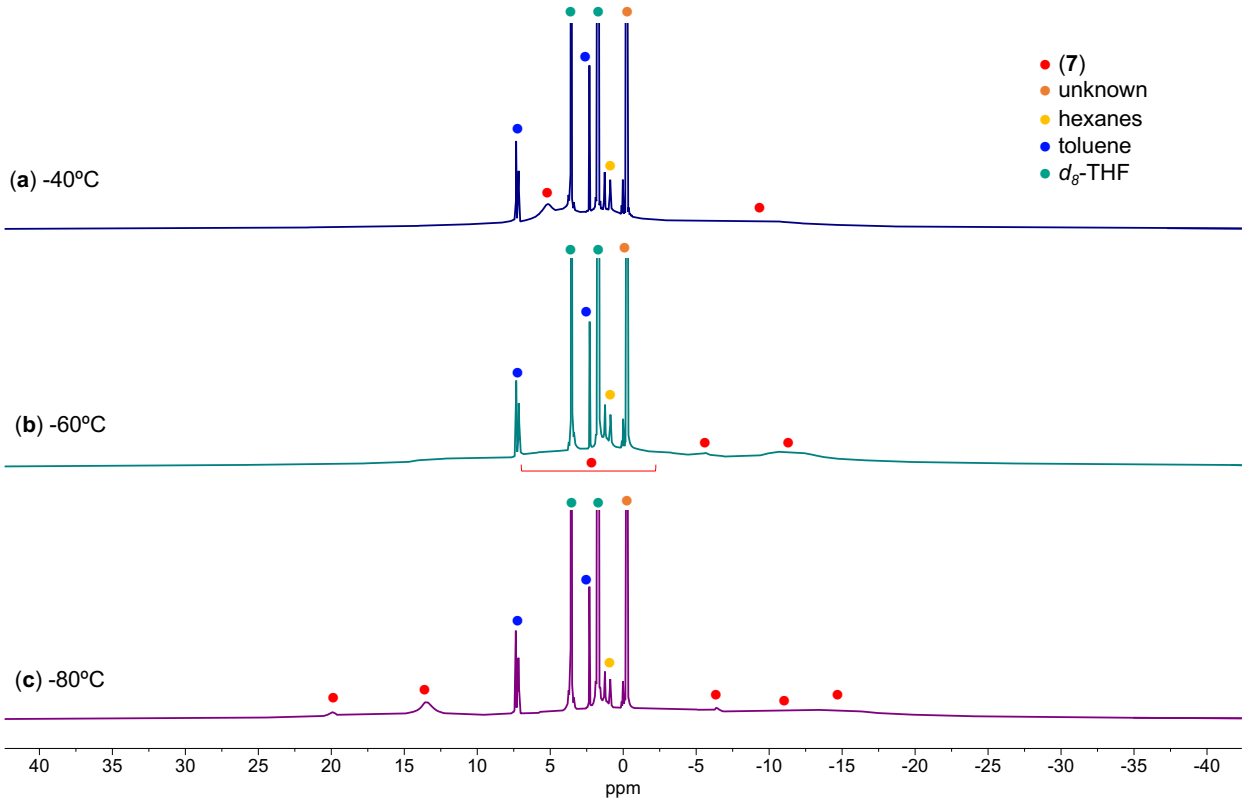

Figure S28. Variable temperature ^{1}H NMR (400 MHz, d_8-THF, (**a**) 233K, (**b**) 213K, and (**c**) 193K) spectra of $[K_3\{U^{V}(OSi(O^{t}Bu)_3)_2(N(SiMe_3)_2)\}_2(\mu\text{-}N)(\mu\text{-}\eta^2\text{:}\eta^2\text{-}N_2)]$, **7**, after 15 minutes at -80°C. Decomposition is observed immediately with formation of an unknown species at -0.2 ppm, and over 24 hours at -40°C.

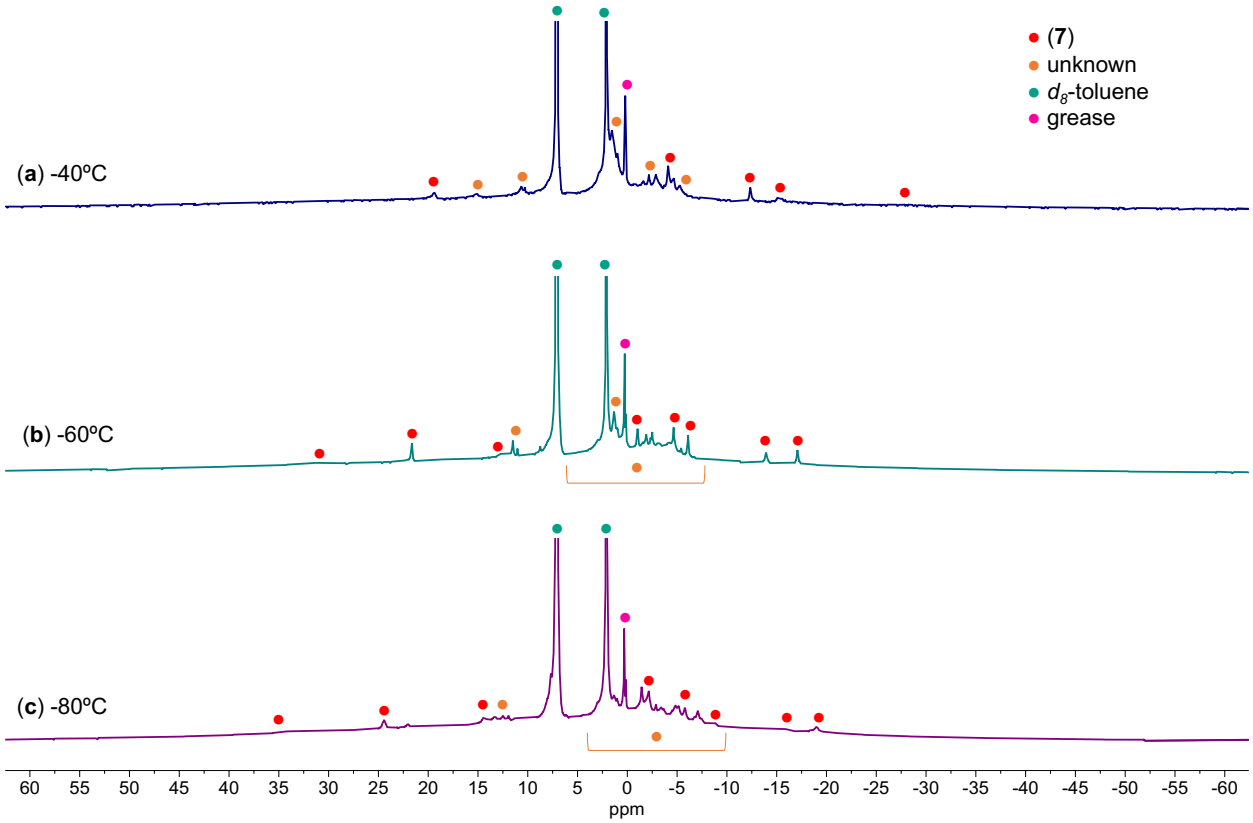

Figure S29. Variable temperature ^{1}H NMR (400 MHz, d_8-THF, (**a**) 233K, (**b**) 213K, and (**c**) 193K) spectra of the stability of $[K_3\{U^{V}(OSi(O^{t}Bu)_3)_2(N(SiMe_3)_2)\}_2(\mu\text{-}N)(\mu\text{-}\eta^2\text{:}\eta^2\text{-}N_2)]$, **7**, in THF. Complex **7** was dissolved in THF for 15 minutes at -80°C, then the solvent was removed under vacuum, and redissolved in d_8-toluene.

S5.4. NMR spectra for the reactivity of heteroleptic-nitride complexes.

S5.4.1. Reactivity of complexes, 1 and 4.

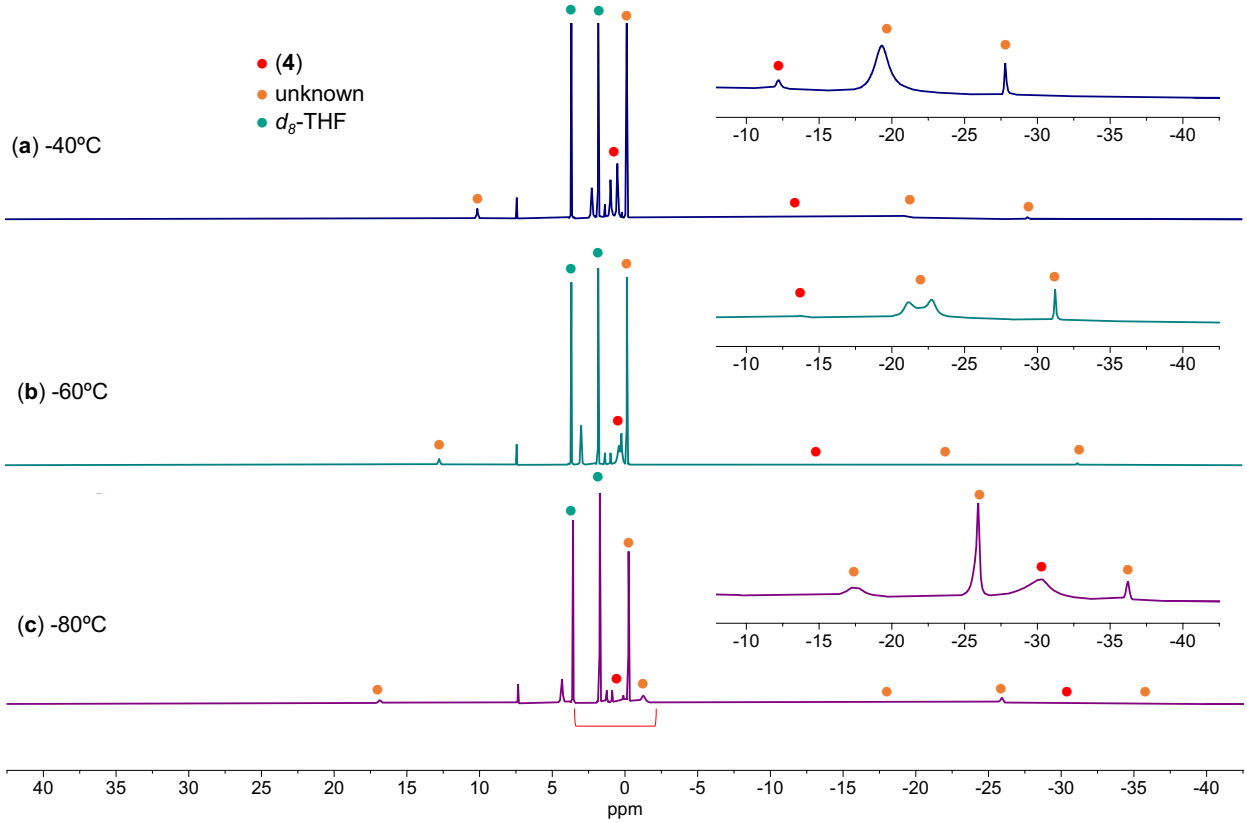

Figure S30. Variable temperature ^{1}H NMR (400 MHz, d_8-THF, (**a**) 233K, (**b**) 213K, and (**c**) 193K) spectra of complex **1** in the presence of 10.0 equiv. KC_8 at -40°C.

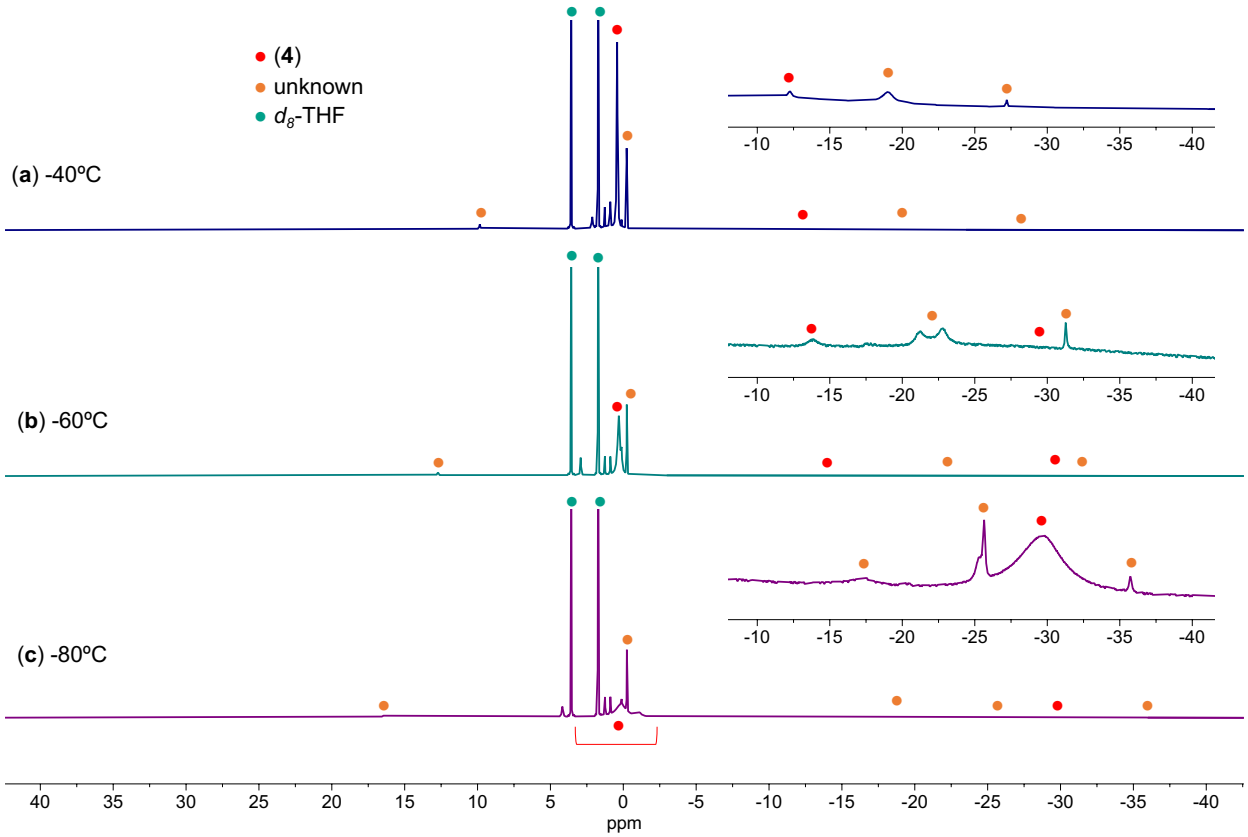

Figure S31. Variable temperature ^{1}H NMR (400 MHz, d_8-THF, (**a**) 233K, (**b**) 213K, and (**c**) 193K) spectra of complex **1** in the presence of 10.0 equiv. KC_8 at -80°C.

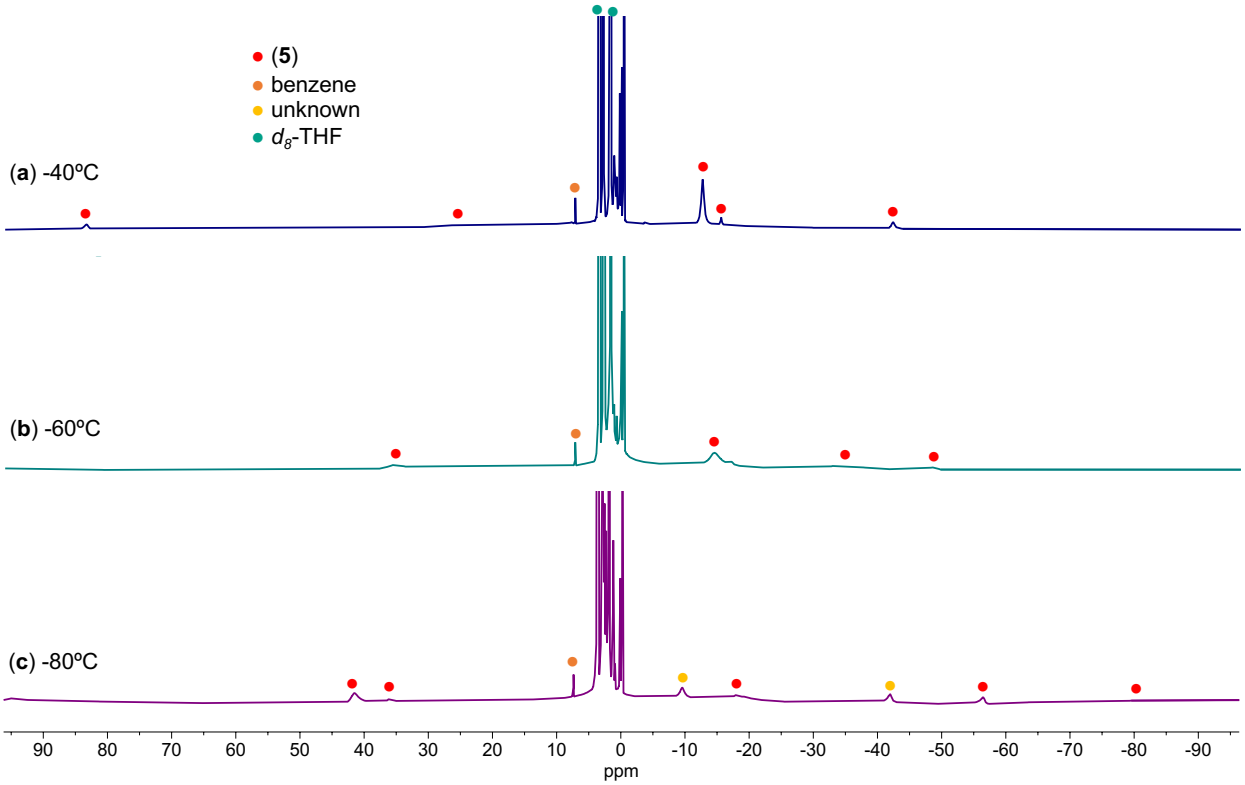

Figure S32. Variable temperature ^{1}H NMR (400 MHz, d_8-THF, (**a**) 233K, (**b**) 213K, and (**c**) 193K) spectra of complex **4** in the presence of 2.0 equiv. 2.2.2-cryptand at -40°C, forming complex **5**.

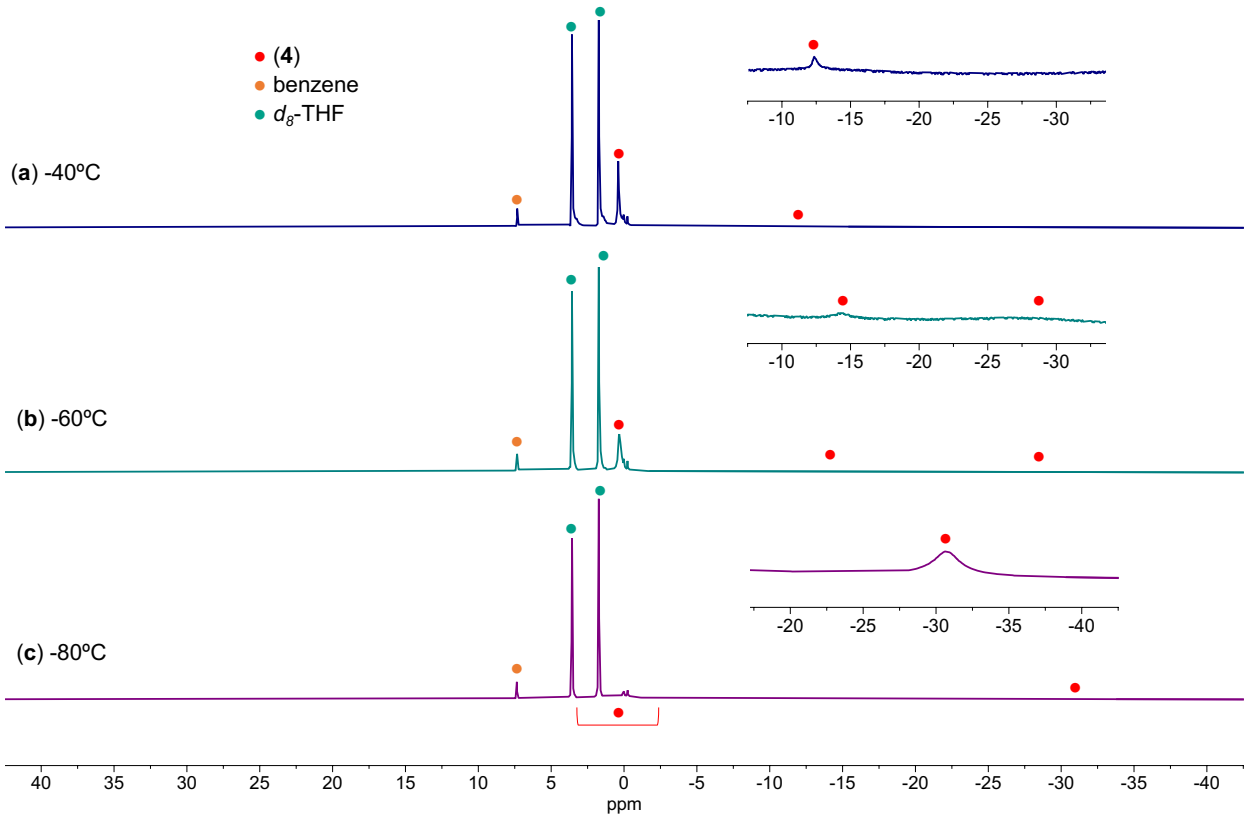

Figure S33. Variable temperature ^{1}H NMR (400 MHz, d_8-THF, (**a**) 233K, (**b**) 213K, and (**c**) 193K) spectra of complex **4** in the presence of 1 atm N_2 at -80°C.

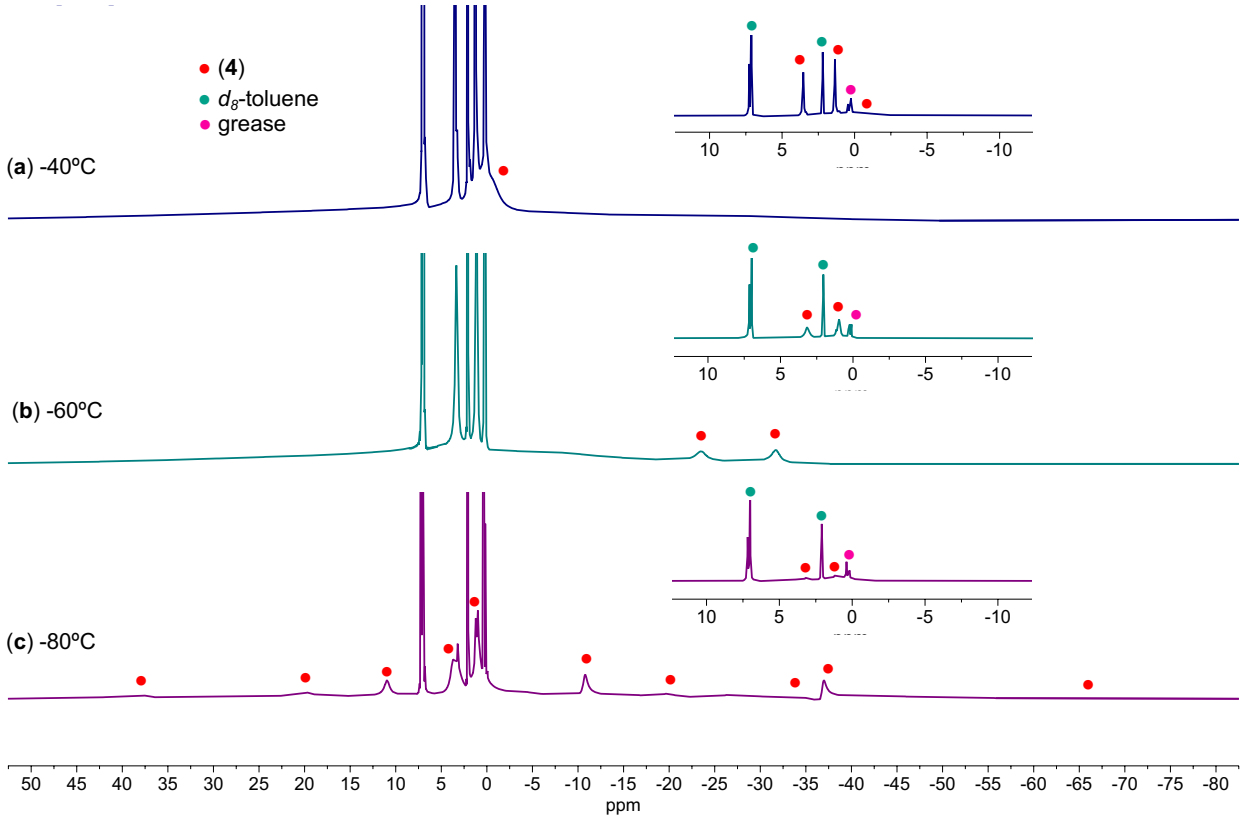

Figure S34. Variable temperature ^{1}H NMR (400 MHz, d_8-toluene, (**a**) 233K, (**b**) 213K, and (**c**) 193K) spectra of complex **4** in the presence of 1 atm N_2 at -80°C.

S5.4.2. Reactivity of complex 3-Cs.

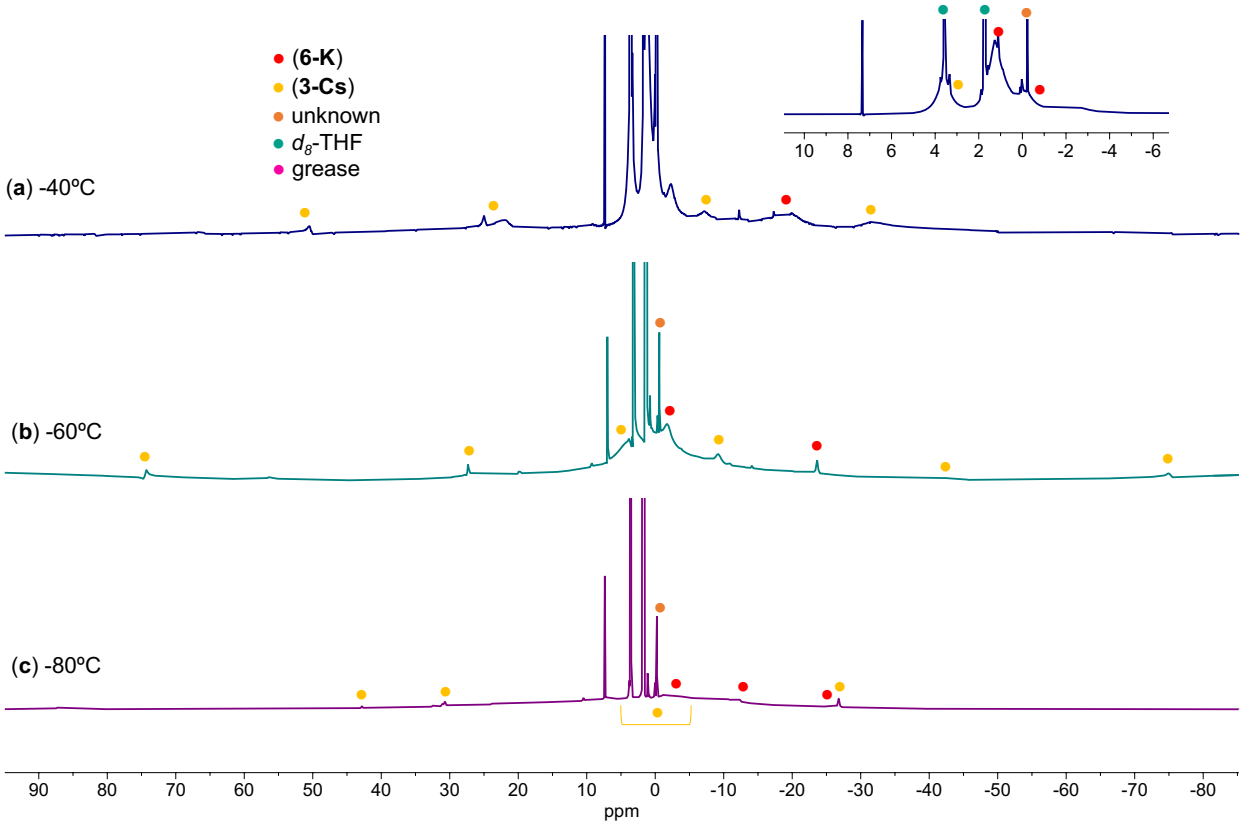

Figure S35. Variable temperature ^{1}H NMR (400 MHz, d_8-THF, (**a**) 233K, (**b**) 213K, and (**c**) 193K) spectra of complex **3-Cs** in the presence of 1.0 equiv. KC_8 at -40°C, generating a mixture of complex **3-Cs** and **6-K**.

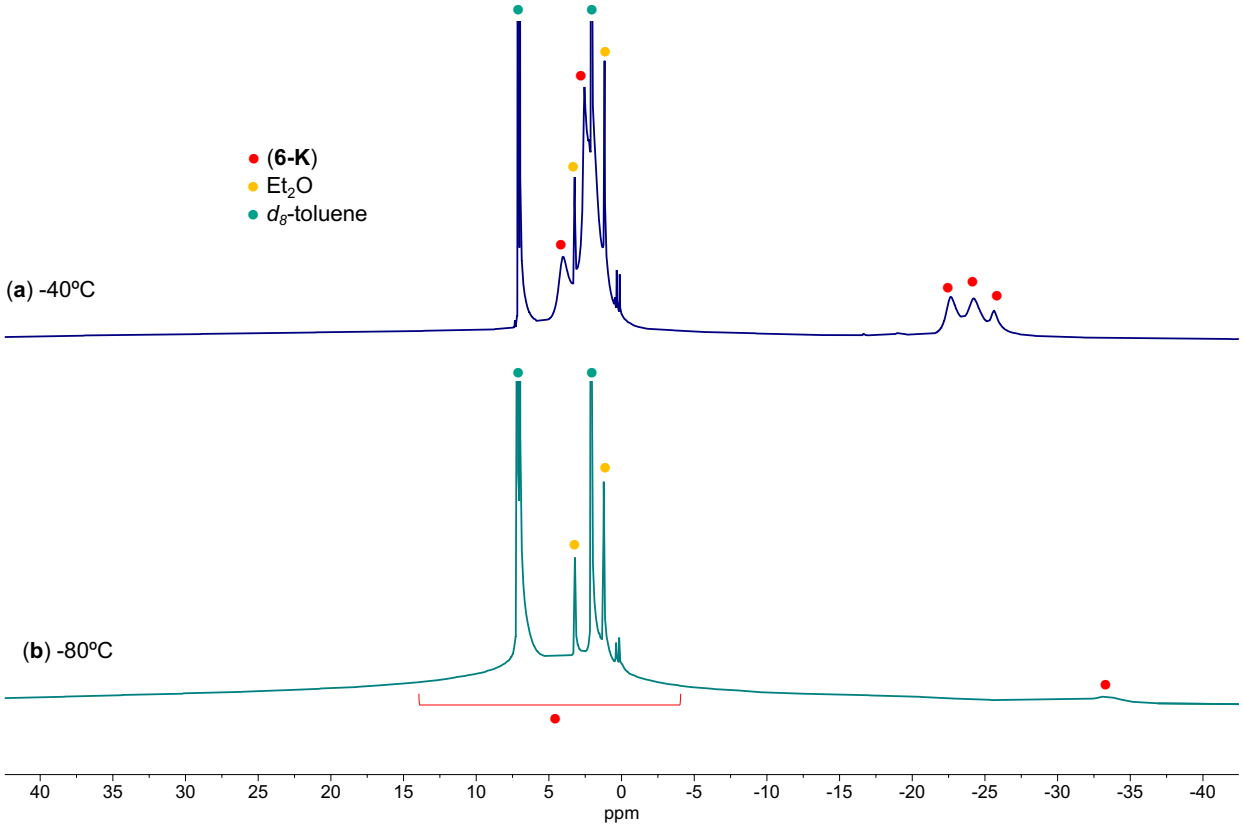

Figure S36. Variable temperature ^{1}H NMR (400 MHz, d_8-toluene, (**a**) 233K, and (**b**) 193K) spectra of the reaction mixture of complex **3-Cs** in the presence of 10.0 equiv. KC_8 in Et_2O at -40°C, generating **6-K** as the major product.

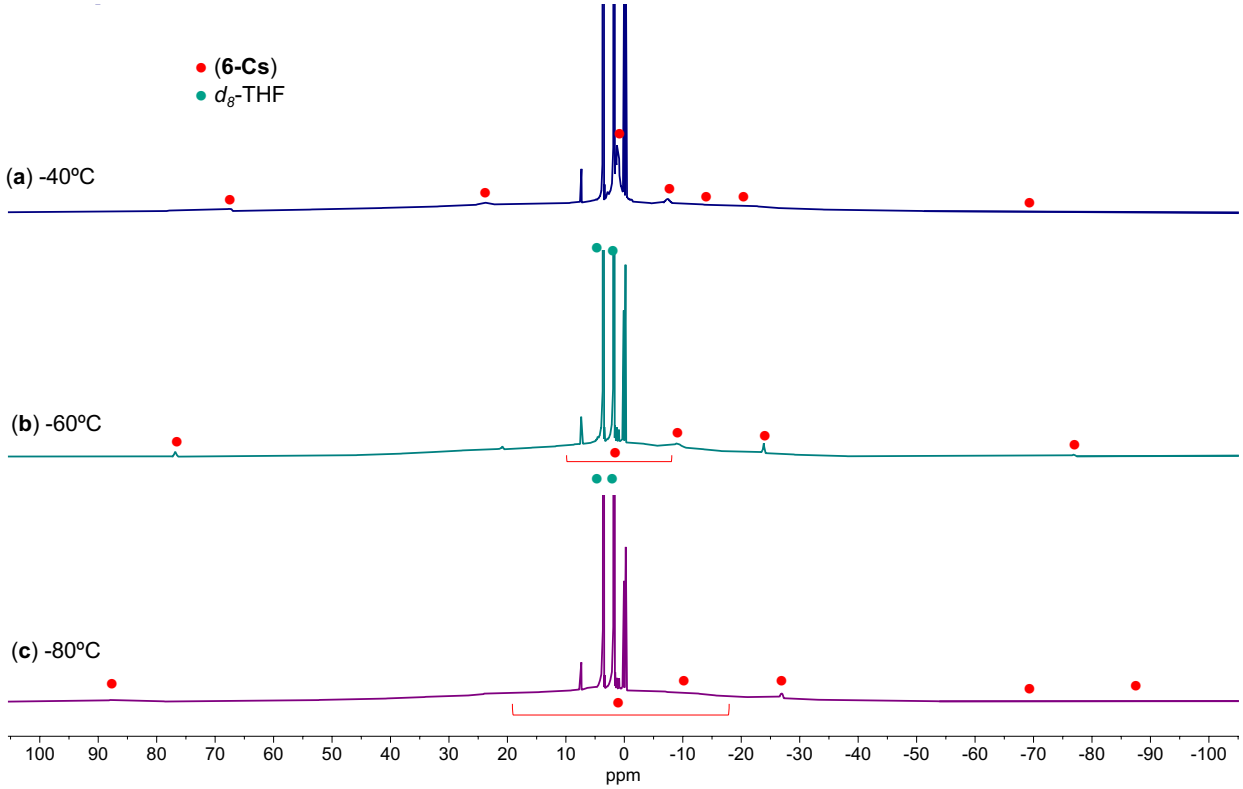

Figure S37. Variable temperature ^{1}H NMR (400 MHz, d_8-THF, (**a**) 233K, (**b**) 213K, and (**c**) 193K) spectra of complex **3-Cs** in the presence of 10.0 equiv. CsC_8 at -40°C, generating **6-Cs** as the only product.

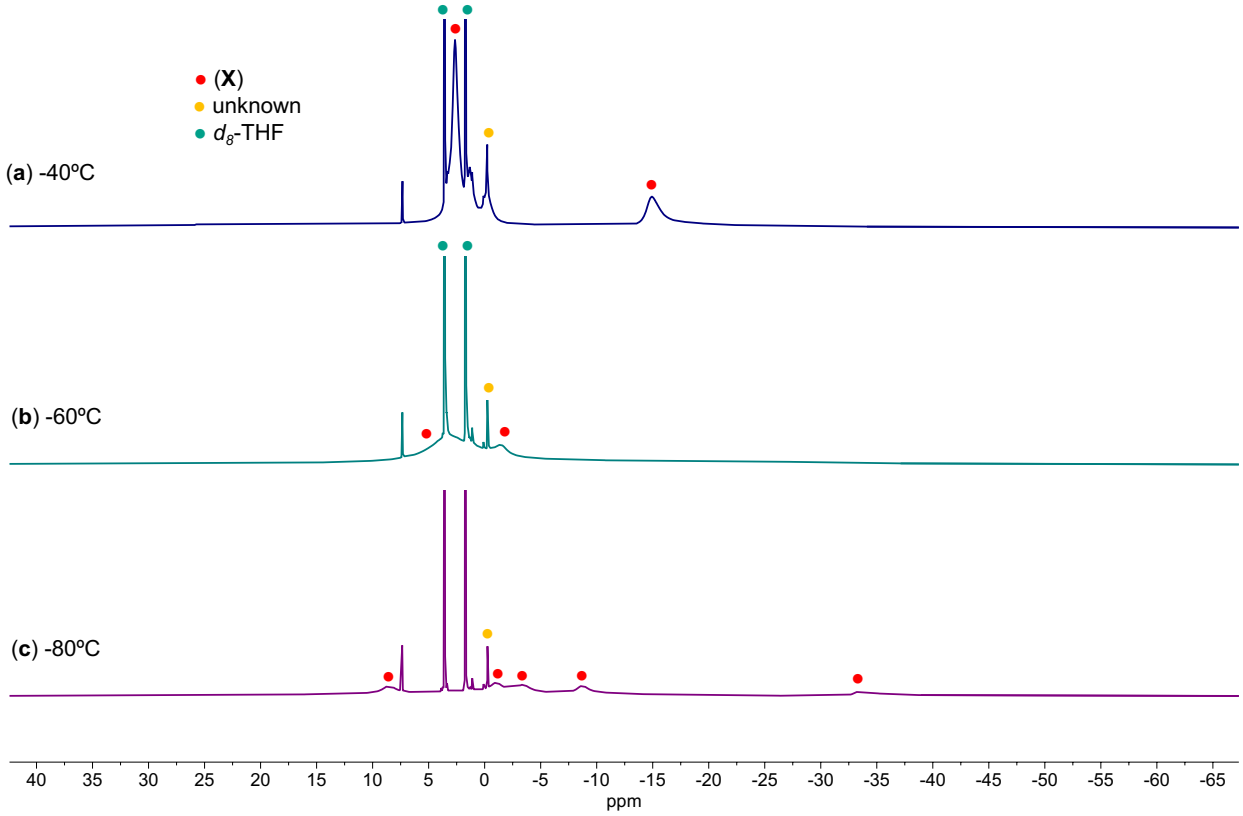

Figure S38. Variable temperature ^{1}H NMR (400 MHz, d_8-THF, (**a**) 233K, (**b**) 213K, and (**c**) 193K) spectra of complex **3-Cs** in the presence of 10.0 equiv. KC_8 at -80°C, generating **X** as the only product.

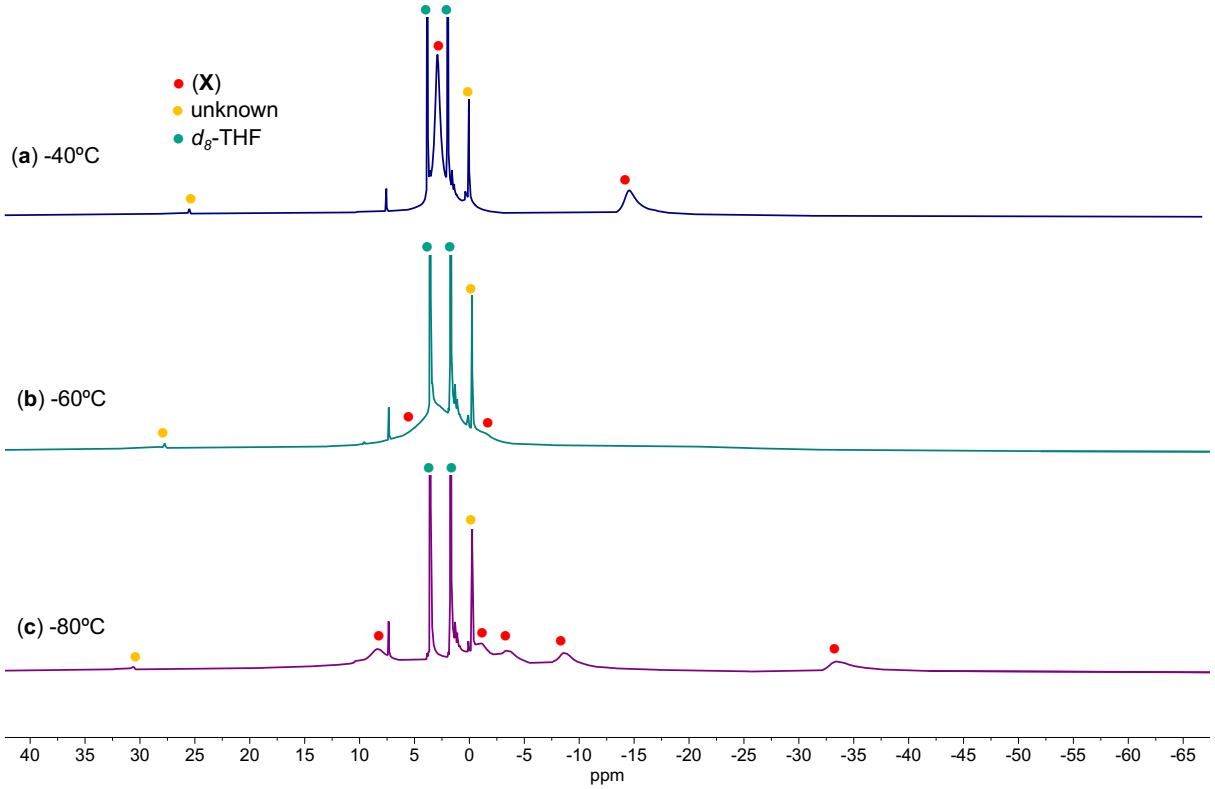

Figure S39. Variable temperature ^{1}H NMR (400 MHz, d_8-THF, (**a**) 233K, (**b**) 213K, and (**c**) 193K) spectra of complex **3-Cs** in the presence of 10.0 equiv. KC_8 at -40°C, generating **X** as the major product.

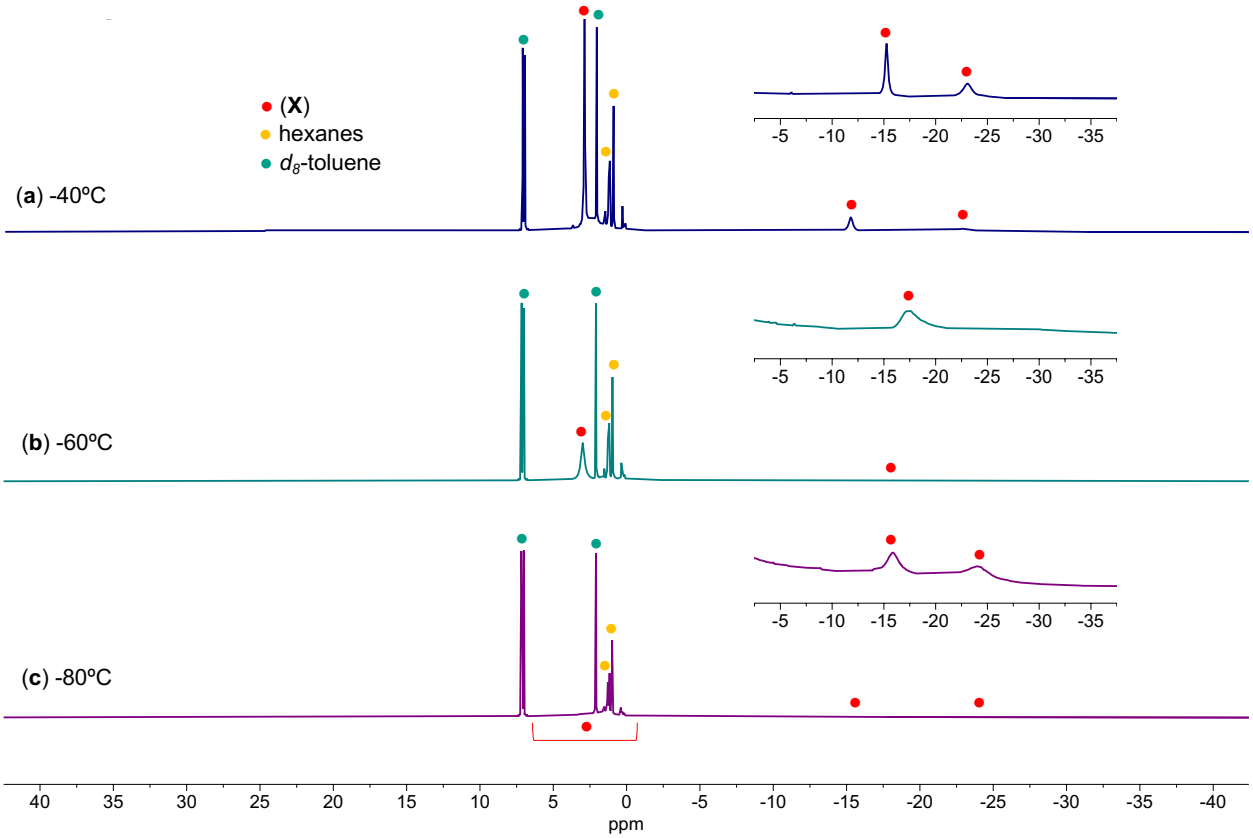

Figure S40.Variable temperature ^{1}H NMR (400 MHz, d_8-toluene (**a**) 233K, (**b**) 213 K, (**c**) 193K) spectra after extraction of the reaction mixture of complex **3-Cs** in the presence of 10.0 equiv. KC_8, generating **X** as the major species.

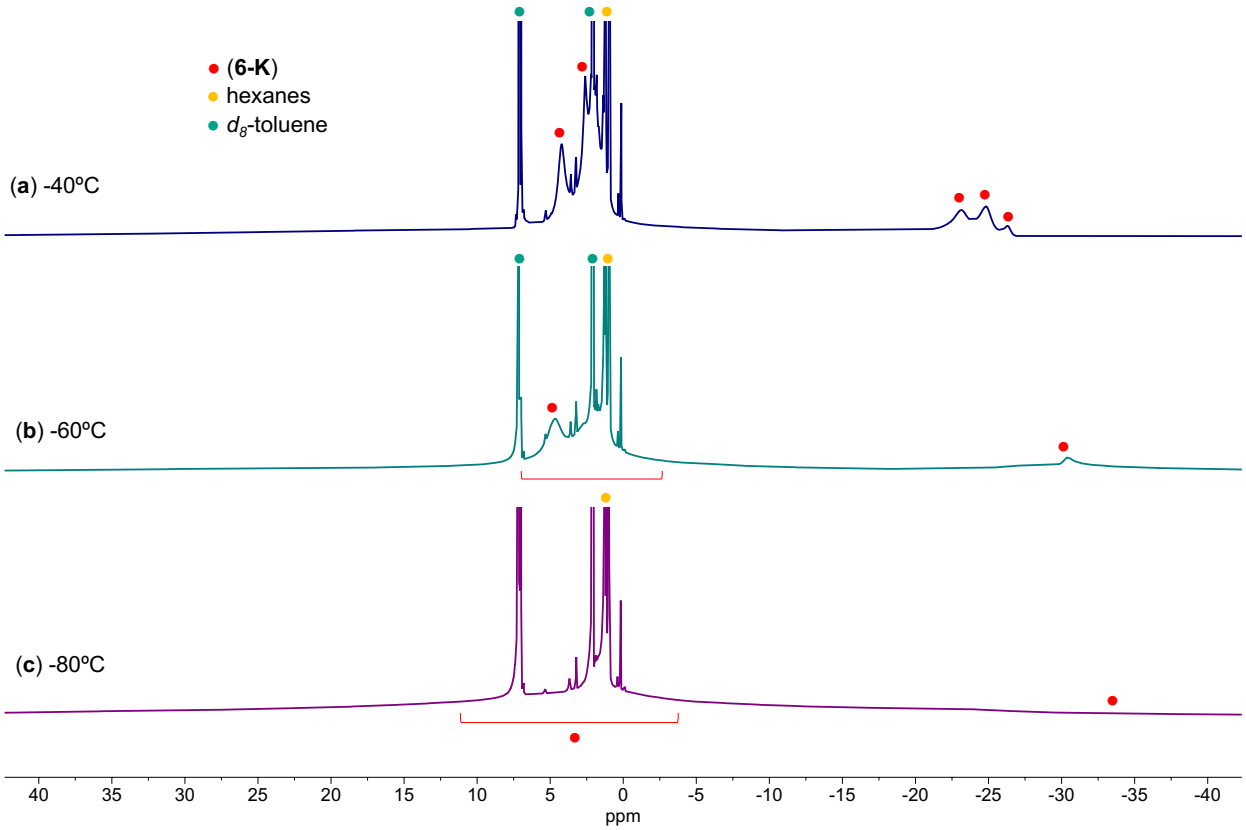

Figure S41. Variable temperature ^{1}H NMR (400 MHz, d_8-toluene, (**a**) 233K, (**b**) 213K, and (**c**) 193K) spectra of complex **X** at -40°C for 24 hours in d_8-toluene, resulting in complex **6-K** as the major species.

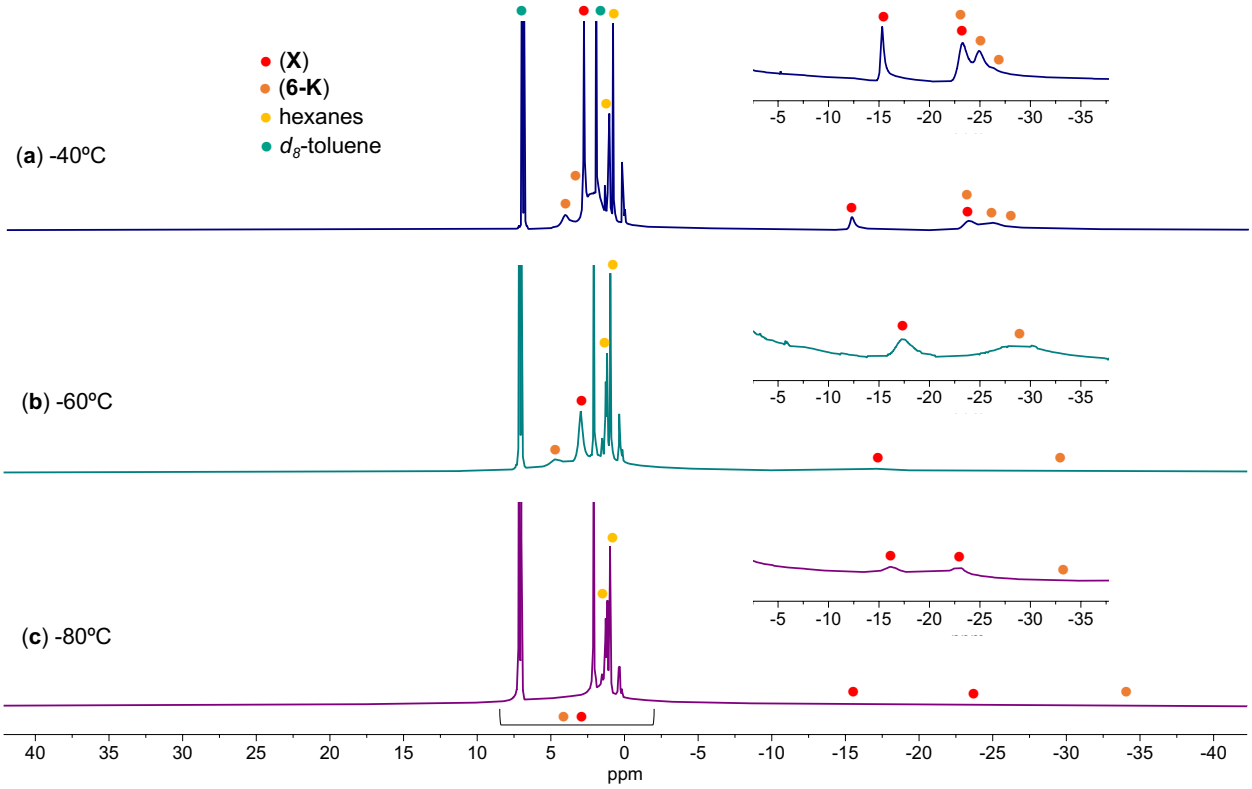

Figure S42.Variable temperature ^{1}H NMR (400 MHz, *d*$_8$-toluene (**a**) 233K, (**b**) 213 K, (**c**) 193K) spectra of a 1:1 mixture of complex **6-K** and *in situ* generated **X** at -40°C, demonstrating complexes **6-K** and **X** are different species.

S5.4.3. Reactivity of complexes 6-K, 6-Cs, X, and 7.

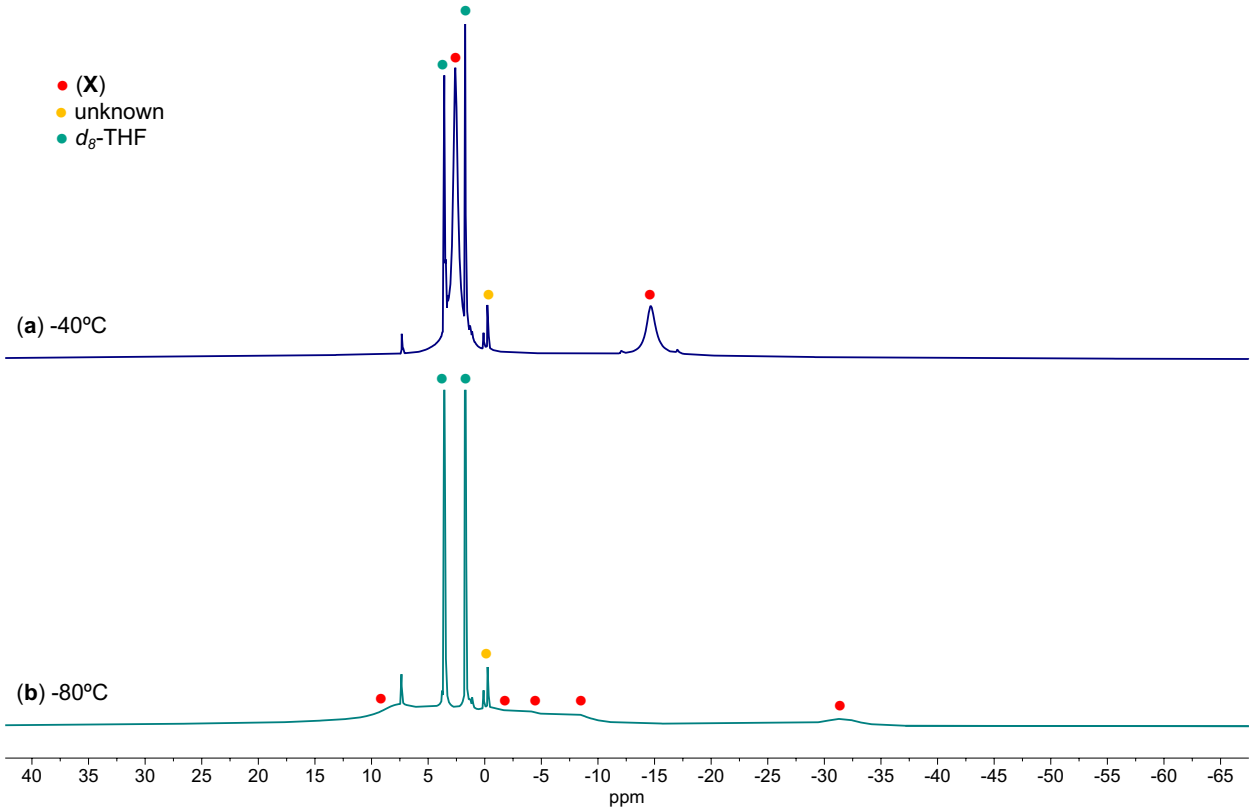

Figure S43. Variable temperature ^{1}H NMR (400 MHz, d_8-THF, (**a**) 233K and (**b**) 193) spectra of complex **6-K** in the presence of 10.0 equiv. KC_8 at -40°C, generating **X** as the major product.

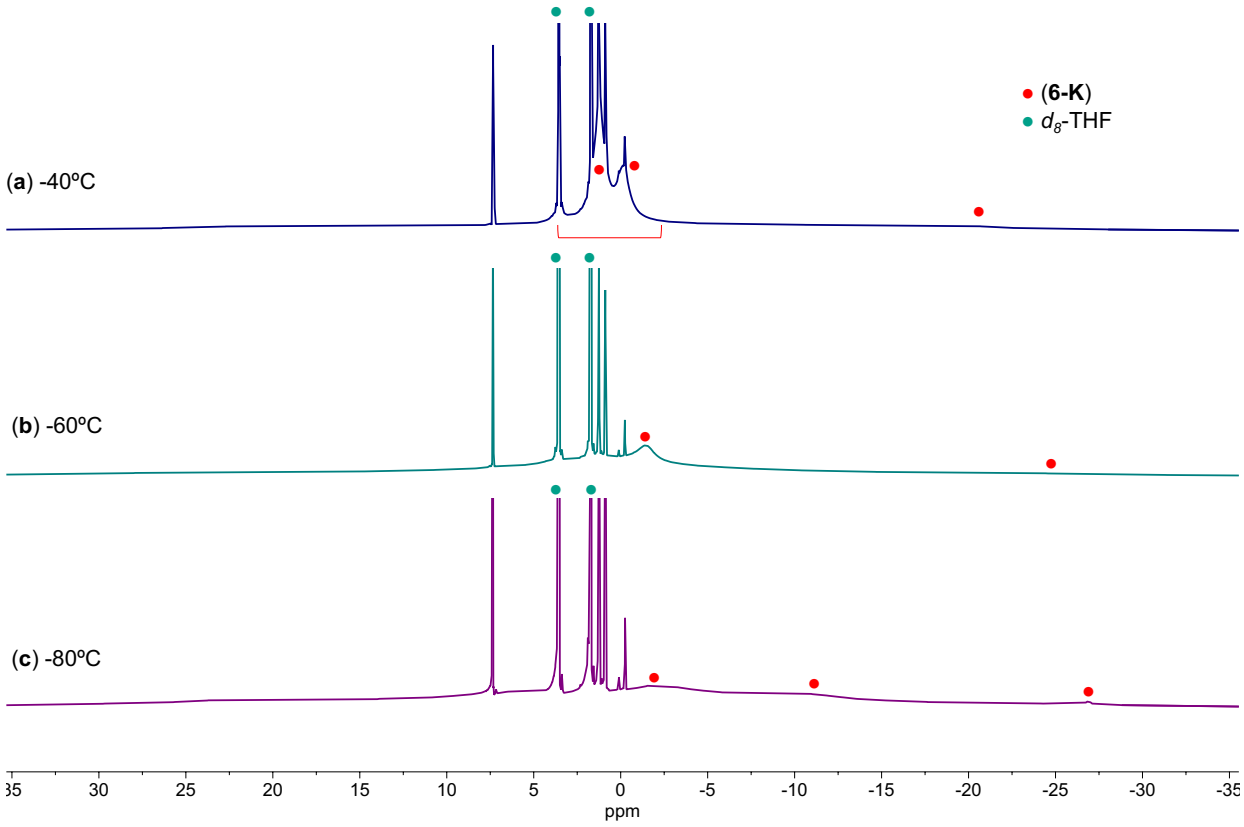

Figure S44. Variable temperature ^{1}H NMR (400 MHz, d_8-THF, (**a**) 233K, (**b**) 213K, and (**c**) 193K) spectra of complex **6-K** in the presence of 1 atm N_2 at -80°C.

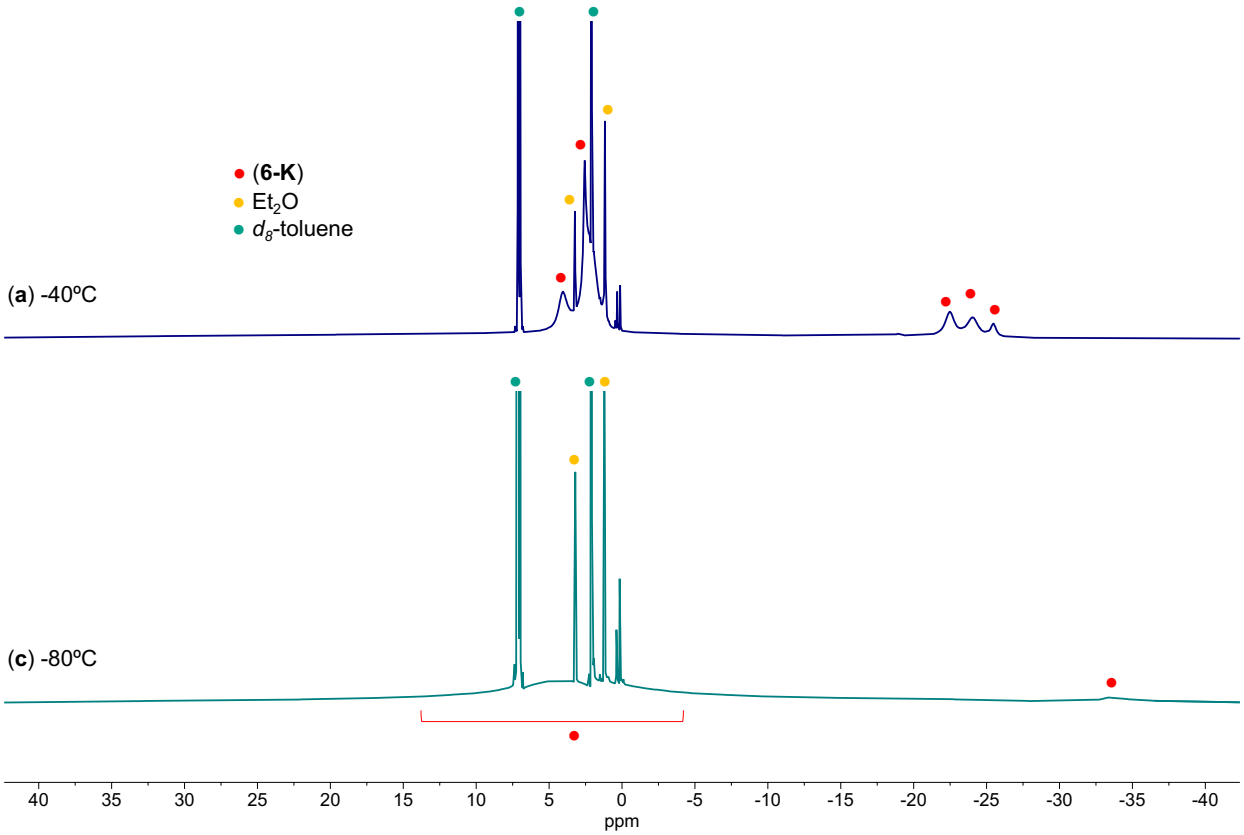

Figure S45. Variable temperature ^{1}H NMR (400 MHz, d_8-toluene, (**a**) 233K and (**c**) 193K) spectra of complex **6-K** in the presence of 1 atm N_2 at -80°C.

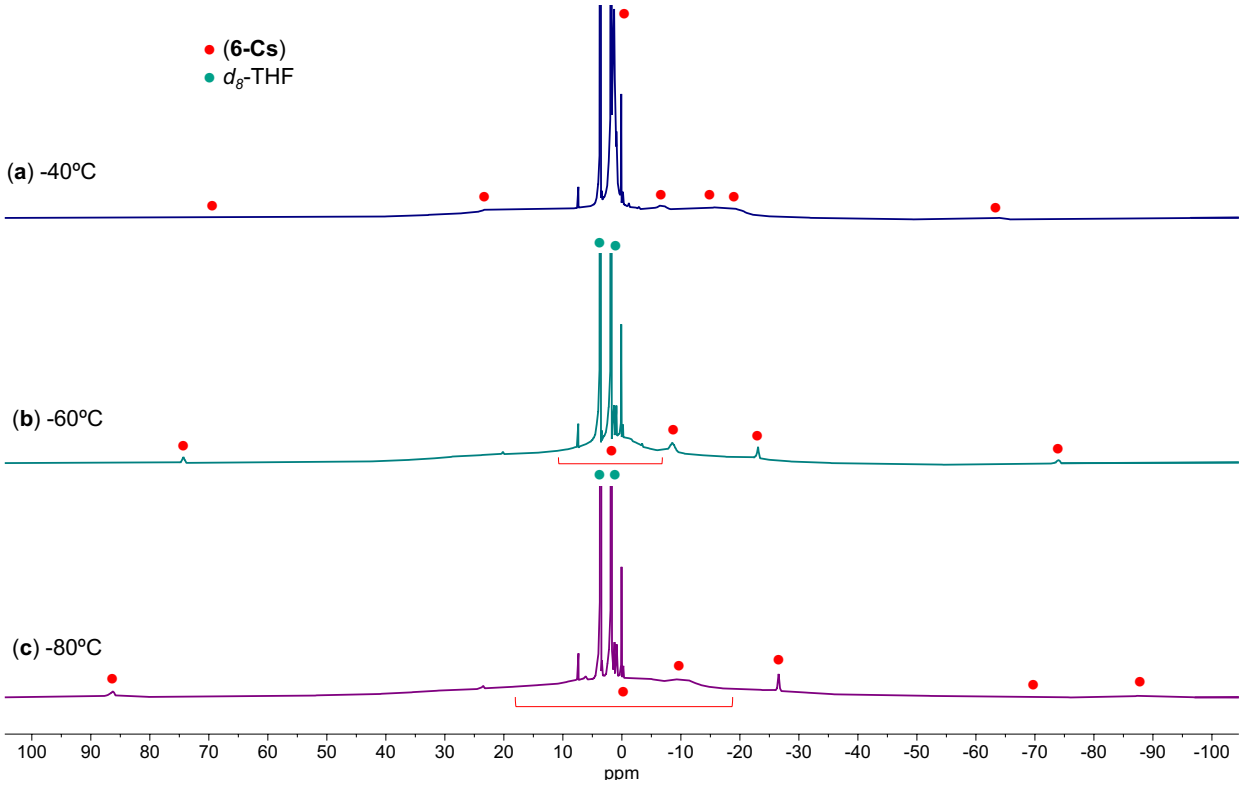

Figure S46. Variable temperature ^{1}H NMR (400 MHz, d_8-THF, (**a**) 233K, (**b**) 213K, and (**c**) 193K) spectra of complex **6-Cs** in the presence of 1 atm N_2 at -80°C.

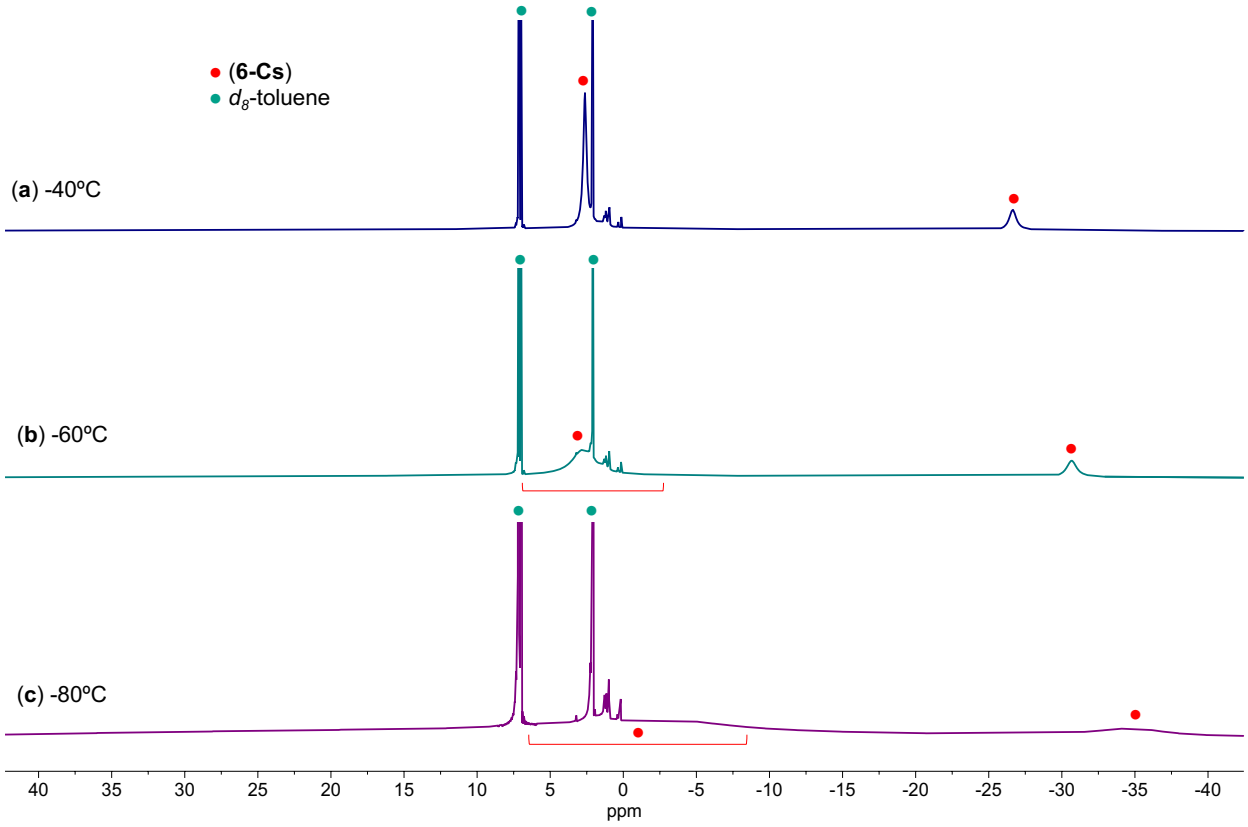

Figure S47. Variable temperature ^{1}H NMR (400 MHz, d_8-toluene, (**a**) 233K, (**b**) 213K, and (**c**) 193K) spectra of complex **6-Cs** in the presence of 1 atm N_2 at -80°C.

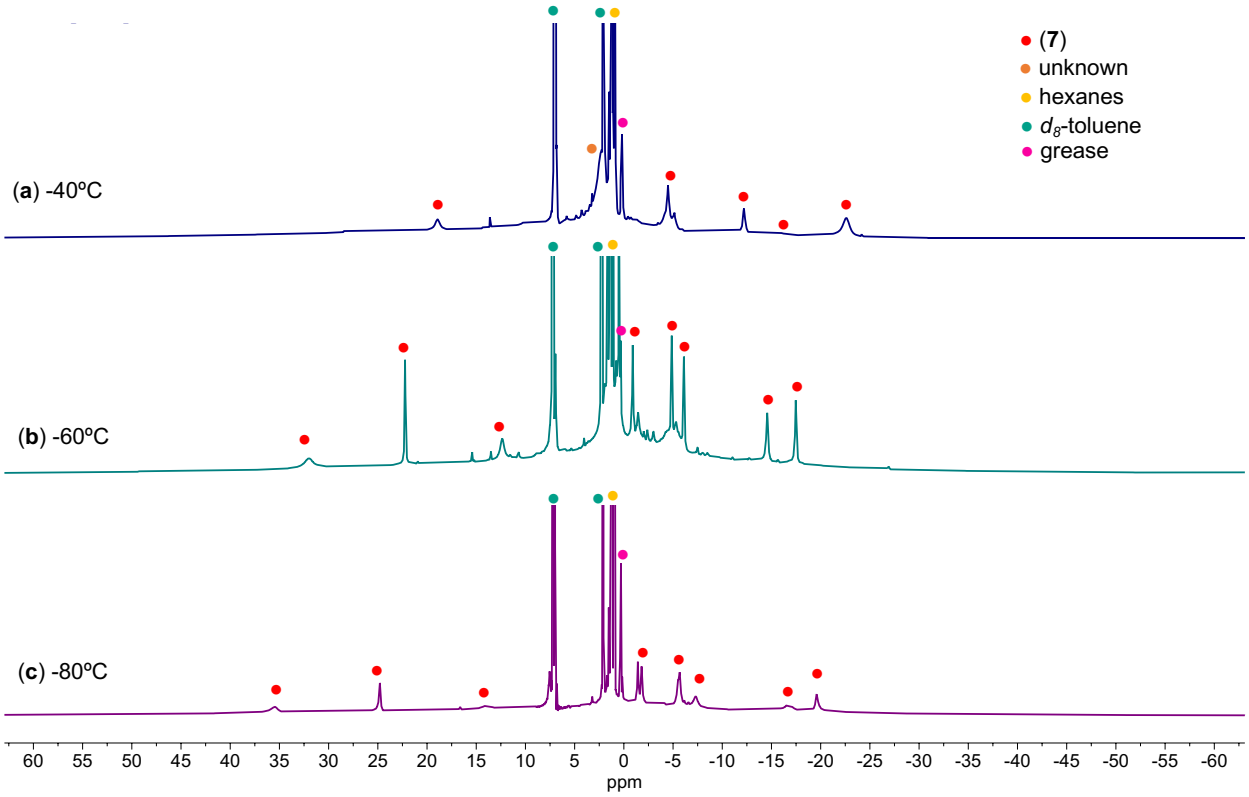

Figure S48. Variable temperature ^{1}H NMR (400 MHz, d_8-toluene, (**a**) 233K, (**b**) 213K, and (**c**) 193K) spectra of complex **X** in the presence of 1 atm N_2 at -100°C, resulting in complex **7** as the major species.

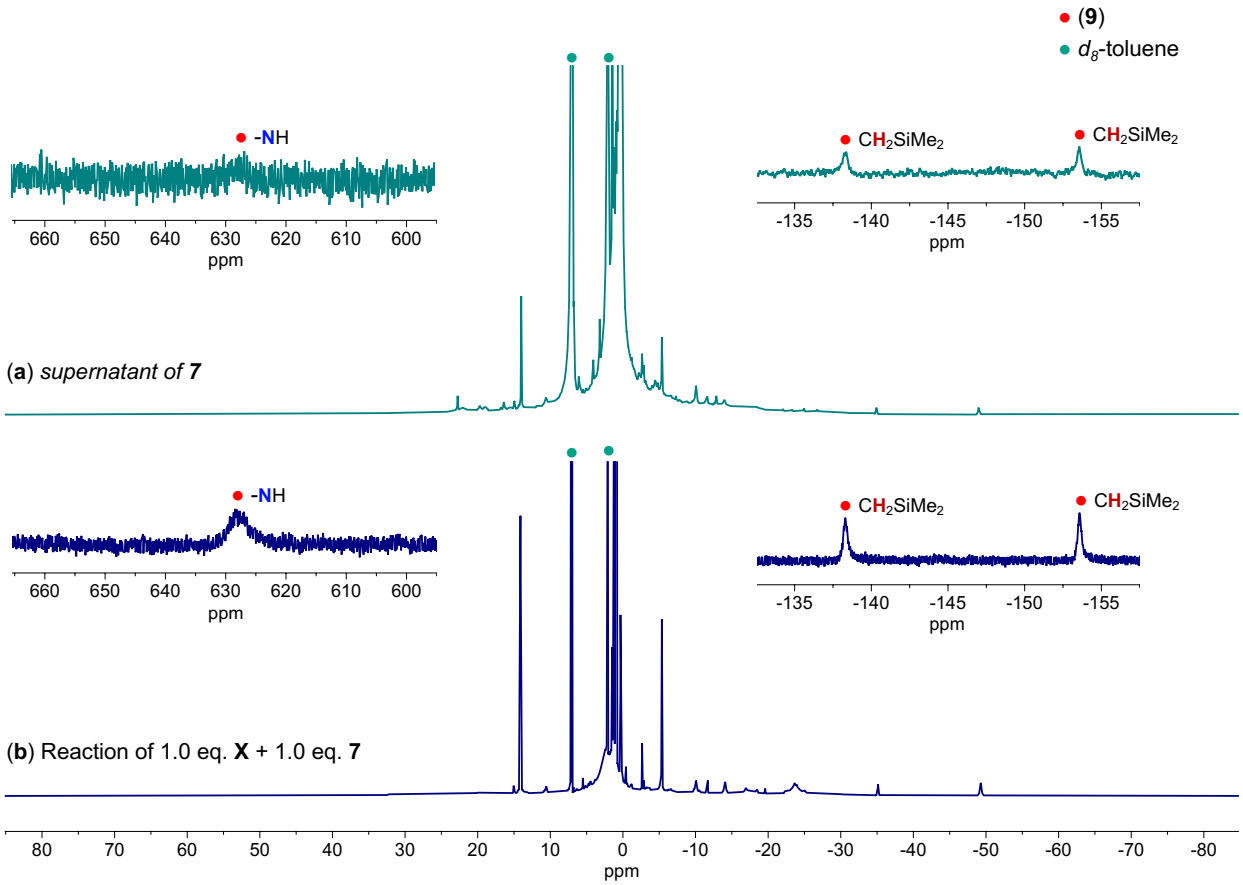

Figure S49. ^{1}H NMR (400 MHz, d_8-toluene, 233K) spectra of the (**a**) supernatant from the synthesis of complex **X**, which is comparable to the spectrum for the (**b**) reaction of complexes **X** and **7**.

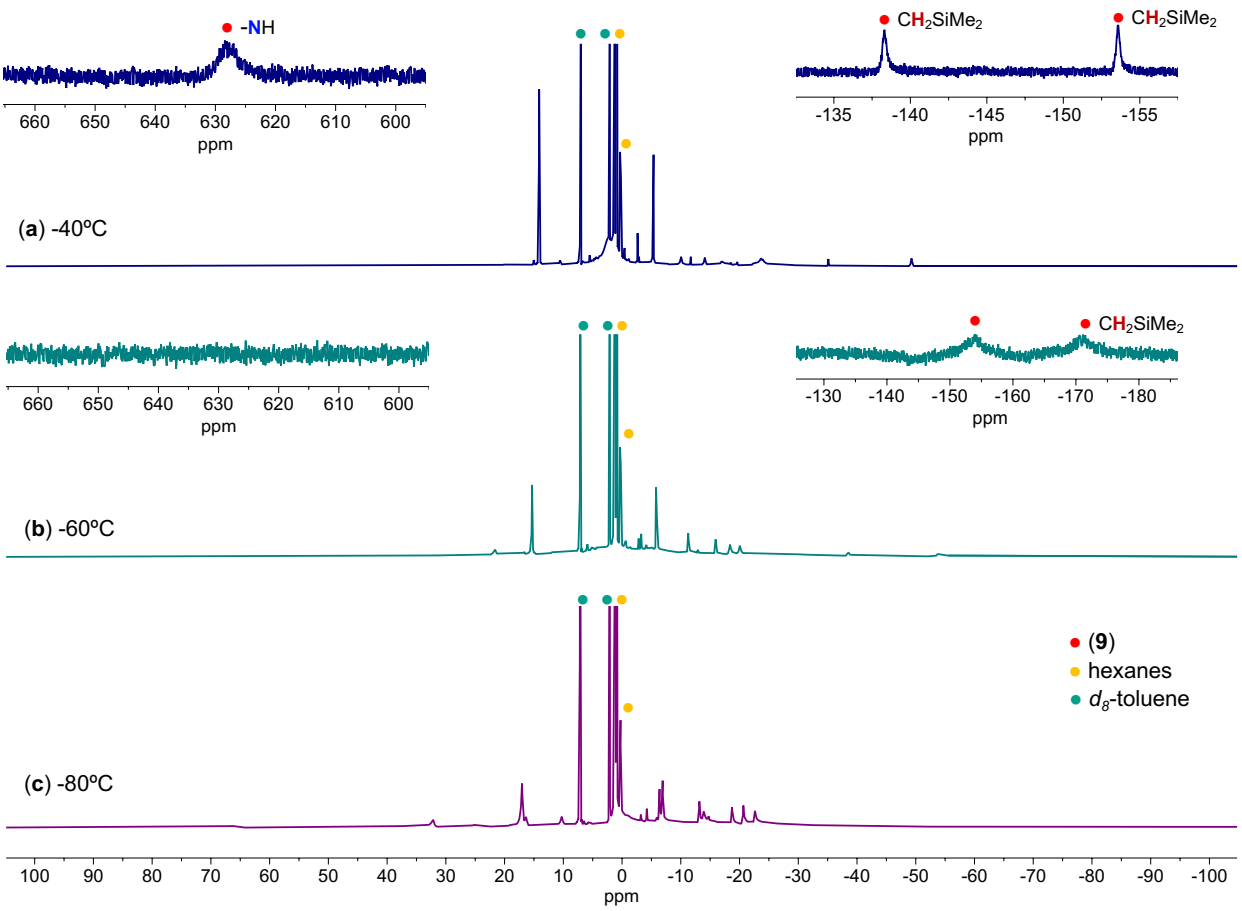

Figure S50. Variable temperature ^{1}H NMR (400 MHz, d_8-toluene, (**a**) 233K, (**b**) 213K, and (**c**) 193K) spectra of complex **7** in the presence of 1.0 equiv. of *in-situ* generated complex **X**, forming complexes **9**, **3-K**, and unknown species.

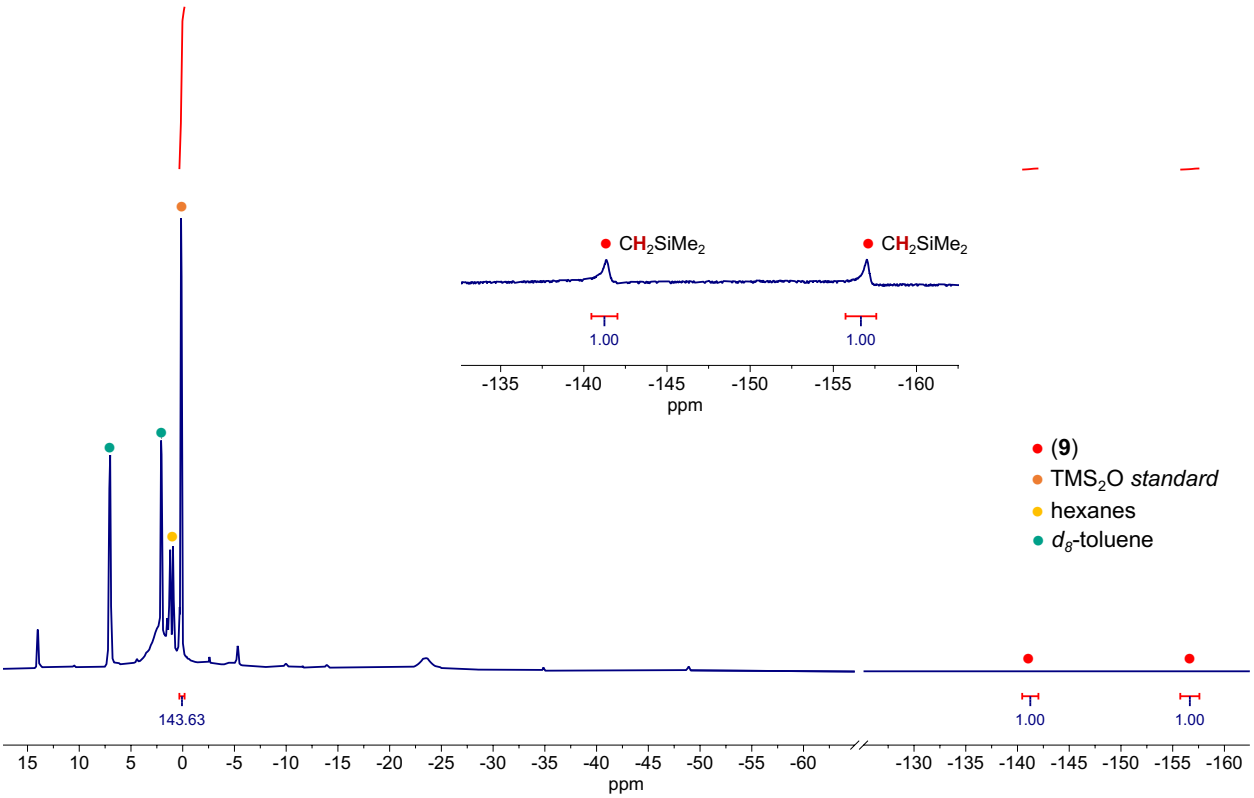

Figure S51. Variable temperature ^{1}H NMR (400 MHz, d_8-toluene, 233K) spectrum of complex **7** in the presence of 1.0 equiv. of *in-situ* generated complex **X**, forming complexes **9**, **3-K**, and unknown species. The spectroscopic yield of complex **9** (51% yield) was determined by adding TMS_2O as an internal standard.

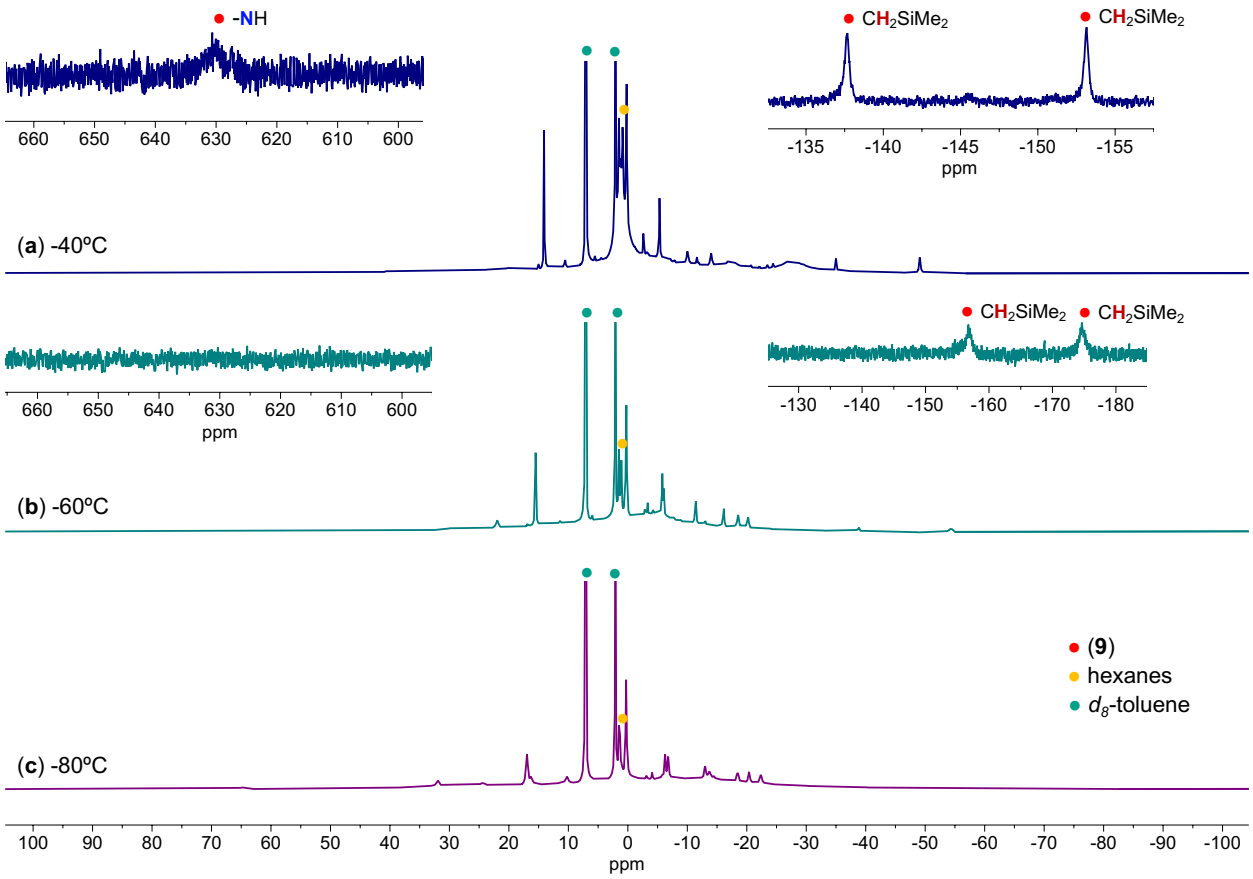

Figure S52. Variable temperature ^{1}H NMR (400 MHz, d_8-toluene, (**a**) 233K, (**b**) 213K, and (**c**) 193K) spectra of isolated crystals from the reaction of complex **7** in the presence of 1.0 equiv. of *in-situ* generated complex **X**. The crystals still display a mixture of species of complexes **9**, **3-K**, and an unknown.

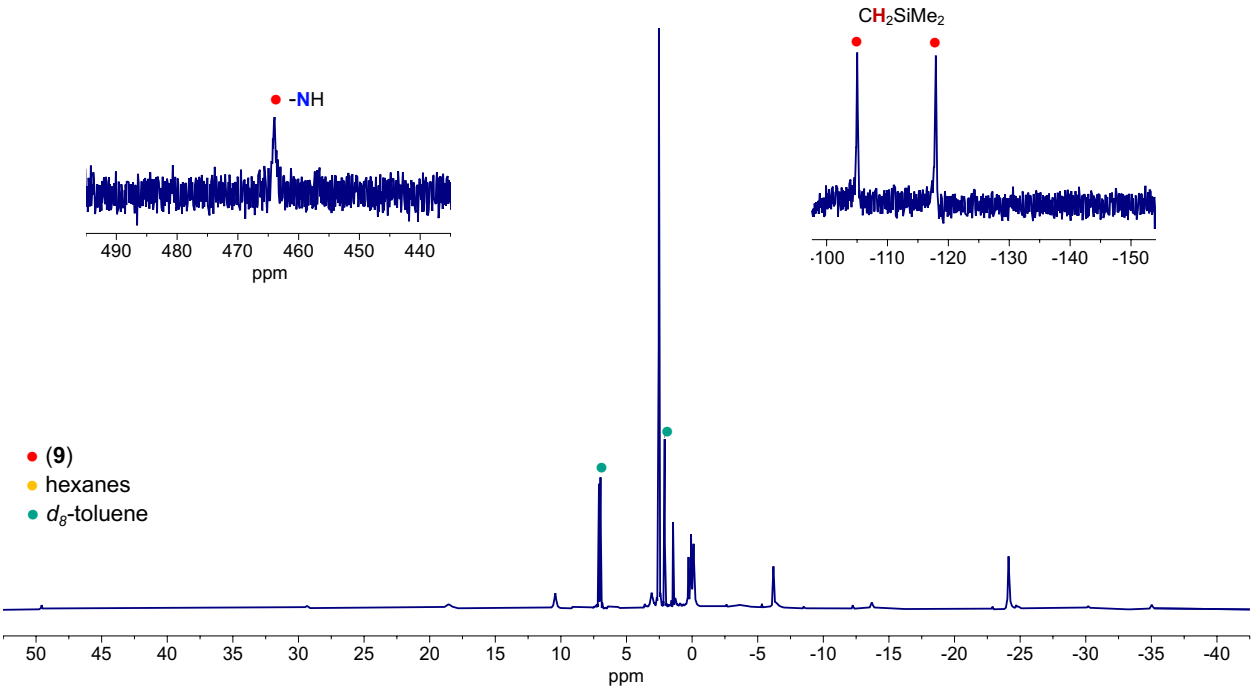

Figure S53. ^{1}H NMR (400 MHz, d_8-toluene, 298K) spectrum of isolated crystals from the reaction of complex **7** in the presence of 1.0 equiv. of *in-situ* generated complex **X**. The crystals still display a mixture of species of complexes **9**, **3-K**, and an unknown.

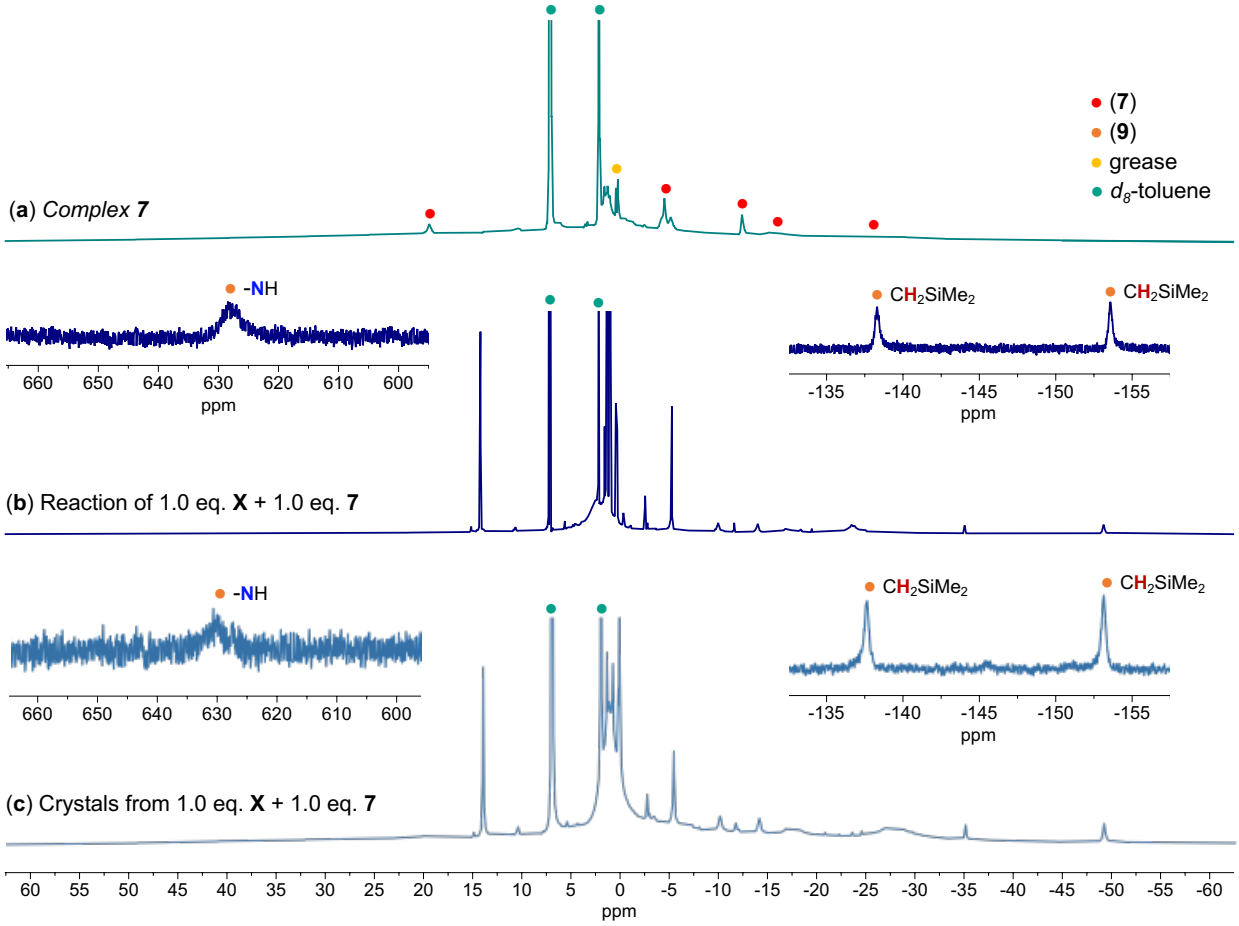

Figure S54. ^{1}H NMR (400 MHz, d_8-toluene, 233K) spectra of (**a**) isolated complex **7**, (**b**) reaction of complex **7** in the presence of 1.0 equiv. of *in-situ* generated complex **X**, (**c**) isolated crystals from the reaction of complex **7** in the presence of 1.0 equiv. of *in-situ* generated complex **X**.

S5.5. NMR spectra for the formation of NH_3 and $N(SiMe_3)_2$-containing species from addition of HCl.

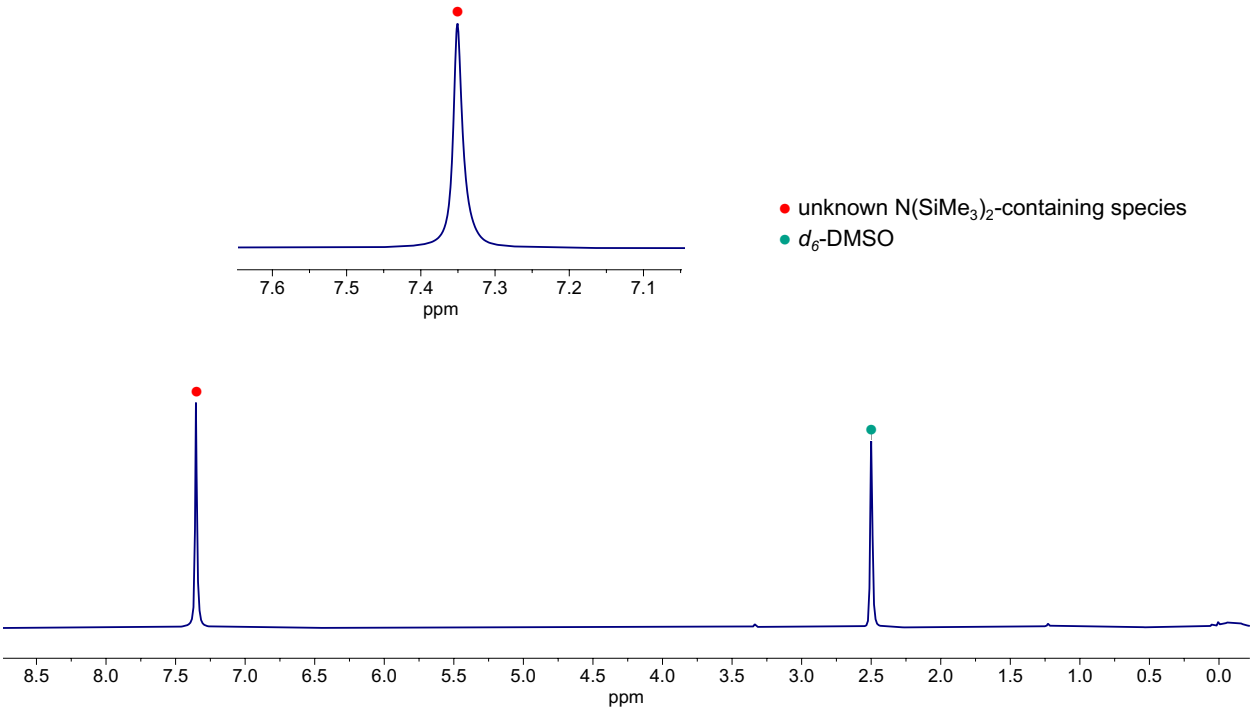

Figure S55. ^{1}H NMR (400 MHz, d_6-DMSO, 298K) spectrum of a $N(SiMe_3)_2$-containing species (δ 7.35 ppm) formed after addition of $KN(SiMe_3)_2$ and HCl (1M in Et_2O).

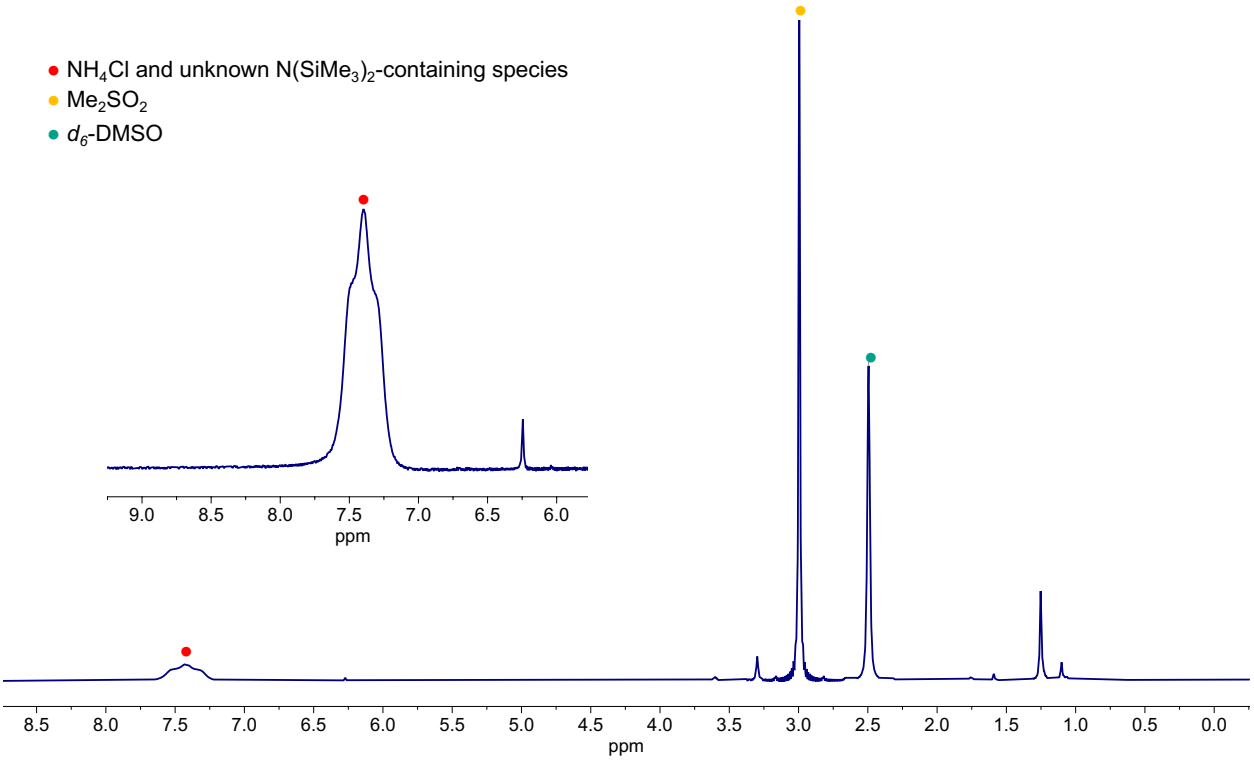

Figure S56. ^{1}H NMR (400 MHz, d_6-DMSO, 298K) spectrum of a mixture of NH_4Cl and an unknown $N(SiMe_3)_2$-containing species (see **Figure S55**) formed after addition of complex **3-Cs** and HCl (1M in Et_2O). Me_2SO_2 added as an analytical standard and obtained with a 120s relaxation delay.

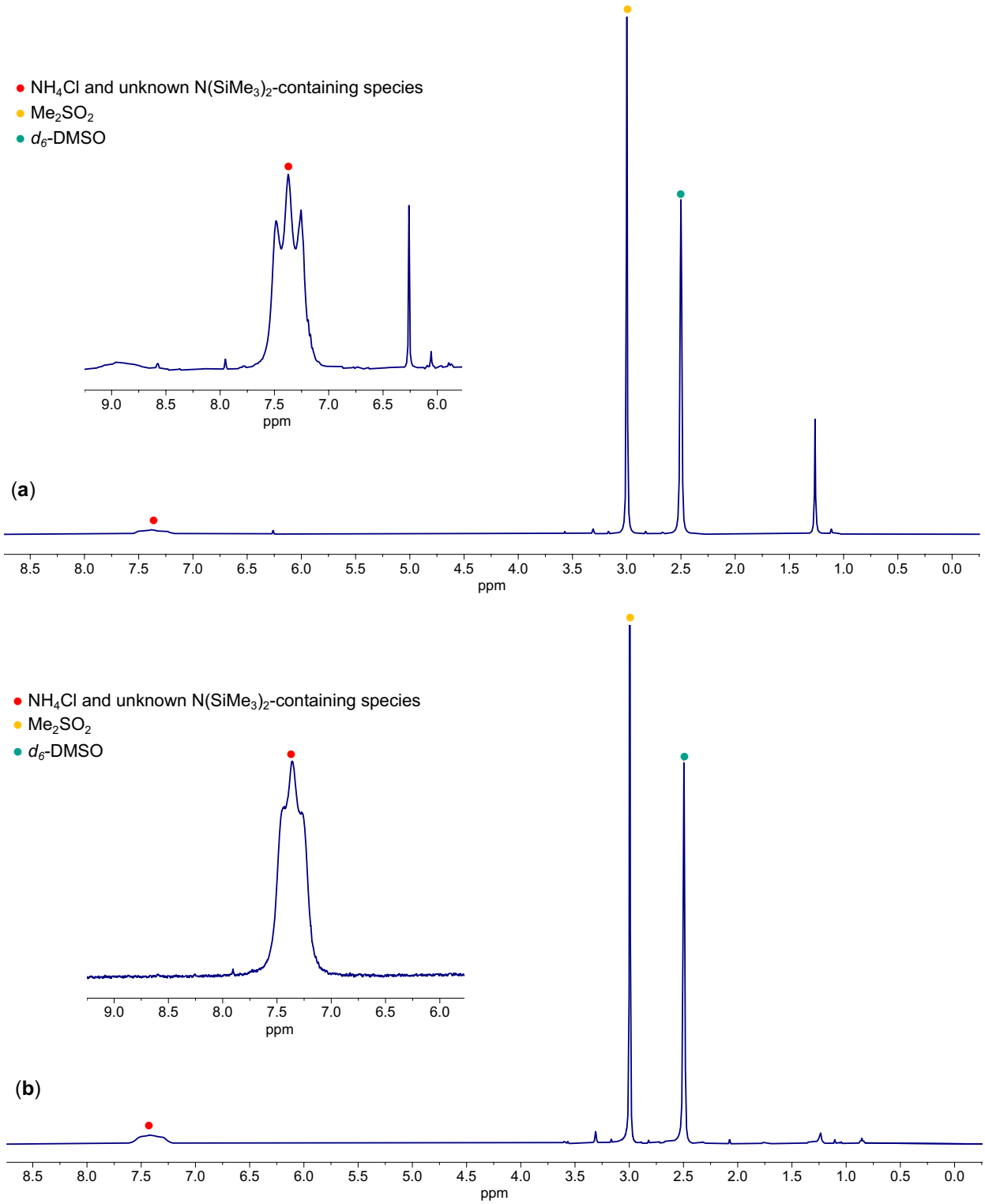

Figure S57. ^{1}H NMR (400 MHz, d_6-DMSO, 298K) spectra of a mixture of NH_4Cl and an unknown $N(SiMe_3)_2$-containing species (see **Figure S55**) formed after addition of either complex (**a**) **7** or (**b**) **7-$^{14/15}$N** and HCl (1M in Et_2O). Me_2SO_2 added as an analytical standard and obtained with a 120s relaxation delay.

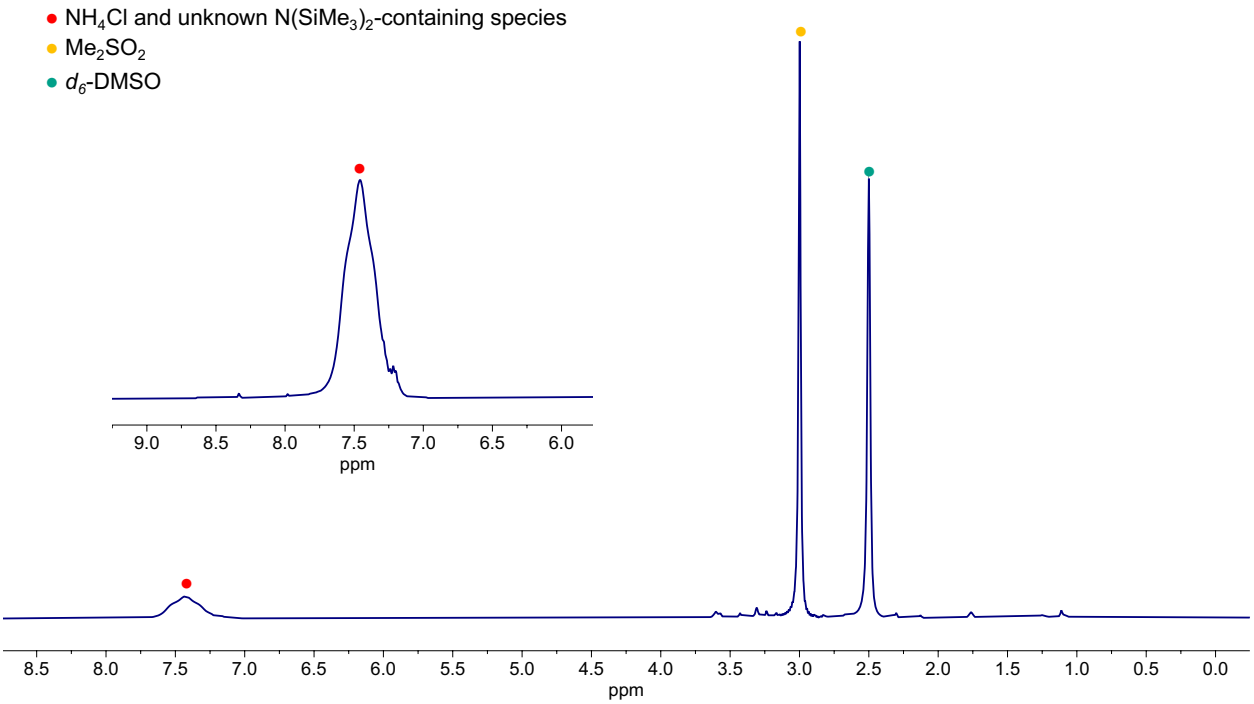

Figure S58. ^{1}H NMR (400 MHz, *d*$_6$-DMSO, 298K) spectra of a mixture of NH_4Cl and an unknown $N(SiMe_3)_2$-containing species (see **Figure S55**) formed after addition of HCl (1M in Et2O) to the *in-situ* generated complex **X**. Me_2SO_2 added as an analytical standard and obtained with a 120s relaxation delay.

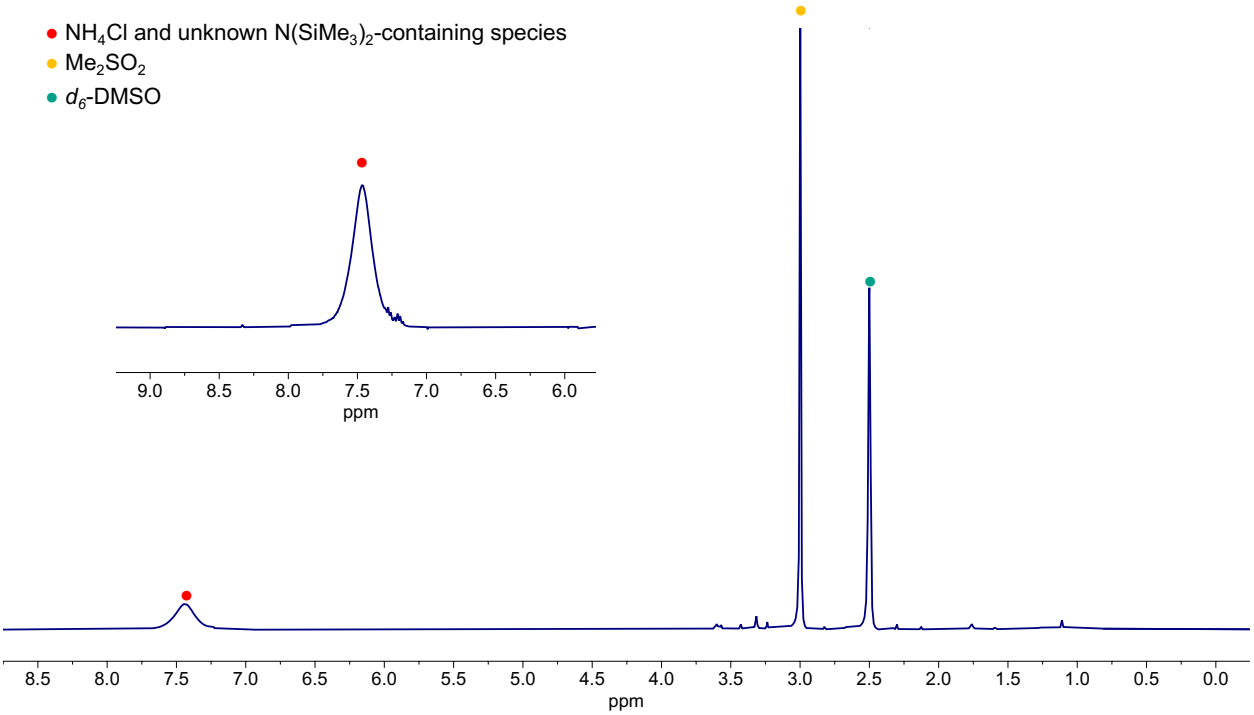

Figure S59. ^{1}H NMR (400 MHz, *d*$_6$-DMSO, 298K) spectra of a mixture of NH_4Cl and an unknown $N(SiMe_3)_2$-containing species (see **Figure S55**) formed after addition of HCl (1M in Et2O) to the reaction mixture of 1.0 equiv. of *in-situ* generated **X** and complex **7**. Me_2SO_2 added as an analytical standard and obtained with a 120s relaxation delay.

S6. X-Ray Crystallography Data

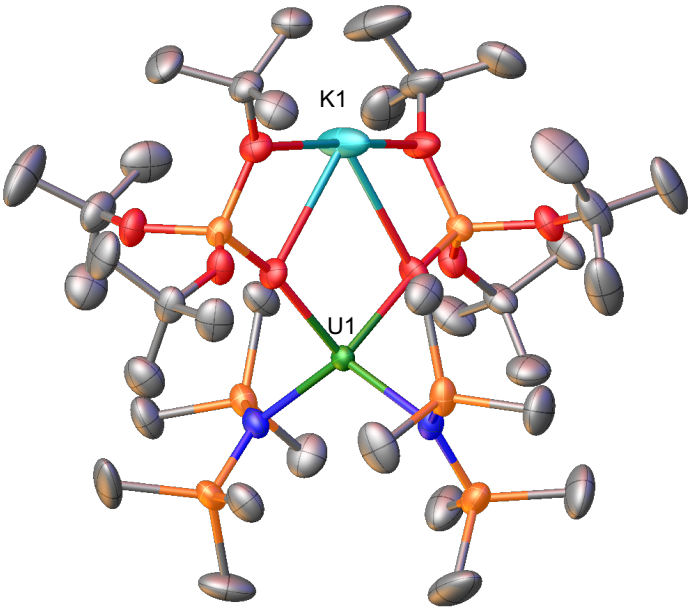

Figure S60. Molecular structure of [{U^{III}(OSi(O^{t}Bu)$_3$)$_2$)(N(SiMe$_3$)$_2$)$_2$}K], **2**, with thermal ellipsoids drawn at the 50% probability level. Hydrogen atoms have been omitted for clarity. Pertinent bond lengths: U1–K1 (3.755(10)Å).

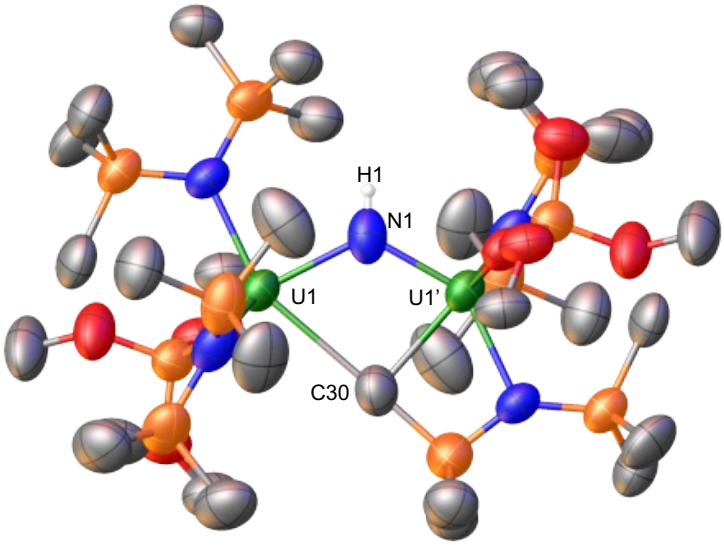

Figure S61. Molecular structure of [((Me$_3$Si)$_2$N)$_2$$U^{IV}$(OSi(O^{t}Bu)$_3$)(μ-NH)(*μ*-*κ*^{2}:*C,N*–CH$_2$SiMe$_2$NSiMe$_3$)-U^{III}(N(SiMe$_3$)$_2$)(OSi(O^{t}Bu)$_3$)][{K(2.2.2-cryptand)}$_2$], **5**, with thermal ellipsoids drawn at the 50% probability level. Hydrogen atoms and methyl groups on the OSi(O^{t}Bu)$_3$)$_3$ ligands have been omitted for clarity. Pertinent bond lengths described in Table 1. The U–NH–U bond angle (119.5(6)º) and distances (U1: 2.184(11), U1': 2.355(12) Å) are significantly longer than the parent nitride complex **4** (163.9(3)°; U2: 1.995(4), U1: 2.210(4)Å) and are consistent with the previously reported U(IV)/U(III) imido cyclometalate complex, (117.5(7)°; 2.151(15), 2.139(12)Å).[2]

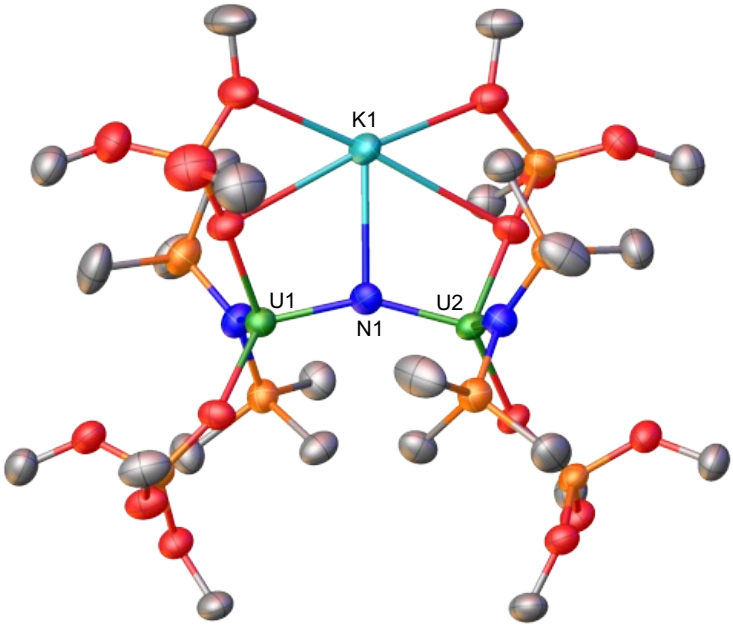

Figure S62. Molecular structure of [K{U^{IV}(OSi(O^{t}Bu)$_3$)$_2$(N(SiMe$_3$)$_2$)}$_2$(μ-N)], **3-K**, with thermal ellipsoids drawn at the 50% probability level. Hydrogen atoms and methyl groups on the OSi(O^{t}Bu)$_3$)$_3$ ligands have been omitted for clarity. Pertinent bond lengths and angles: U1–N1 (2.054(7)Å); U2–N1 (2.065(7)Å); N1–K1 (2.876(7)Å); U1–N1–U2 (154.0(4)º).

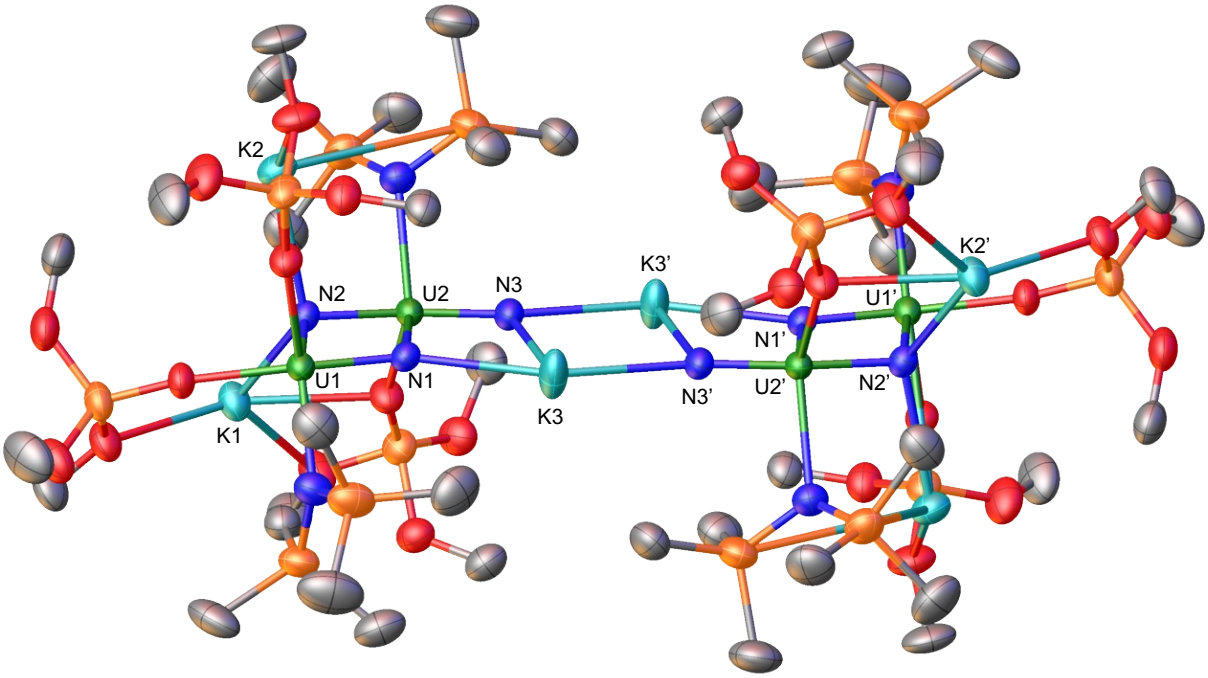

Figure S63. Molecular structure of [K$_3${U^{VI}(OSi(O^{t}Bu)$_3$)$_2$(N(SiMe$_3$)$_2$)(≡N)}(μ-N)$_2${U^{V}(OSi(O^{t}Bu)$_3$)$_2$(N(SiMe$_3$)$_2$)}]$_2$, **8**, with thermal ellipsoids drawn at the 50% probability level. Hydrogen atoms and methyl groups on the OSi(O^{t}Bu)$_3$)$_3$ ligands have been omitted for clarity. Pertinent bond lengths described in Table 2.

S7. EPR and Magnetism Data

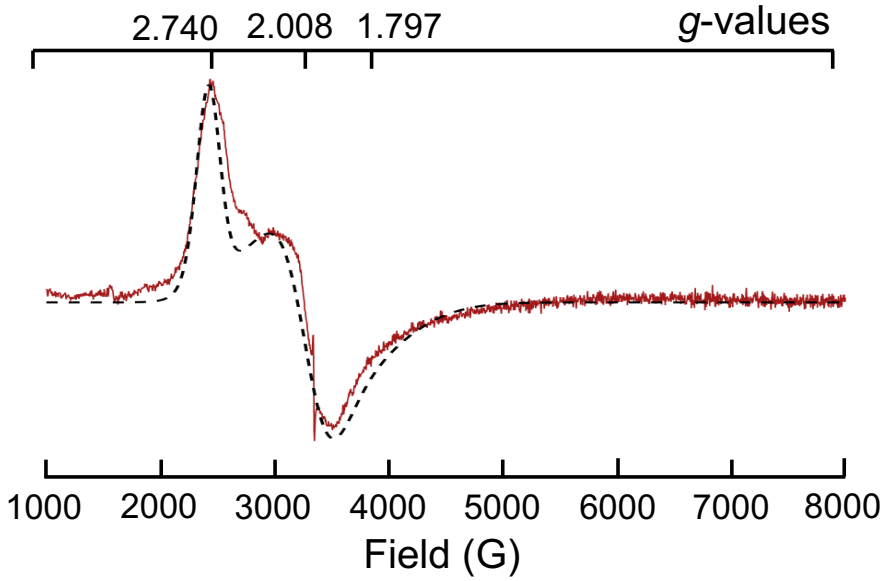

Figure S64. X-band (9.40 GHz) EPR spectrum of **7** (15.0 mg) suspended in 0.3 mL of toluene at 6 K (*red line*, experiment; *black dashed line*, fit to two $5f^1$ ions). The plot was fit to an axial set of *g*-values ($g_1 = 2.740$; $g_2 = 2.008$; $g_3 = 1.797$).

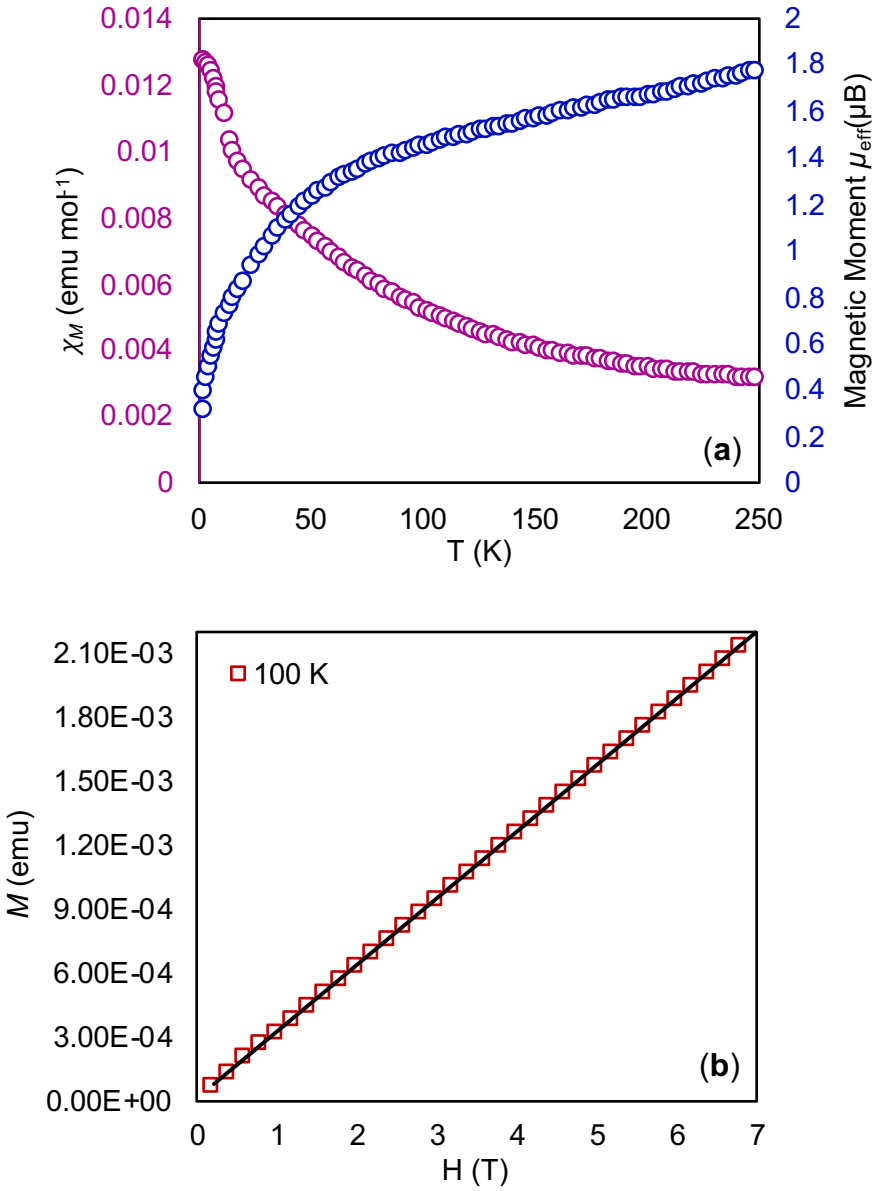

Figure S65. (**a**) Temperature-dependent SQUID magnetization data (1 T) for complex **7**, plotted as the magnetic susceptibility, χ_M (purple), and magnetic moment, μ_{eff} (blue), versus temperature. (**b**) Magnetization data for complex **7** at 100 K from 0.2 to 7 T to check to ferromagnetic impurities.

S8. Supplementary Schemes

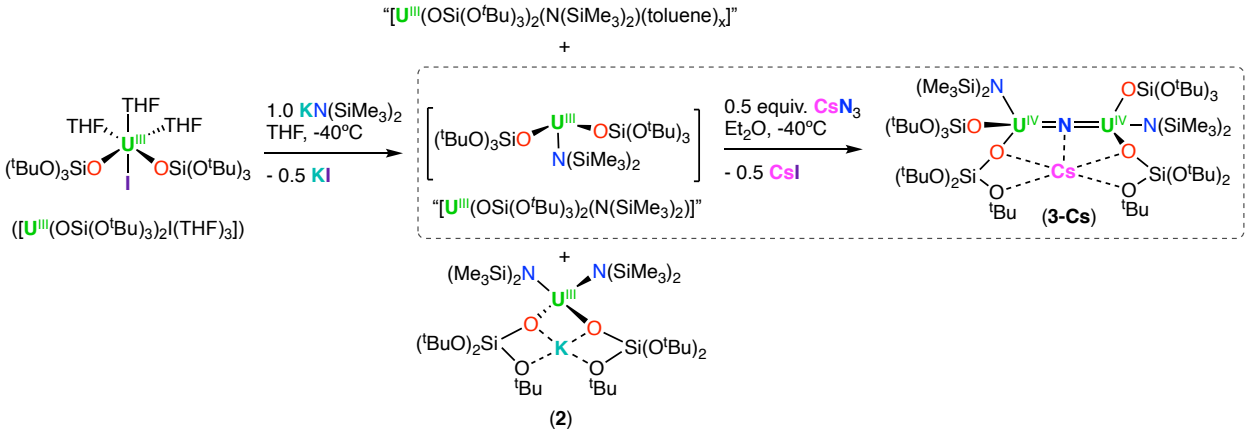

Scheme S1. Synthesis of complex **3-Cs**.

S9. References

1. C. T. Palumbo, L. Barluzzi, R. Scopelliti, I. Zivkovic, A. Fabrizio, C. Corminboeuf and M. Mazzanti, *Chem. Sci.*, 2019, **10**, 8840-8849.
2. C. T. Palumbo, R. Scopelliti, I. Zivkovic and M. Mazzanti, *J. Am. Chem. Soc.*, 2020, **142**, 3149-3157.
3. S. Stoll and A. Schweiger, *J. Magn. Reson.*, 2006, **178**, 42-55.
4. G. A. Bain and J. F. Berry, *J. Chem. Educ.*, 2008, **85**, 532.
5. *CrysAlis^{Pro}*, Rigaku Oxford Diffraction, release 1.171.41.113a, 2021.
6. G. M. Sheldrick, *Acta Cryst. Section A*, 2015, **A71**, 3-8.
7. G. M. Sheldrick, *Acta Cryst. Section C*, 2015, **C71**, 3-8.
8. L. Barluzzi, PhD. EPFL, 2021.
9. V. Mougel, C. Camp, J. Pécaut, C. Copéret, L. Maron, C. E. Kefalidis and M. Mazzanti, *Angew. Chem. Int. Ed.*, 2012, **51**, 12280-12284.
10. C. Camp, J. Pécaut and M. Mazzanti, *J. Am. Chem. Soc.*, 2013, **135**, 12101-12111.